Atom Transfer Radical Polymerization of Bio-based Methacrylates for Applications in Super Varnishes

Masa Alrefai

Department of Chemical Engineering

McGill University

Montreal, Quebec, Canada

July 2021

A thesis submitted to McGill University in partial fulfillment of the requirements of the degree of Master of Engineering

Abstract

This thesis presents controlled radical polymerization via atom transfer radical polymerization (ATRP) of bio-based monomers to make well-defined polymerswith narrow molecular weight distribution for application in varnish formulations.

Initially, traditional ATRP was used to synthesize homopolymers of isobornyl methacrylate (IBOMA) and a methacrylic ester with an average aliphatic side chain consisting of 13 carbon bonds (C13MA). Statistical copolymers of poly(IBOMA-*stat*-C13MA) with varying IBOMA:C13MA ratios were synthesized, kinetics and molecular characteristics were evaluated and reactivity ratios were determined to predict copolymer compositions from an initial monomer composition. The reactions were conducted at 80°C with the bromine-based initiator 4-(2-isobutyrate ethyl morpholine bromide) (ME-Br). Based on the gravimetric conversion analysis and gel permeation chromatography (GPC), the IBOMA and C13MA-rich compositions were all polymerized in a controlled manner (defined as a linear increase in number average molecular weight M_n with conversion up to 99% and low dispersity (Đ=1.16-1.52)). Differential scanning calorimetry (DSC) and thermogravimetric analysis (TGA) studies were performed to evaluate thermal transitions and thermal stability of the copolymers. The glass transition temperatures were found to be 118°C and -45°C for poly(IBOMA) and poly(C13MA), respectively. Post-polymerization treatments and purification were performed on the resulting polymers in order to remove the metal catalyst residue.

A reduced catalyst ATRP method, activator regenerated by electron transfer (ARGET ATRP), is an environmentally friendly ATRP method that can efficiently produce tailor-made polymer structures with only ppm amounts of copper, thereby eliminating post-polymerization purification.

ARGET ATRP was explored initially for the synthesis of IBOMA homopolymers. Different reaction parameters, including temperature, type of initiator and solvent, and concentration of solvent, catalyst, ligand, and reducing agent were all investigated. The reaction parameters were optimized to obtain a well-controlled polymerization with a linear increase in number average molecular weight M_n with conversion up to 97% and a relatively low dispersity (Đ=1.5-1.7). The optimized reaction conditions were then utilized to synthesize homopolymers of C13MA and statistical copolymers (poly(IBOMA-*stat*-C13MA)) with different IBOMA:C13MA ratios. The reactions were well controlled with conversion up to 99% and low dispersity (Đ=1.5). These results suggest the successful incorporation of sustainably sourced monomers into copolymers with a broad range of tunable glass transition temperatures via ARGET ATRP. Further, polymers were prepared to include the epoxy-functional monomer glycidyl methacrylate (GMA) to enhance adhesion properties for the varnish. Therefore, IBOMA/C13MA/GMA terpolymers were synthesized in a well-controlled manner with conversion up to 79% and low dispersity (Đ=1.5). The resulting resins were used to prepare varnish formulations that were tested for minimal drying time and impact resistance.

Abrégé

Cette thèse présente la polymérisation radicalaire contrôlée par la méthode de transfert d'atomes (ATRP) de monomères bio-sourcés pour synthétiser des polymères bien définis, avec une distribution de masse molaire étroite, pour les utiliser dans le domaine des vernis.

Premièrement, l'ATRP traditionnelle est utilisée pour synthétiser des homopolymères de méthacrylate d'isobornyle (IBOMA) et d'un ester méthacrylique ayant une chaîne latérale aliphatique moyenne constituée de 13 liaisons de carbone (C13MA). Des copolymères statistiques de poly (IBOMA-stat-C13MA) avec différentes quantités d'IBOMA/C13MA sont synthétisés, leur cinétique et leurs caractéristiques moléculaires sont évaluées ainsi que les rapports de réactivité sont déterminés pour anticiper les compositions des copolymères à partir du mélange de monomère initiale. Les réactions sont réalisées à 80 °C avec un initiateur à base de brome (4- (2-isobutyrate éthyl morpholine bromure ou ME-Br). En se basant sur l'analyse de conversion gravimétrique et sur les résultats extraits de la chromatographie sur gel perméable (GPC), c'est conclu que toutes les compositions riches en IBOMA et C13MA se sont polymérisées de manière contrôlée (définie comme une augmentation linéaire de la masse molaire moyenne en nombre M_n avec une conversion jusqu'à 98% et une faible dispersité (Đ = 1,16-1,52)). Des études de calorimétrie différentielle à balayage (DSC) et d'analyse thermogravimétrique (TGA) sont réalisées pour évaluer les transitions thermiques et la stabilité thermique des copolymères. Les températures de transition vitreuse se sont avérées être de 118 ° C et -45 ° C pour le poly (IBOMA) et le poly (C13MA), respectivement. Une série de purification est effectuée sur les polymères synthétisés afin d'éliminer le résidu de catalyseur métallique.

L’ATRP à catalyseur réduit, activateur régénéré par transfert d'électrons (ARGET ATRP), est une méthode d’ATRP plus environnementale qui peut produire avec efficacité des structures polymériques sur mesure avec seulement des faibles quantités (ppm) de cuivre, éliminant ainsi la purification de post-polymérisation. ARGET ATRP est explorée au début pour la synthèse d'homopolymères à base d’IBOMA. Différents paramètres de réaction, y compris la température, le type d'initiateur et de solvant ainsi que la concentration du solvant, du catalyseur, du ligand et de l'agent réducteur sont tous étudiés. Les paramètres de réaction sont optimisés pour obtenir une polymérisation bien contrôlée avec une augmentation linéaire de la masse molaire moyenne en nombre M_n avec une conversion jusqu'à 97% et une faible dispersité (Đ = 1,5-1,7). Les conditions de réaction optimisées sont ensuite utilisées pour synthétiser des homopolymères de C13MA et des copolymères statistiques (poly (IBOMA-stat-C13MA)) avec différentes quantités d’ IBOMA/C13MA. Les réactions sont bien contrôlées avec une conversion jusqu'à 99% et une faible dispersité (Đ = 1,5). Ces résultats suggèrent l'incorporation réussie de monomères issus de sources renouvelables dans des copolymères avec une large marge de températures de transition vitreuse ajustables à travers ARGET ATRP. En outre, des polymères sont préparés pour inclure le monomère de méthacrylate de glycidyle à fonction époxy (GMA) pour améliorer les propriétés d'adhésion du vernis. Par conséquent, les terpolymères IBOMA/C13MA/GMA sont synthétisés d'une manière bien contrôlée avec une conversion jusqu'à 79% et une faible dispersité (Đ = 1,5). Les résines résultantes sont utilisées pour préparer des formulations de vernis qui sont testées pour leur temps de séchage et leur résistance aux chocs.

Acknowledgements

I would like to thank my supervisor, Prof. Milan Marić, for his guidance and supervision throughout my Master's project. I would also like to thank the members of my research group for their support.

I would like to thank the McGill department of Chemical Engineering for providing great research facilities and work environment. A special mention goes to Frank Caporuscio, for his guidance and safety training. Moreover, I would like to thank the McGill department of Chemistry for the analytical equipment used for characterization with a special mention going to Robin Stein for her help in the NMR training and running the NMR samples and for Mr. Petr Fiurasek for is help with the DSC and TGA characterization.

I would like to thank the Natural Sciences and Engineering Research Council (NSERC) and PRIMA Quebec for their financial support. I would also like to thank our industrial partner, SAFRAN, for their support and project funding. I would also like to thank the McGill Department of Chemical Engineering for the Graduate Excellence Fellowship award and the Eugenie Ulmer Lamothe Discretionary Scholarship.

Finally, I would like to thank my family (Mona, Talal, and Abdullah) for their love and support and continuous encouragement. I feel really blessed to have them as my family. I would also like to thank my friends for their love and continuous support and encouragement.

Table of Contents

1. General Introduction

1.1 Protective Coatings

Protective coatings have long been applied in the wood, ceramic, and metal industries with increasingly more demanding requirements needed in current applications [1], [2]. As raw materials and resources become increasingly scarcer, protecting and conserving various substrates is vital. Polymeric materials offer that protection via coatings. Environmental concerns and limited resources have compelled researchers to investigate methods to improve widely used polymerization methods to meet the functional requirements crucial for the application. Recently, there have been significant advancements in controlled macromolecular polymer structures and new synthetic bio-based materials that are applicable to the coatings industry [3].

Wood is widely used in interior and exterior applications to enhance performance and aesthetic appeal. The lifetime of the coatings used to protect the wood is influenced by three main factors: weather, environmental environment, and human usage [4]. One primary concern associated with wood is its weatherability; figure 1.1 provides a summary of the weathering effect on wood. Protective coatings are applied in order to protect the wood from the surrounding conditions, maintain its dimensions and properties, and thus prolong its life [3]. Exterior wood products should be coated for protection against humidity, absorption, and UV light; they are typically acrylic-based binders or fatty acid-containing polyesters [5],[6]. Indoor applications of wood face different stress factors; these include home detergents, mechanical damage, abrasion, scratching, and chemical interactions [7],[8],[9]. Environmental and biological factors are strong influencers because weathering may include exposure to fungi, bacteria and insects, and non-biological factors such as air pollutants [7]. Some essential characteristics that varnish should have include

durability, flexibility, adhesion, tackiness, and resistance to biological agents [7],[10]. More specific characteristics include strong adhesion to the wood surface, resistance to flammability and cracking [11].

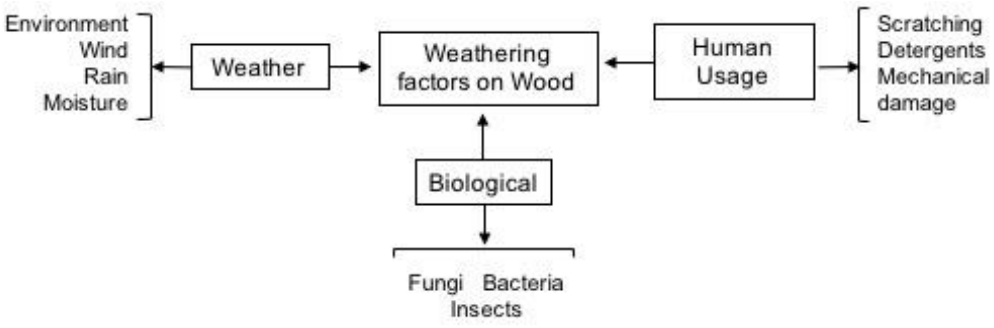

Figure 1.1 Wood weathering factors.

The coating market is large and broad; it includes transportation, living environments, healthcare, leisure, industrial processes, food, cosmetics, and energy. This market was estimated to be around 90×10^9 $ in 2016 and is predicted to reach about 129×10^9 $ by 2022 at a growth rate of 6.1% compounded annually [12].

1.1.1 Coating Formulation

Polymer coatings are formulations that include but are not limited to polymers, which may include. binders, pigments, solvents, and various additives. Binders are the primary ingredient of a coating. They are usually made of polymer resins, and their main function is film formation [12]. Binders must have good adhesion to the substrate and be resistant to chemical and mechanical damage [13]. The integrity of a polymer coating can be established by simply evaporating the solvent, while other coatings must form a network to cure. In the latter case, crosslinking agents are required in order to create the network. Curing is a process of crosslinking that changes the polymer coating in its thermoplastic form into a thermoset on the substrate [12]. Crosslinking or

curing agents are generally small molecules that can react with active groups in the resin to form a crosslinked network [14].

Additives act as effective problem solvers; they are added to enhance the properties of the coatings and solve a production or application problem. Additives include but are not limited to surface modifiers, thickening agents, surface active agents, and coalescing agents [15], [16]. Special effect additives can promote color, light, and weather resistance; they include corrosion inhibitors, thermal and light stabilisers, flame retardants, and photoinitators [16], [17].

The solvent plays an essential role in the coating's production and application. It is a transient state in the coating as it evaporates upon application; thus, it influences the solubility, dispersibility, and stability of components. The nature of the solvent also affects the viscosity, drying, and film formation of the coating [12],[13]. Fillers may be added, organic or inorganic, to adjust the structural and surface properties.

Therefore, by selection and manipulation of these constituents, the coating formulation is carefully designed and selected to obtain desired properties and performance for the final product, as shown in figure 1.2. Some of the considerations include the source of the raw materials and their environmental impact, and the choice of additives, pigments, and solvents. Specific details about the various components are explained further below.

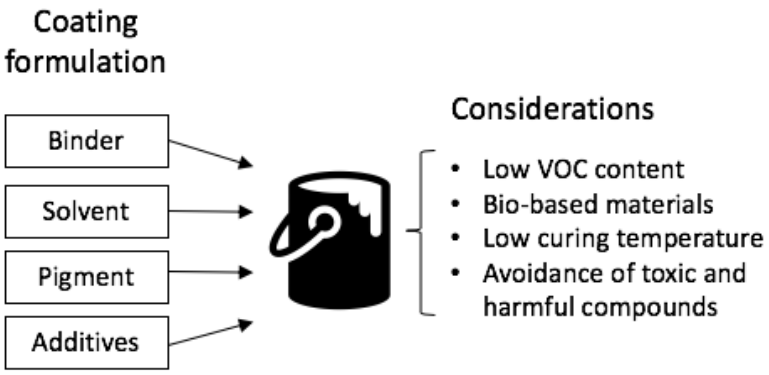

Figure 1.2 Coating formulation and considerations.

1.1.1.1 Binder

The majority of coatings are made of thermoset resins due to their network architecture that provides high resistance to chemicals and mechanical stresses [12],[15]. The main type of thermosetting polymers used for coatings includes phenol-formaldehydes and urea-formaldehydes, epoxies, acrylics and acrylates, isocyanates, polyesters, and alkyds [18]. Acrylic resins have gained a strong foothold in the coatings industry due to their improved flexibility and adhesion compared to other resins [19]. Poly(acrylate)s for solvent-based and waterborne coatings find uses in various areas for coating applications, including automotive, general metal, wood, and business machines coatings [19].

Acrylic homopolymers have a wide range of glass transition temperatures. The proper selection would result in specific glass transition temperatures suitable for various applications [20]. The glass transition temperature T_g is the most important property that influences the processibility of the polymer. Below the glass transition temperature, the polymer behaves like glass and there is no movement in the chains, whereas above the glass transition temperature, the polymer chains flow freely and the polymer behaves like a liquid. The glass transition temperature is indicative of the softness of the polymer, hardness, and low-temperature flexibility [20].

For ease of application, coatings are applied as liquids and then must transform into thermosets through curing. Coating application methods depend on several criteria, including cost, rheology, desired film thickness, the shape of the substrate, and versatility of use. Examples of coating application techniques include brushing, rolling, spraying, blade coating, spin-coating, and electrodeposition [20].

1.1.1.2 Solvent

Solvents pose a serious health and environmental concern. Emissions from organic solvents can cause permanent and irreversible health damage and may even lead to death from long-term exposure [13]. Organic solvents also impact the environment as solvent vapors can contribute to harming the ozone layer in the lower atmosphere and induce respiratory problems [13]. Thus, there has been a significant push to lower volatile organic compounds (VOCs) in paints and coatings. Consequently, the use of solvent must be minimized or even eliminated, which led to the development of new coating technologies that aim to lower the solvent requirement or even eliminate its usage altogether. These technologies include waterborne coatings, solvent-borne high solid content coatings, solventless liquid coatings, and powder coatings [21].

Water-based coatings significantly decrease and may even eliminate VOCs; hence, it poses as a more environmentally friendly alternative [7],[6],[9]. Although they are very promising, some problems are associated with this type of coating, including lower gloss, poor flow, and weather conditions limitations [22]. It is challenging to get the same aesthetic appearance and effects that solvent-based coatings have in water-based coatings [22]. Another problem is the requirement of coalescing agents for waterborne coatings. Due to the rapid increase in viscosity during film formation, coalescing agents are required so that the particles would deform and coalesce to fill the voids formed by the evaporation of water [23].

In contrast, solvent-borne high solid content coatings utilize less solvent with a volatile content of only 10-30% [13]. However, with the lower solvent concentration, the molar mass of the resin should be reduced to obtain the same viscosity. As the molar mass is lowered, the functionality of the chains, the network density, and final resin properties are all affected. The lower molecular weight reduces the concentration of functional groups and the network density, leading to a later gel point and requiring higher conversion to obtain similar network properties [21]. The low solvent content also affects the rheology of the coatings and causes problems in film stability as it may experience sagging (tearing from vertical surfaces). The two main solutions that can be pursued to maintain the same viscosity are to reduce the molar mass of the resin while either keeping the functionality the same or keeping the final network structure the same [21]. The coating solutions prepared are Newtonian fluids in which the viscosity is constant and independent of shear and extension[24]. To achieve high solid content coatings with suitable viscosity, resins with low molecular weight and narrow molecular weight distribution must be used [20].

1.1.2 Copolymers

Polymer resins used in coatings often employ functional copolymers as a component of the coating binder [14]. The properties of the copolymer depend on its homopolymer constituents and its microstructure. In the synthesis of a copolymer, several parameters dictate the morphology and properties of the final product. These include the composition distribution, the ratio of the different monomers in the polymer chain, and in the case of block copolymers, the block length distribution along the chain. These properties are controlled by the nature and the ratios of the monomers [17]. A variety of possible compositions of copolymers include homopolymers and random, block, graft, and gradient copolymers [2],[4].

In block copolymers, the different monomer chains are arranged in a systematic block structure in which monomer units are repeated in distinct segments. In random/statistical copolymers, the monomer units are linked in an essentially random or statistical arrangement dictated by the monomer reactivity ratios [27]. The synthesis of random copolymers, compared to block copolymers, is very easy as it can usually be performed as a one-step copolymerization process. While block copolymers' properties are dependent on the length of their respective blocks, random copolymer properties depend on the ratio of the different chain groups [28] and the reactivity ratios of the constituent monomers [27]. The copolymer architectures can be controlled and manipulated by controlling the solvent used and sometimes using external stimuli such as light and temperature [27].

Therefore, in the production of tailor-made coatings, the polymer resin can be synthesized to have specific properties by manipulating the nature of constituent monomers used and their composition and sequence distribution. For example, the constituent monomers could contain one that is used to enhance crosslinking through a functional group, while the other to adjust the glass transition temperature or other properties of the polymer.

1.1.2.1 Adhesion

When it comes to coatings, especially in a varnish, adhesion is one of the most critical properties. The adhesion of the coating to the wood substrate is essential and critical for its application; it can be achieved if the coating has a low surface tension and subsequently low contact angle [29]. The coating must also have good film flexibility and should be durable for robust applications. These characteristics are associated with the glass transition temperature of the polymer resin; a low glass transition temperature will result in better durability and enhanced film flexibility [29]. The coating must be easy to apply and should deeply penetrate the wood substrate to guarantee protection and

preservation of the wood. This can be achieved with a formulation that has a low viscosity [29]. Poor adhesion of the coating to the wood substrate would lead to water entering the substrate, this may result in the failure of the coating [30].

1.1.2.2 Crosslinking

Crosslinking is crucial for coatings as it determines the properties and performance of the coating film. Molecular weights are usually low for coatings in order to keep the viscosity low, which is very important in applying the film. Introducing crosslinking chemistry into the coating can help impart and enhance many physical and mechanical properties including adhesion to the substrate, durability, and resistance to scratch, abrasion, and chemical stresses [41],[42]. Functional groups can be incorporated into the polymeric matrix through copolymerization of the functional monomer. Several crosslinking chemistries have been studied. For example, carboxyl and hydroxyl functionalities can be incorporated into the polymer latex; melamine–formaldehyde groups or alkyl ether-containing monomers can be added to have crosslinking. These crosslinking chemistries require high curing temperatures (around 140-160 °C); hence, may be impractical and expensive when it comes to industrial application [31]. For the coating to be practical and industrially applicable, the curing should be done at relatively low temperatures and the coating should form a dry tack-free state within a reasonable time. Such fast-drying coatings are usually two-part formulations with a short pot life wherein the resin and the crosslinker are mixed right before application. Some ambient temperature crosslinking chemistries include polycarbodimide crosslinkers with carboxylic acid moieties, acetoacetoxy groups with aldehydes, electron-deficient olefins via Michael addition, and epoxy groups with amines [31].

Curing agents are used to build the polymer networks and stabilize them [14],[33]. They could be polymers with active hydrogen atoms like those found in acetoacemides and acetoacetoxy groups.

These polymers do not crosslink by themselves, but they crosslink rapidly in the presence of diamines. They are added to enhance the crosslinking in the coating formulations, giving enhanced properties like hardness, fast crosslinking, and water resistance [34]. Glycidyl acrylate (GA) and glycidyl methacrylate (GMA), shown in figure 1.3, are monomers that can be added to introduce epoxy functionality to the polymer; they can be incorporated into the polymer matrix by copolymerization [31], [35]. The oxirane ring in these monomers gives them the ability to react with various functional groups, including carboxylic acids, hydroxyls and amines, allowing chemical modification of the base polymer [35].

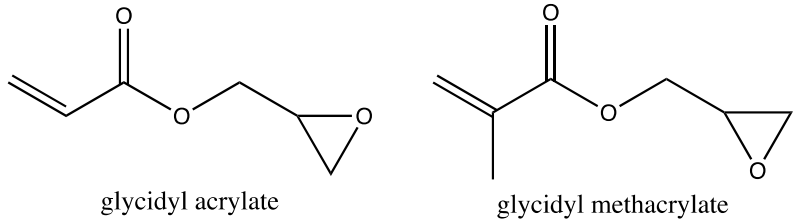

Figure 1.3 The structures of glycidyl acrylate (GA) and glycidyl methacrylate (GMA).

An amine crosslinking agent can then be added to the polymeric resin in the dispersed state. The crosslinking reaction between amino groups and the epoxy groups, shown in figure 1.4, occurs at ambient temperature and begins as soon as the amine diffuses and reaches the epoxy groups attached to the polymer chain. The diamine should dissolve into the polymer and diffuse rapidly as the solvent starts to evaporate, thus forming an initial uniform film as the coating dries. This will allow all the amine groups to react with the epoxy groups in the film effectively [31].

Epoxy resins have good adhesion to most substrates, high toughness, good chemical resistance, hardness and strength, and heat and moisture resistance [21]. Due to this versatility, epoxy resins are used in various coatings applications in nearly all fields. They are used as protective primer coatings in the automotive, aerospace, and marine industries; and in fiber-reinforced plastics and composites in the aerospace industry [21].

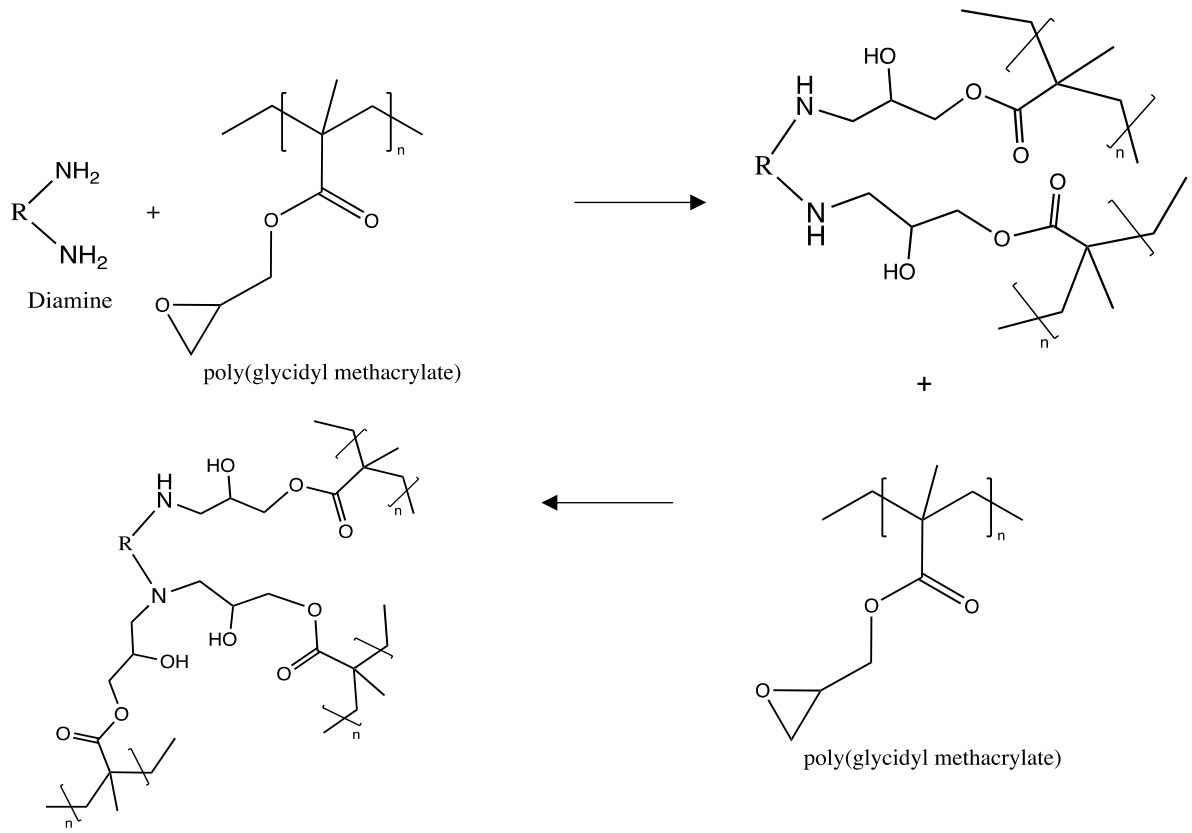

Figure 1.4 The crosslinking reaction of a diamine with the epoxy functional group (GMA).

In conclusion, precise control of the polymer's structure and molecular weight to obtain the required viscosity and carefully adjust the coating properties and optimize performance. Control of polymerization permits synthesis of low molecular weight copolymers in which functional monomers can be incorporated to make low viscosity coatings, which also enables the use of less solvent in the coating process.

1.2 Renewable Resources

Replacing conventional chemicals with bio-based ones in different market applications, including paints and coatings, has been promoted [36]. The use of bio-based materials is nothing new; natural resins have been used for thousands of years. Shellac, which is made of insect excrement, was used as an electrical insulator coating and still is used as a wood coating, a binder, and as an encapsulate for pharmaceutical and food supplements [37],[38]. Another example would be rosin, made from pine trees, that is still used for inks [18]. In the 19th century, raw materials were chemically modified, because of their difficulty in processing, to produce cellulose derivatives that can be used in coatings. An important example would be cellulose nitrate, invented in 1869, which was used in textile coatings and inks [39].

The utilization of bio-based substitutes in the chemical industry is one of the principles of green chemistry [40]. Biomass, wood, plant oils, polysaccharide, and other natural resources are used to substitute fossil fuels and derivatives. Products such as coatings, packaging materials, and bio-based chemicals can be obtained from these resources [41],[42],[43]. The global market of bio-based chemicals was estimated to be around 50 million tonnes in 2012 [44] and has grown to approximately 90 million tonnes in 2020 [45]. Various biomass fractions have been utilized to produce renewably sourced polymers, including polyesters, polyacrylates, polyurethane, polyamides, epoxy resins, and vinyl copolymers [3]. However, it should be noted that the use of bio-based precursors and solvents introduces some variability to the process in comparison to synthetic chemicals due to variations in the bio-source.

1.2.1 Bio-based Monomers

Increasingly in the polymer coatings industry, petroleum-derived monomers are being substituted with monomers made from renewable resources like carbohydrates and vegetable oils [40],[46]. The latter is an excellent choice due to their abundance, low price, and their non-toxic and biodegradable nature [47],[48]. Vegetable oils contain triglycerides; the degree of unsaturation and stereochemistry determines their chemical and physical properties. Triglycerides in vegetable oils can be chemically modified and reacted to enhance cross-linking, adhesion, and other coatings properties [49]. Their ability to dry and form films makes them suitable for application in coatings. Studies have shown that vegetable oils will be of great importance for the synthesis of polymers and the subsequent cross-linking systems for coatings [43],[47].

Many examples exist of bio-based monomers [18]. In particular, acrylates are relevant to this thesis. One important example of a bio-based monomer, derived from pine sap, would be isobornyl methacrylate (IBOMA) which is 71% bio-based [50]. IBOMA is a very useful functional monomer, often copolymerized in tandem with other unsaturated monomers. Properties that IBOMA imparts include gloss, hardness, and resistance to scrub, water, UV radiation, and chemicals. IBOMA is an environmentally friendly monomer due to its low volatility and high boiling point which reduces its pollution and environmental toxicity [51]. Poly(IBOMA) has a high glass transition temperature of around 125°C, making it suitable to be used as the hard monomer when copolymerized with other monomers [50]. Its introduction to polymers significantly improves heat resistance and reduces the polymers' viscosity [31], [51], [53]. Another example of a partially sustainably sourced monomer is the vegetable-oil-based methacrylic ester similar to lauryl methacrylate (C13MA, average alkyl side chain length = 13 carbons). It is a

hydrophobic methacrylate with a very low glass transition temperature of around -46°C [52]. The structures of IBOMA and C13MA are shown in figures 1.5 and 1.6, respectively.

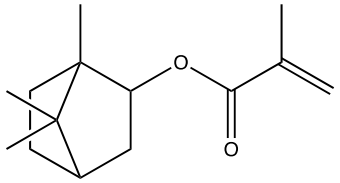

Figure 1.5: IBOMA structure.

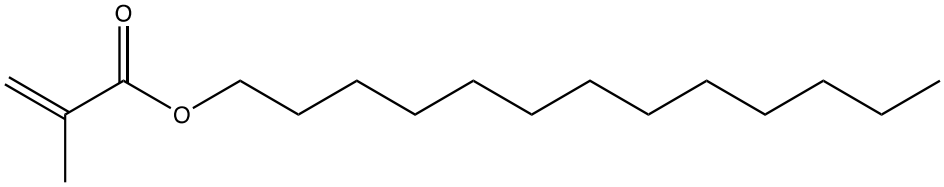

Figure 1.6 C13MA structure.

1.2.2 Bio-based Solvents

Following the third principle of green chemistry, synthetic methods should be designed in order to minimize the use of hazardous chemicals and to use and generate substances that pose little or no toxicity to the environment or human health [54]. Solvents account for the vast majority of waste generated in chemical processes [54]. Therefore, notable efforts have been directed towards developing and using green solvents; researchers are replacing solvents with environmentally friendly alternatives [55]. Fulfilling the seventh principle of green chemistry, several green or bio-based solvents have been proposed to replace traditional solvents; some examples include glycerol, glycerol ethers, 2-methyl tetrahydrofuran (2-MeTHF), valerolactone, ethyl lactate, and cyclopentyl methyl ether [55]. On this basis, 2-methyl tetrahydrofuran (2-MeTHF) is a bio-based solvent that can be produced from renewable resources such as furfural or levulinic acid [56]. 2-MeTHF has similar properties to THF; some of its physical and chemical properties include low miscibility with water, high stability, and a relatively high boiling point of around 80°C. It is a commercially available alternative solvent that easily degrades and is bio-based [56], [57].

Another example of a bio-based solvent is Cyrene (also known as dihydrolevoglucosenone or 6,8-dioxabicyclo[3.2.1]octanone) which is touted as a alternative to REACH restricted solvents N, N-dimethylformamide (DMF), and N-methyl- 2-pyrrolidone (NMP) [58]. Cyrene can be synthesized from biomass (cellulose) in a two-step process where it initially forms LGO levoglucosenone, then Cyrene, as shown in figure 1.7 [58].

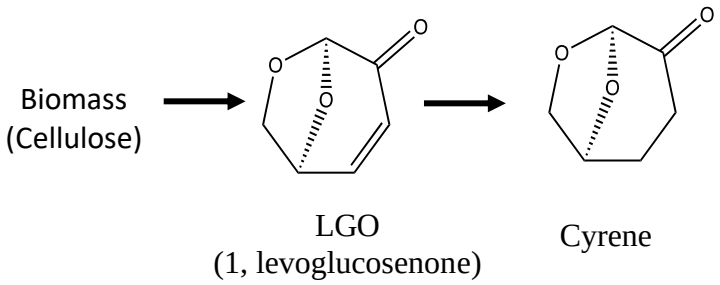

LGO
(1, levoglucosenone)

Cyrene

Figure 1.7 The synthesis of Cyrene from biomass.

The use of renewable resources in the synthesis of the resins, in compliance with the principles of green chemistry, will help reduce the environmental damage caused by traditionally used petroleum-based chemicals. It is also a step forward in sustainability as it is a move towards the production of "green" materials and more environmentally friendly chemical processing.

1.3 Atom Transfer Radical Polymerization

1.3.1 Free Radical Polymerization

Free radical polymerization is a versatile polymer synthesis technique and is highly applicable industrially as it is tolerant to a wide range of solvents and functional groups [59]. Free radical polymerization is used to produce a wide range of industrially relevant polymers such as poly(styrene), poly(methyl methacrylate), poly(vinyl acetate), and branched poly(ethylene). The mechanism for free radical polymerization involves initiation, propagation, and termination. In initiation, free radicals are formed through thermal or photochemical initiation that in turn initiate the monomers by adding to the carbon-carbon double bond. This creates propagating radicals that propagate further through the addition of monomer, thus creating propagating chains. Termination then occurs in two modes, combination or disproportionation, to form dead polymers. However, the main drawback of free radical polymerization is that it terminates very quickly due to the propagating radical chain ends' highly reactive nature [17]. The radicals' fast-terminating nature does not allow enough time to control polymerization; hence, it is impossible to control the molecular weight, structure and topology of the resulting polymer. Polymer scientists aimed to slow down or retard the termination of radicals to gain control over the reaction. It was found that this can be accomplished via an equilibrium where the active chain ends are capped reversibly and stay in a dormant state. The chains are then reactivated briefly to add more monomer units in a controlled manner [60].

1.3.2 Controlled Radical Polymerization

Controlled radical polymerization methods (CRP), also known more correctly as reversible deactivation radical polymerization (RDRP), are radical polymerization methods that demonstrate the chain end fidelity in a manner akin to truly living polymerizations as the life of the propagating

chain is prolonged, and termination is suppressed [60],[61]. These methods utilize a dynamic equilibrium between an active state of growing radicals and a dormant state of inactive species. The equilibrium ideally lies on the dormant side, thus keeping the active radicals' concentration to a minimal level to avoid termination and thus permitting linear chain growth with monomer conversion. Successful controlled radical polymerization is achieved when the initiator is consumed early in the reaction, and the chain transfer and termination reactions are negligible [17]. This will allow high control levels over polymerization, allowing the synthesis of uniform macromolecules with predetermined molecular weight and functionality with narrow molecular weight distribution and a high degree of chain-end fidelity [60].

Therefore, controlled radical polymerization methods enable the production of polymers with defined architectures and chain length with a wide range of different compositions, structures, and topologies [2], [25]; some of the structures that these macromolecules can have include star, comb, linear, hyperbranched, and network structures.

Materials with well-defined microstructures that can be made with RDRP include coating components, adhesives, lubricants, surface modifiers, surfactants, gel and hydrogels, and advanced electronic and biochemical materials [25],[62]. RDRP methods can be used to adjust the functionality and viscosity of the coating formulation; in coating applications specifically, controlled radical polymerization methods prove to be very effective due to the narrow molecular weight distribution of the resulting polymer. The low dispersity (Đ) obtained from RDRP indicates the formation of polymer chains of uniform length which results in low viscosity polymers. In coating applications, low viscosity polymers enable higher solid content and lower solvent requirements; it also gives smoother hardening during the curing stage, which optimizes the coating film properties [17].

Moreover, different desirable properties for the coating can be achieved by manipulating the following parameters: polymerization efficiency, solvent used, activator/deactivator ratio, reaction temperature and time, and the incorporation of additives. The sequence and duration of the reagent addition dictates the efficiency of polymerization conversion. The activator/deactivator ratio is manipulated to create a balance between control and conversion. It is clear that specialized coatings require well-defined and functionalized materials; this level of control can be achieved through controlled radical polymerization methods [17].

Over the past 30 years, there have been significant advancements in controlled radical polymerization (RDRP as stated earlier) methods. These methods include nitroxide mediated radical polymerization (NMR) [63], also termed as stable free radical polymerization (SFRP) [64], atom transfer radical polymerization (ATRP) [26], and reversible addition-fragmentation chain transfer (RAFT) [65].

1.3.3 Atom Transfer Radical Polymerization

Amongst the variants of controlled radical polymerizations, atom transfer radical polymerization (ATRP) has emerged as a very powerful and versatile controlled polymerization method. It is considered a mature polymerization technique due to its efficiency, versatility, and applicability in the lab and on an industrial scale [66]. Since its discovery in 1995 by Matyjaszewski [67] and Sawamoto [68], ATRP has been used to synthesize many polymers from a variety of monomers including styrenics, (meth)acrylates, (meth)acrylamides, and acrylonitrile [69]. ATRP allows the synthesis of polymers with low Đ and predetermined molecular weights, complex architectures, and high chain-end functionality [8],[17]. It has been used to synthesize nanostructured materials including controlled complex polymer architectures, hybrids, and bioconjugates [26]. ATRP can be carried out in bulk and aqueous dispersed media [71]; it was successfully carried out in several

polymerization systems including emulsion [72], mini-emulsion [84],[85], and micro-emulsion systems [75]. ATRP does not have demanding reaction conditions as it is tolerant to low concentrations of impurities and recent advances in ATRP methods are even tolerant of oxygen [61]. ATRP has been commercialized and is currently used in seventeen different industrial licenses spanning various applications such as coatings, adhesives, dispersants, lubricants, gels, sealants, and hybrids, thermoplastic elastomers, and electronic biomaterials [66], [76].

1.3.3.1 Atom Transfer Radical Polymerization: Mechanism

ATRP derives its name from the key elementary reaction responsible for the polymer chain growth which is the atom transfer step. ATRP originates from atom transfer radical addition (ATRA) reactions that are catalyzed by a transition metal complex. It is related to reactions like transition-metal-catalyzed telomerization reactions and transition metal initiated redox processes and inhibition with transition metal compounds. Although these reactions have activation and deactivation, they do not provide efficient reversibility [77]. ATRP is a reversible termination controlled radical polymerization method; the mechanism, shown in figure 1.8 [78], involves ligand coupling to a metal complex (that is usually a copper complex (Mt^n-Y/Ligand). Initiation occurs by transferring the halogen atom (X) from an alkyl halide to the metal complex. This results in an alkyl radical (R•) that acts as the initiator. The radical will combine with a monomer forming a monomer-ended radical that reacts with the oxidized metal complex (X-Mt^{n+1}-Y/Ligand), forming the lower oxidation state (n) metal species with an extended halide (P_n-X). [67].

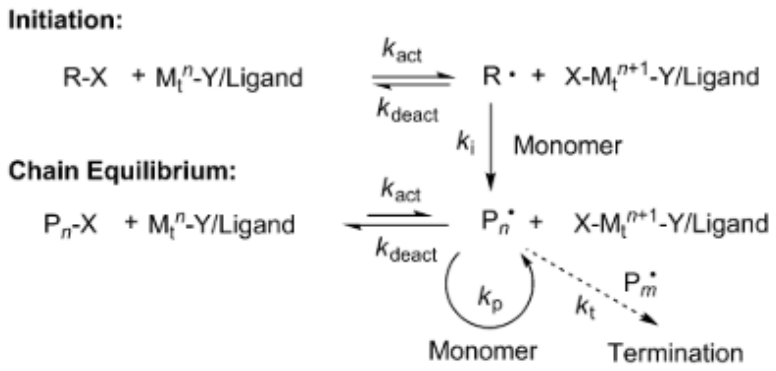

Figure 1.8 General mechanism for ATRP [78].

In the activation step, the metal complex is oxidized to its higher oxidation state, and it abstracts the halogen atom, leaving the propagating polymer chain available for monomer addition. In deactivation, the polymer chain is capped with the halogen atom again and cannot propagate; thus it is inactive or dormant again. The activation and deactivation steps proceed with the rate constants k_{act} and k_{deact} respectively. The dynamic exchange between activation and deactivation is one of the most critical parameters of ATRP. Control relies on the domination of deactivation over the equilibrium so that the monomers propagate slowly. When the concentration of dormant species is high and the initiator concentration is low, the conversion is high and low molecular weight distribution is obtained [25],[67]. Termination can occur through radical coupling or disproportionation, but a very low portion, no more than 5%, of the chains terminate during polymerization. ATRP is a well-controlled polymerization reaction in which molecular weight increases linearly with conversion. Higher Đ is usually observed initially as monomer units are added in activation but the Đ then decrease with conversion as the concentration of the deactivator species increases and the concentration activator species decreases [77].

1.3.3.2 Atom Transfer Radical Polymerization: Chemistry

The main components of ATRP are monomer, initiator, metal catalyst complexed with a ligand, and solvent. ATRP can be applied to a wide variety of monomers that contain substituents that can

stabilize the propagating radicals. Some of the monomers include styrenes, (meth)acrylates, (meth)acrylamides, dienes, and acrylonitrile [79]. The initiator plays an important role in ATRP as the initiator's concentration determines the number of growing polymer chains. Alkyl halides (RX) are typically used in ATRP where the halogen is usually chlorine or bromine. The halide exchanges rapidly between the growing polymer chain and the transition metal complex. Initiation should be fast compared to propagation and side reactions should be minimal. Besides alkyl halides, other potential ATRP initiators include halogenated alkanes, benzylic halides, α-haloesters, α-haloketones, α-halonitriles, and sulfonyl halides. Common monomers, initiators, and ligands typically used in ATRP are shown in figure 1.9 [78].

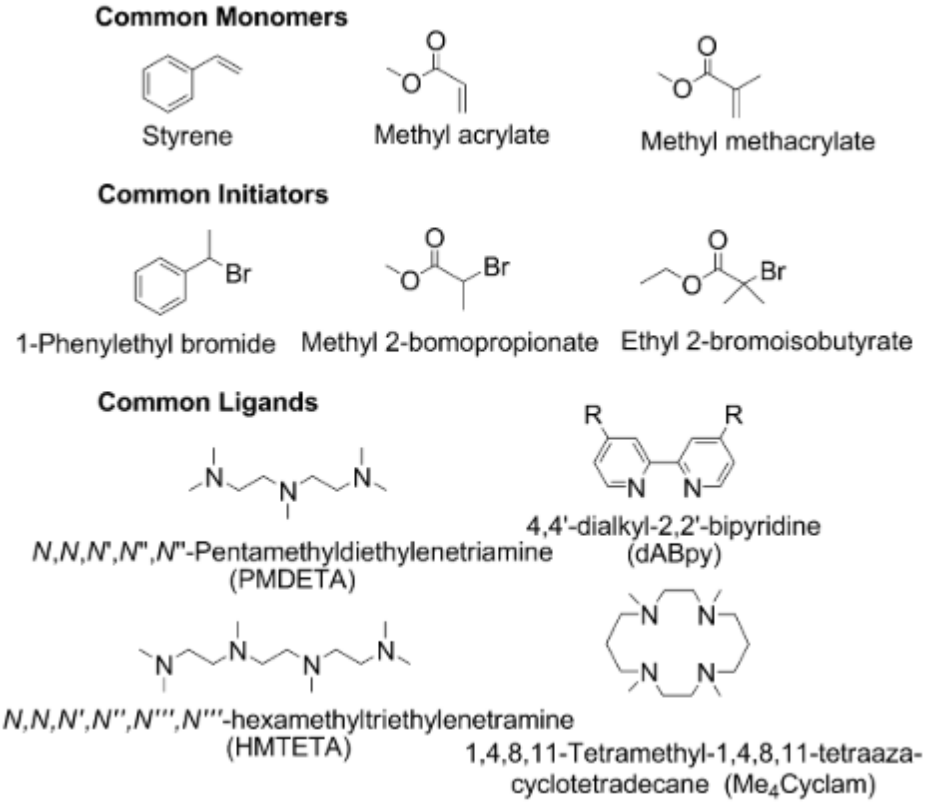

Figure 1.9 Common ATRP monomers, initiators, and ligands [78].

The catalyst is a critical part of ATRP as it determines the position of the equilibrium and facilitates the halogen exchange cycle. Copper catalysts are most commonly used due to their binding

versatility, performance, and cost [77]. Other potential transition metal catalysts include iron, cobalt, rhodium, palladium, and nickel. A ligand is also required in ATRP; the ligand forms a complex with the transition metal to solubilize it and adjust the redox potential and halogenophilicity of the metal center. The ligands typically used are nitrogen-based monodentate, bidentate and multidentate compounds, all of which have been successfully employed in ATRP [79]. Finally, as ATRP can be carried out in bulk, solution, suspension, emulsion, and mini-emulsion, a solvent may be required. Various solvents could be used including benzene, toluene, anisole, diphenyl ether, water, and many others [77]. The potential for chain transfer is an important factor that influences the choice of solvent. Considering chain transfer constants, toluene and xylene can be used as ATRP solvents when the targeted molecular weight is low (M_n < 20,000 g/mol). Other factors influence the choice of solvent include the solubility of monomers and solvent interactions with the catalyst system [79].

1.3.3.3 Atom Transfer Radical Polymerization: Drawbacks

Due to the environmental issues the world is currently facing, there has been a drive in the chemical and polymer industry to apply green chemistry principles to develop eco-friendly techniques and use less toxic substances in processes [80]. Companies are focusing on sustainable development and eco-friendly processes by reducing the energy requirements in their operations and avoiding harmful waste. Similar sustainability efforts have been directed towards the improvement in ATRP to make it more environmentally friendly or green. Efforts in green ATRP have been directed towards using green solvents, lowering catalyst concentrations, and synthesizing degradable polymers [60]. ATRP utilizes a metal complex as a catalyst to mediate its dynamic equilibrium. The use of the metal catalyst is the main weakness of ATRP as it causes discoloration of the final polymer product and requires extensive treatment to be removed [81], [82]. The metal catalyst,

typically copper, can be toxic and is harmful to the environment once discarded [83]. Furthermore, the discoloration of the polymer product is a problem in terms of industrial application, especially in biochemical and electrical applications. In order to remove the coloured catalyst residue, several post-polymerization and purification steps are required. Purification methods include washing, extraction, precipitation, and filtration through an adsorption medium like silica gel or aluminium oxide [82], [83]. These purification techniques are impractical and sometimes inapplicable on a large scale. The repetitive purification cycles have a very high cost due to the excessive use of solvents and adsorption media. Furthermore, the separation can be very challenging and will cause some loss of polymer product. Other more advanced methods for purification that were investigated include biphasic separation and solid supported catalyst. In both these systems there was a loss of control over ATRP and they resulted in high dispersity of chains [82].

1.3.4 Atom Transfer Radical Polymerization: Reduced Catalyst Methods

Ultimately, the green route to polymerization via ATRP would be through the reduction or elimination of the metal catalyst. However, lowering the concentration of the metal catalyst leads to an accumulation of the (Mt^{n+1}) deactivator complex, which in turn significantly retards and eventually halts the reaction preventing the reaction from reaching high conversion [84],[83]. Upon careful inspection of the ATRP rate law (eq. 1.1) [85], it can be seen that the rate is dependent on the ratio of the activator and deactivator species [Mt^{n}] and [Mt^{n+1}] respectively, and independent of the absolute concentration of the metal complex.

$$R_p = k_p[M][P^\bullet] = k_p K_{eq}[M][I]_0 \frac{[Mt^n]}{[X - Mt^{n+1}]}) \qquad \text{eq. 1.1}$$

In equation 1.1, [M], [P•], and $[I]_0$ are concentrations of monomer, propagating species, and initiator, respectively. Also, k_p is the propagation rate constant and K_{eq} is the ATRP equilibrium constant; and $[Mt^n]/[Mt^{n+1}]$ is the molar ratio of the concentrations of the copper activator and deactivator species) [85]. Therefore, in theory, the amount of metal catalyst used, which is typically copper, can be reduced as long as the ratio of Cu(II) to Cu(I) is maintained. However, a sufficient concentration of the deactivator species $[X\text{-}Mt^{n+1}]$ should be available as the molecular weight and the dispersity (Đ) of the polymer are dependent on the concentration of the copper deactivating species as shown in equation 1.2.

$$Đ = 1 + \frac{1}{DP_n} + \left(\frac{k_p[R-X]_0}{k_{da}[X-Mt^{n+1}]}\right)\left(\frac{2}{p} - 1\right) \qquad \text{eq.1.2}$$

Here, $Đ = M_w/M_n$, DP_n is the number average degree of polymerization, k_p and k_{da} are the propagation and deactivation rate constants, $[R\text{-}X]_0$, and $[X\text{-}Mt^{n+1}]$ are the concentrations of initiator and deactivator, respectively; and p is the conversion.

In order to adjust the catalytic requirements of the ATRP system, an alteration of the initiation method is required to allow the regeneration of the lower oxidation state in order to push the reaction forward. This can be achieved using ppm amounts of copper and environmentally benign reducing agents such as iron, sugar, ascorbic acid, and even light and electricity. Several initiation methods have been developed for ATRP. The different initiation methods all follow the same ATRP reaction mechanism but vary in terms of the concentration and amount of metal complex used, the oxidation state of the added transition metal, and the procedure of activating the metal complex [4],[16]. These methods include, but are not limited to, reverse ATRP [86], simultaneous reverse and normal initiation (SR&NI) [87], activator regenerated by electron transfer

(AGET)[88], activator regenerated by electron transfer (ARGET) [88], initiators for continuous activator regeneration (ICAR) [89], and photo-induced ATRP [90],[91].

1.3.4.1 Activators Generated by Electron Transfer (AGET) ATRP.

AGET ATRP (Activators are Generated by Electron Transfer) is an ATRP method that uses electron transfer to reduce the metal complex from its higher oxidation state Cu(II); a reducing agent that does not form radicals is used [88]. In the AGET mechanism, the reducing agent reduces the higher oxidation state metal complex to the lower oxidation state activating species, which activates the ATRP reaction. The reducing agent used in this method facilitates initiation, controls the rate of propagation, and aids in removing dissolved oxygen from the system [74]. In AGET ATRP, the higher oxidation state catalyst complex is reduced prior to normal initiation and only a low concentration of the catalyst is required. This method is tolerant to air as the catalyst used is a stable higher oxidation state metal complex, making it a simple, robust, and versatile method. Although AGET provides a very convenient initiation method, the amount of metal complex used in not reduced as desired; thus, a more advanced variation of AGET, Activator Regenerated by Electron Transfer (ARGET), was developed.

1.3.4.2 Activator Regenerated by Electron Transfer (ARGET) ATRP

ARGET is an electron transfer technique in which the activator species is continuously regenerated from the deactivator species. It is considered an environmentally friendly polymerization procedure because it uses only ppm amounts of catalyst in the presence of a reducing agent. This method is very similar to AGET discussed above, except that it uses a high excess of reducing agent [92].

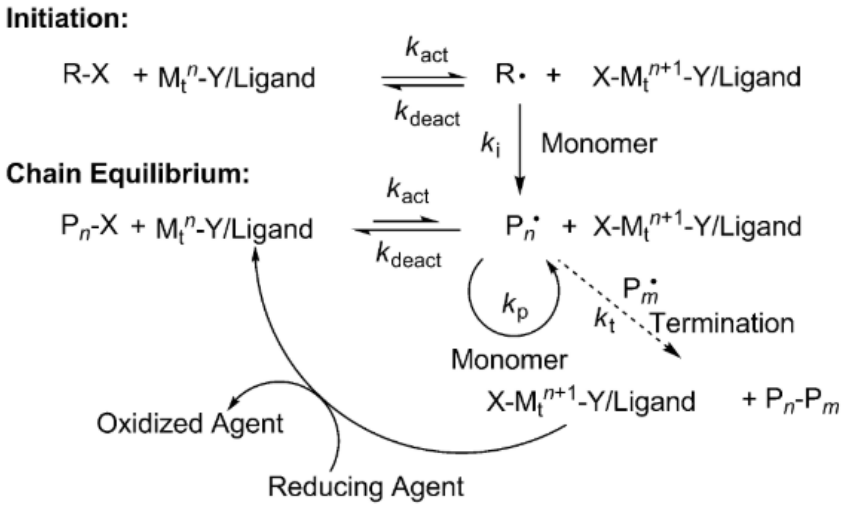

Figure 1.10 Mechanism for ARGET ATRP [78].

1.3.4.2.1 ARGET mechanism

In the mechanism for ARGET ATRP, shown in figure 1.10 [78], an excess of reducing agent is used to regenerate the Mt^{n+1} complex, typically Cu(II), continuously [84],[83]. The reducing agent reduces the Mt^{n+1} deactivating species to the Mt^{n} activating species which prolongs the life of the propagating chains and allows the reaction to reach higher conversion. This method prevents the reaction from slowing down or stopping as it avoids the build-up of Mt^{n+1} deactivating complex. The reducing agent's selection is the key to successful ARGET as it should continuously regenerate the activator while avoiding any side reactions [84].

1.3.4.2.2 Reducing agent

The most commonly used reducing agents for ARGET and AGET include ascorbic acid, tin(II) 2-ethyl hexanoate, glucose, hydrazine, and phenols [49],[50]. The regeneration of the higher oxidation state complex by the reducing agent tin(II) 2-ethyl hexanoate ($Sn(EH)_2$) is shown in equation 1.3.

$$Sn(EH)_2 + 2Cu^{II}X_2/Ligand \rightleftharpoons Sn(EH)_2X_2 + 2Cu^{I}X/Ligand \qquad \text{eq. 1.3}$$

The excess reducing agent allows polymerization to reach higher conversion and molecular weights while retaining chain-end functionality as the catalyst induced side reactions are eliminated [83]; it also helps scavenge and remove the oxygen from the process [84].

1.3.4.2.3 Ligand

Expensive ligands, such as tris((N,N-dimethyl-amino)-ethylamine (Me6-TREN) and tris(2-pyridylmethyl)amine (TPMA) [95], are commonly used in ARGET ATRP due to their high activity and ability to form stable metal complexes [96], [97]. These ligands form complexes that have equilibrium constants several magnitudes higher than other lower activity ligands. As the expensive ligands are problematic when it comes to the industrialization of the process, other cheaper ligands with lower activity have been investigated for application in ARGET ATRP. These include N,N,N′,N″,N″-pentamethyldiethylenetriamine (PMDETA), diethylenetriamine (DETA), and 2,2'bipyridine (bpy) [98]. The main drawback associated with ARGET is that in order to maintain control over the polymerization process a high excess of ligand is required. The ligand must be at least three to ten times in molar excess to achieve control over the polymerization by stabilizing the metal complex and protecting it from side reactions. Possible destabilizing side reactions including monomer complexation with catalyst and complexation of catalyst with Lewis acids formed from the reduction mechanism [30],[49]. Moreover, the excess ligand not only complexes and stabilizes the metal complex, but also acts as a reducing agent that aids in the success of ARGET ATRP [92]. PMDETA, used in high excess, was successfully employed in ARGET ATRP; some examples include the synthesis of poly(methyl methacrylate) [99] and amphiphilic block copolymers [96]. Moreover, recent work done by Cunningham et al showed the success of ARGET ATRP with a stoichiometric ratio of ligand (TPMA) to copper [93].

1.3.4.2.4 Catalyst concentration

One of the main advantages of ARGET ATRP is that the catalyst concentration, typically copper, can be reduced to trace amounts of several ppm of the monomer concentration. Control over the polymerization reaction is maintained due to the regeneration of the activating species by the reducing agent; the reducing agent will compensate any loss of Cu(I) species in termination by maintaining the concentration of the activator species through constant regeneration. However, the concentration of catalyst cannot simply be reduced drastically as a minimum concentration of copper must be present to ensure the reaction proceeds. The ratio of the catalyst to the initiator is an important factor that determines the minimum copper concentration requirement. Under typical ATRP conditions, as much as 1-10% of chains terminate [84]; therefore, the amount of copper initially added to the system should not be below 10mol% of the initiator to avoid complete consumption of copper if 10% of the chains terminate [84],[100]. Thus, the required copper concentration is influenced by the amount of terminating chains which depends on the radical concentration and rate of termination according to equation 1.4 [100]. Note that k_t is the rate constant for termination, $[P^\bullet]$ is the concentration of propagating radicals and t is the time below.

$$-\Delta[\mathrm{Cu}] = [P_t] = k_t[P^\bullet]^2 t \qquad \text{eq. 1.4}$$

The stability of the metal complex also plays a role in controlling the reaction as it influences the ratio of copper to initiator [96]. The target degree of polymerization (DP) is another factor that affects the minimum concentration of catalyst necessary. A study done by Matyjaszewski and co-workers on the influence of ligand and DP of the copper concentration requirement shows that at higher DP, lower catalyst concentration is required [95]. It also shows that for the same target DP,

a higher concentration of the copper catalyst is required when using lower activity ligands such as PMDETA and DETA [95].

ARGET was successfully employed in the synthesis of poly(butyl acrylate) with 50 ppm of Cu(II) with a target DP of 500, whereas a higher concentration of 500 ppm was required to achieve the same Đ with a DP of 50 [96]. In another work, the concentration of copper was successfully reduced to only 10 ppm of copper in the polymerization of styrene using ARGET ATRP [100]. Much progress has been accomplished by ARGET ATRP, and it has proven to be an effective, robust, and environmentally friendly ATRP method. New advances with lower ligand requirements and trace amounts of copper catalyst used show the industrial viability of this method and its potential to be adopted on an industrial scale. ARGET ATRP demonstrated good control and successfully synthesized well-defined colorless polymers using only trace amounts of the copper catalyst [94],[101],[102].

It can be concluded that ATRP is a very attractive and industrially viable method for making polymers with well-defined polymers structures with controlled architectures and properties. The advancements in ATRP and the different initiation methods developed have allowed the synthesis of controlled polymer structures with only trace amounts of catalysts, thus eliminating the need for purification and post-polymerization treatment. This chapter reviewed exhaustively the advancements in ATRP and the various ATRP initiation methods revealing the vast literature and rapid discoveries making ATRP even more suitable for industrial applications. I will use traditional ATRP and the reduced catalyst method ARGET ATRP in my thesis work to take advantage of some of these advances to to produce cutting-edge polymeric coatings that meet specific properties and criteria as set out by the industrial partner.

2. Research objectives & Methodology

2.1 Research objectives

The objective of the thesis work is to produce advanced polymeric coatings that meet specific criteria for adhesion, anti-flammability, and shelf-life as dictated by the industrial partner's benchmark. Specifically, the polymer will be synthesized via atom transfer radical polymerization (ATRP) as the narrow molecular weight distribution resulting from this polymerization will result in low viscosity solutions, which facilitates spraying or deposition of the coating. The specific objectives for this thesis are as follows:

1) Apply traditional ATRP to synthesize homo/copolymers of the commercial bio-sourced methacrylic monomers (isobornyl methacrylate (IBOMA) and an alkyl methacrylate with average chain length of 13 CH_2 units (C13MA) as a viable coatings formulation with narrow molecular weight distribution for low viscosity solutions.
2) Predict copolymer composition via reactivity ratio and evaluate the thermal properties of the resulting copolymers as coating performance depends on resin glass transition temperature.
3) Reduce concentration of ATRP metal catalyst to ppm levels to eliminate discolouration while maintaining high control over polymerization and narrow molecular weight distributions.
4) Evaluate advanced ATRP methods such as activators regenerated by electron transfer (ARGET) ATRP, to further reduce and even eliminate the metal catalyst used in order to have an environmentally friendly controlled polymer synthesis with minimal post-polymerization purification requirements.

5) Use ARGET ATRP to synthesize colorless terpolymers with additional curing functionality to enhance coating durability. Compare the coatings' appearance and adhesion to previous coatings derived from nitroxide mediated polymerization (NMP) and establish an alternative coating technology via controlled radical polymerization for aircraft interiors.

2.2 Methodology

Initially, traditional ATRP was used to synthesize homopolymers of isobornyl methacrylate (IBOMA) and methacrylic ester 13 (C13MA). Statistical copolymers poly(IBOMA-*stat*-C13MA) with different IBOMA:C13MA ratios were synthesized to examine the kinetics and the reactivity ratios of IBOMA/C13MA polymerizations. The reactions were conducted at 80°C with the bromine-based initiator 4-(2-isobutyrate ethyl morpholine bromide) (ME-Br), copper (I) bromide, and PMDETA as a catalyst/ligand complex in diphenyl ether. The conversion was determined gravimetrically and molecular weight distribution was measured using gel permeation chromatography (GPC); plots of number average molecular weight versus conversion were constructed to assess the chain end fidelity (linear plots suggest an active polymerization center). Chain-end fidelity was tested by a chain-extension experiment using the previously formed polymer as the macroinitiator for a second batch of monomer. Differential scanning calorimetry (DSC) and thermogravimetric analysis (TGA) studies were performed to study thermal stability and transitions of the polymers. Post-polymerization treatments and purification were performed to remove the metal catalyst residue in the polymer. Finally, the incorporation of other monomers with useful functional groups to the IBOMA/C13MA system was done; glycidyl methacrylate (GMA) was added to impart epoxy functionality to the resin via the synthesis of statistical

terpolymers of IBOMA/C13MA/GMA. The epoxy could be used in subsequent curing reactions when coated.

A reduced catalyst ATRP method, activator regenerated by electron transfer (ARGET ATRP), is a more environmentally friendly ATRP method that can efficiently produce tailor-made polymer structures with only ppm amounts of copper, unlike traditional ATRP. ARGET ATRP was explored for the homopolymerization of IBOMA initially. Different reaction parameters, including temperature, type of initiator and solvent, and concentration of solvent, catalyst, ligand, and reducing agent were all investigated. The reaction parameters were optimized to obtain a well-controlled polymerization with a linear increase in number average molecular weight versus conversion, a hallmark of truly living polymerizations. The optimized reaction conditions were then utilized to synthesize homopolymers of C13MA and statistical copolymers poly(IBOMA-stat-C13MA) with different IBOMA:C13MA ratios. Polymers were prepared for use in varnish formulations in which the epoxy-functional monomer glycidyl methacrylate (GMA) was incorporated to enhance the adhesive properties of the resin. Resin solutions were prepared, and coatings were made and applied with a bench-top film applicator and compared to benchmark tests.

2.2.1 Materials

Isobornyl methacrylate (IBOMA, >99%) and a mixture of alkyl methacrylates with an average chain length of 13 carbons (C13MA, >99%) were obtained from Evonik. Glycidyl methacrylate (GMA , >99%) was obtained from Sigma-Aldrich. The monomers were purified to remove the inhibitor by passing through a column of basic alumina (Brockmann, Type 1, 150 mesh, Sigma-Aldrich) mixed with 5 wt % calcium hydride (90–95% reagent, Sigma-Aldrich) and then stored in

a sealed round bottom flask under a head of nitrogen in a refrigerator until needed. Ethyl α-bromoisobutyrate (EBiB 98%), copper (I) bromide (99%), copper (II) bromide (99%), tin(II) 2-ethyl hexanoate (92.5-100%), and silica gel (Davisil grade 633, pore size 60 Å, 200-425 mesh particle size) were all obtained from Sigma-Aldrich and used as received. Toluene (≥99%), tetrahydrofuran (THF, 99.9% HPLC grade), methanol (MeOH, ≥99%), and dimethylformamide (DMF, 99.8%) were obtained from Fisher Scientific and used as received. The deuterated chloroform ($CDCl_3$, ≥99%) used as a solvent for proton nuclear magnetic resonance (^1H NMR) was purchased from Cambridge Isotopes Laboratory. Priamine 1075-LQ-(GD) dimer diamine, used as a crosslinker in the coating formulation, was obtained from Croda. 4-(2-isobutyrate ethyl morpholine bromide) (ME-Br), the initiator for methacrylic homopolymers, was previously prepared according to the following procedure adapted from the literature [1,2].

2.2.2 Synthesis of Homopolymers and Copolymers of IBOMA and C13MA by Atom Transfer Radical Polymerization (ATRP).

For the homopolymerization of IBOMA, in a 100 mL round bottom three-necked reactor flask was added 0.17 g (0.66 mmol) of ME-Br initiator along with 14.81g (0.066 mol) of the previously purified IBOMA monomer so that the target number average degree of polymerization (DP) was 100 based on the monomer to initiator ratio; this corresponds to a target molecular weight (Mn=22.3 kg/mol). In a separate sealed flask was added 0.047 g (0.33 mmol) Cu(I)Br, 0.114 g (0.66 mmol) of the ligand (pentamethyl diethylenetriamine, PMDETA) and 14.81 g of diphenyl ether solvent. The diphenyl ether has to be warmed gently in order to melt it and facilitate removal from the bottle. A nitrogen purge was applied for 30 minutes to each flask to remove any dissolved oxygen. The contents of the flask containing Cu(I)Br/PMDETA/solvent were transferred by cannula under pressure to the reactor. The reactor was heated to 80^{o}C at a rate of about 5^{o}C/min.

In most cases, the greenish solutions became progressively browner, as the temperature increased to above 50^{o}C, indicating oxidation of some of the copper species. When the temperature reached 80^{o}C, the time of reaction was taken as zero. Samples were taken periodically and quenched in non-solvents to precipitate the polymer. After 60 minutes, the heating was stopped, and the reactor contents were poured into a non-solvent to precipitate the desired polymer. For the systems initiated by ME-Br, poly(IBOMA) samples were precipitated in methanol.

The product was filtered under vacuum and then re-dissolved in tetrahydrofuran (THF). Silica gel was then added to remove the catalyst. The silica became blue due to catalyst absorption and was filtered. The filtrate containing the polymer dissolved in the solvent was re-precipitated with the appropriate non-solvent, which was methanol in this case. The product was then dried in a vacuum oven overnight. The dried samples were then weighed to determine the gravimetric yield and also analyzed by gel permeation chromatography (GPC) to determine the molecular weight distribution. For the specific sample cited here, the P(IBOMA)-ME-Br conversion was 73%. The molecular weight of the P(IBOMA) using gel permeation chromatography (GPC) according to poly(methyl methacrylate) standards in tetrahydrofuran (THF) was number average molecular weight M_n = 17.7 kg/mol, weight average molecular weight M_w = 22.6 kg/mol and $Đ = M_w/M_n$= 1.28. The same procedure was followed for the copolymerization of IBOMA and C13MA; the experimental conditions for the synthesis of the homopolymers and copolymers of IBOMA and C13MA are summarized in table 2.1, and an overview of the copolymer synthesis of IBOMA and C13MA is shown in figure 2.1

Table 2.1 The feed concentrations for the homopolymers and copolymers of IBOMA and C13MA with different ratios of IBOMA and C13MA synthesized by traditional ATRP using ME-Br initiator in 50wt% diphenyl ether at 80°C.

Experiment ID	$[ME\text{-}Br]_0$ (M)	$[Cu(I)Br]_0$ (M)	$[PMDETA]_0$ (M)	$[IBOMA]_0$ (M)	$[C13MA]_0$ (M)	f_0[a] IBOMA	Temp (°C)
IB_C13MA_1	0.024	0.011	0.023	2.431	0.000	1	80
IB_C13MA_2	0.024	0.011	0.023	2.160	0.240	0.9	80
IB_C13MA_3	0.025	0.011	0.024	1.637	0.702	0.7	80
IB_C13MA_4	0.025	0.012	0.024	1.141	1.141	0.5	80
IB_C13MA_5	0.025	0.012	0.024	0.668	1.558	0.3	80
IB_C13MA_6	0.026	0.012	0.025	0.217	1.956	0.1	80
IB_C13MA_7	0.026	0.012	0.025	0.000	2.148	0	80

a. The initial molar fraction of IBOMA in the initial feed

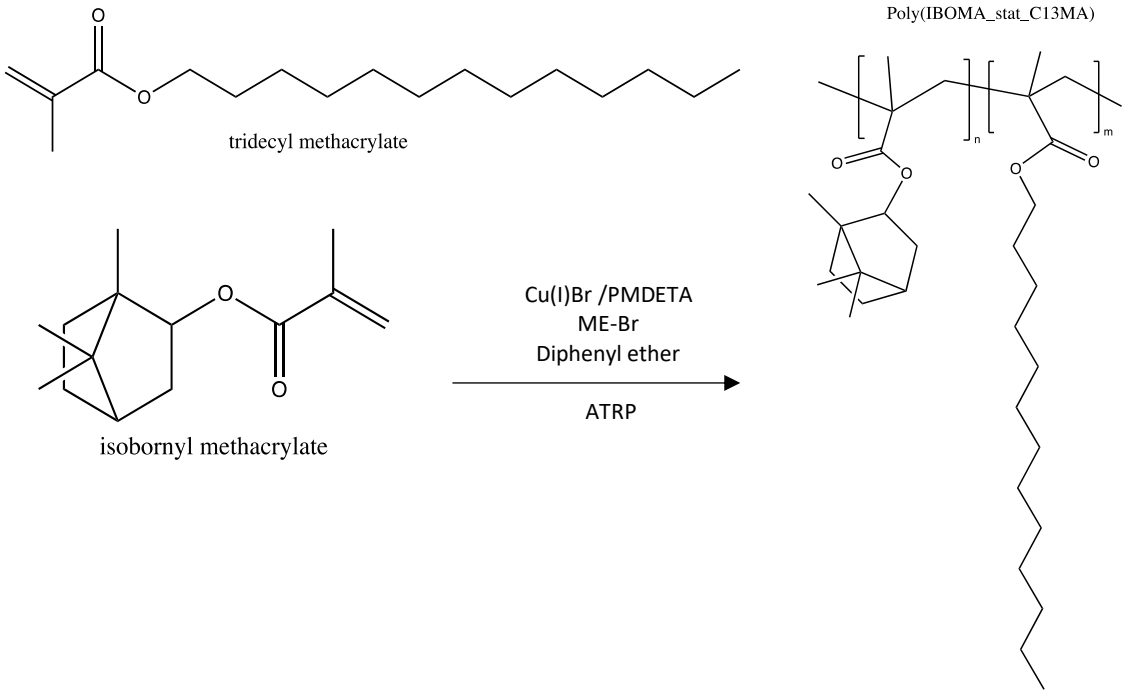

Figure 2.1 Co-polymerization of IBOMA and C13MA via traditional ATRP with Cu(I)Br, PMDETA, and diphenyl ether at 80°C.

2.2.3 Synthesis of Homopolymers by Activator Regenerated by Electron Transfer Atom Transfer Radical Polymerization (ARGET ATRP).

An example of the ARGET reaction given below is the homopolymerization of isobornyl methacrylate using the ethyl α-bromoisobutyrate (EBiB) initiator; a summary of the experiments performed is given in table 2.2. In a 100 mL round bottom three-necked reactor flask was added 0.12 g (0.62 mmol) of EBiB initiator along with 13.67 g (0.0615 mol) of the previously purified IBOMA monomer so that the target number average degree of polymerization was 100 based on the monomer to initiator ratio; this corresponds to a target molecular weight (Mn=22.3 kg/mol). Then 3.4 mg (0.015 mmol) Cu(II)Br, 0.04 g (0.2 mmol) of the ligand (pentamethyl diethylenetriamine, PMDETA), 0.06 g (0.15 mmol) of $Sn(EH)_2$ reducing agent and 13.67 g of toluene solvent were added. A nitrogen purge was applied for 30 minutes to each flask to remove any dissolved oxygen. The reactor was heated to 80 ^{o}C at a rate of about 5°C/min. In most cases, the colorless solution became more opaque with a hint of a light blue color, as the temperature increased above 50 ^{o}C, indicating oxidation of some of the copper species. When the temperature reached 80^{o}C, the time of reaction was taken as zero. Samples were taken periodically and quenched in non-solvents to precipitate the polymer. After 60 minutes, the heating was stopped, and the reactor contents were poured into a non-solvent to precipitate the desired polymer. For the systems initiated by EBiB, P(IBOMA) samples were precipitated in methanol. The product was filtered under vacuum and then dried in a vacuum oven overnight at room temperature. The dried samples were then weighed to determine the gravimetric yield and also analyzed by gel permeation chromatography (GPC) to determine the molecular weight distribution. For the specific sample cited here, the P(IBOMA)-EBiB conversion was 97%. The molecular weight of the P(IBOMA) using gel permeation chromatography (GPC) according to poly(methyl methacrylate) standards in

tetrahydrofuran (THF) was number average molecular weight M_n = 20.6 kg/mol weight average molecular weight M_w = 35.0 kg/mol and $Đ = M_w/M_n$ = 1.65.

Table 2.2 Homopolymerization of IBOMA via ARGET ATRP experiments with variable conditions (solvent, reaction temperature, and reactants feed ratio).

Experiment ID	Temp (∘C)	Initiator	Ligand [PMDETA]	[$CuBr_2$] (ppm)	[PMDETA] /[$CuBr_2$]	Solvent	[Solvent]	Reducing agent [$Sn(EH)_2$]
AR_IB_1	90	ME_Br	0.009	250	10	DPE	1.420	0.0133
AR_IB_2	80	ME_Br	0.007	500	6	DPE	3.180	0.0089
AR_IB_4	80	ME_Br	0.018	500	15	toluene	5.867	0.0089
AR_IB_5	80	ME_Br	0.009	250	15	toluene	5.867	0.0091
AR_IB_6	90	ME_Br	0.009	250	15	toluene	5.867	0.0091
AR_IB_7	85	ME_Br	0.009	250	15	toluene	5.867	0.0091
AR_IB_8	75	ME_Br	0.009	250	15	toluene	5.867	0.0091
AR_IB_9	80	EBiB	0.009	250	15	toluene	5.867	0.0091
AR_IB_10	80	EBiB	0.009	250	10	toluene	5.867	0.0061
AR_IB_11	80	EBiB	0.018	500	10	toluene	5.867	0.0125

2.2.4 Synthesis of IBOMA/C13MA Copolymers and IBOMA/C13MA/GMA Terpolymers by ARGET ATRP

An identical reactor/condenser system and reactants feed ratio as for the synthesis of the homopolymers of IBOMA by ARGET ATRP described in the previous section was used to prepare the copolymers and terpolymers of IBOMA/C13MA and IBOMA/C13MA/GMA. The experimental conditions for the synthesis of the copolymers of IBOMA and C13MA are shown in table 2.3; similar to the IBOMA homopolymers, the copolymers were prepared with a target molecular weight of 22.3 kg/mol (corresponding to target DP=100 for poly(IBOMA)). The copolymers were synthesized via ARGET ATRP at 80°C with EBiB initiator in 50wt% toluene

solution with a feed ratio of $[EBiB]_0/[SnEH_2]_0/ [CuBr_2]_0 /[PMDETA]_0$ = 1/0.25/0.025/0.25. The monomer concentrations were calculated based on the target DP, moles of initiator, and the initial mole fraction of the respective monomers. Terpolymers of IBOMA/C13MA/GMA were also prepared according to the diagram shown in figure 2.2. Similarly, the terpolymers of IBOMA/C13MA/GMA were prepared with a target molecular weight of 22.3 kg/mol via ARGET ATRP at 80°C with EBiB initiator in 50wt% toluene solution with a feed ratio of $[EBiB]_0/[SnEH_2]_0/ [CuBr_2]_0 /[PMDETA]_0$ = 1/0.37/0.025/0.25; a summary of the experimental conditions is shown in table 2.4. The following example is given for the terpolymer ARG_IB_ C13MA_GMA. EBiB (0.12 g), IBOMA (5.47 g), C13MA (6.59 g), GMA (1.75 g), Cu(II)Br (0.0034g), and $Sn(EH)_2$ (0.09 g) were added to the reactor along with toluene (14.52 g). After purging with nitrogen for 30 min at room temperature, heating was started at 5°C/min up to the set point of 80°C. Purging was continued with nitrogen throughout the reaction. When the reactor temperature reached 80°C, the time was noted as the beginning of the polymerization. Samples were removed periodically with a syringe for the kinetic study until the end of experiments. The polymer was then precipitated into methanol. The methanol was then decanted to remove any unreacted monomer. This was followed by drying overnight in the fume hood, and then it was dried for 3-4 days in the vacuum oven at room temperature to remove any remaining solvent. The conversion was determined gravimetrically and the M_n and $Đ$ were characterized by GPC relative to PMMA standards at 40°C. For this particular experiment, the final conversion was 79% after 80 min with M_n =19 kg/mol and $Đ$ = 1.5. Further, the copolymerization of IBOMA and C13MA was studied in terms of reactivity ratios and the resulting glass transition temperatures of the copolymers.

Table 2.3 Experimental conditions for the synthesis of copolymers of IBOMA and C13MA via ARGET ATRP at 80°C in 50wt% toluene solution with a feed ratio of $[EBiB]_0/[SnEH2]_0/[CuBr2]_0$ /$[PMDETA]_0$ = 1/0.25/0.025/0.25.

Experiment ID	Temp (°C)	$f_{IBOMA,0}$[a]	Cu(II)Br (ppm)[b]
AR_10_IB	80	1	250
ARG_10_IB_C13MA_70_30	80	0.7	250
ARG_10_IB_C13MA_30_70	80	0.3	250
ARG_10_C13MA_100	80	0	250

a. The initial molar fraction of IBOMA in the initial feed.
b. The amount of copper was calculated on a molar basis as the ratio of the concentration of catalyst to monomer reported in ppm, ex: [Cu(II)Br]:[IBOMA]=250 ppm.

Table 2.4 Experimental conditions for the synthesis of terpolymers of IBOMA/C13MA/GMA via ARGET ATRP at 80°C in 50wt% toluene solution with a feed ratio of $[EBiB]_0/[SnEH2]_0/[CuBr2]_0$ /$[PMDETA]_0$ = 1/0.37/0.025/0.25.

Experiment ID	Temp (°C)	$f_{0.IBOMA}$[a]	$f_{0.C13MA}$[a]	$f_{0.GMA}$[a]	Mn_{target} (kg/mol)	Cu(II)Br [b] (ppm)
AR_IB_C13MA_GMA_1	90	0.4	0.4	0.2	22.3	250
AR_IB_C13MA_GMA_2	80	0.4	0.4	0.2	22.3	200
AR_IB_C13MA_GMA_3	80	0.4	0.4	0.2	12.0	250

a. The initial molar fraction of monomers in the initial feed.
b. The amount of copper was calculated on a molar basis as the ratio of the concentration of catalyst to monomer reported in ppm.

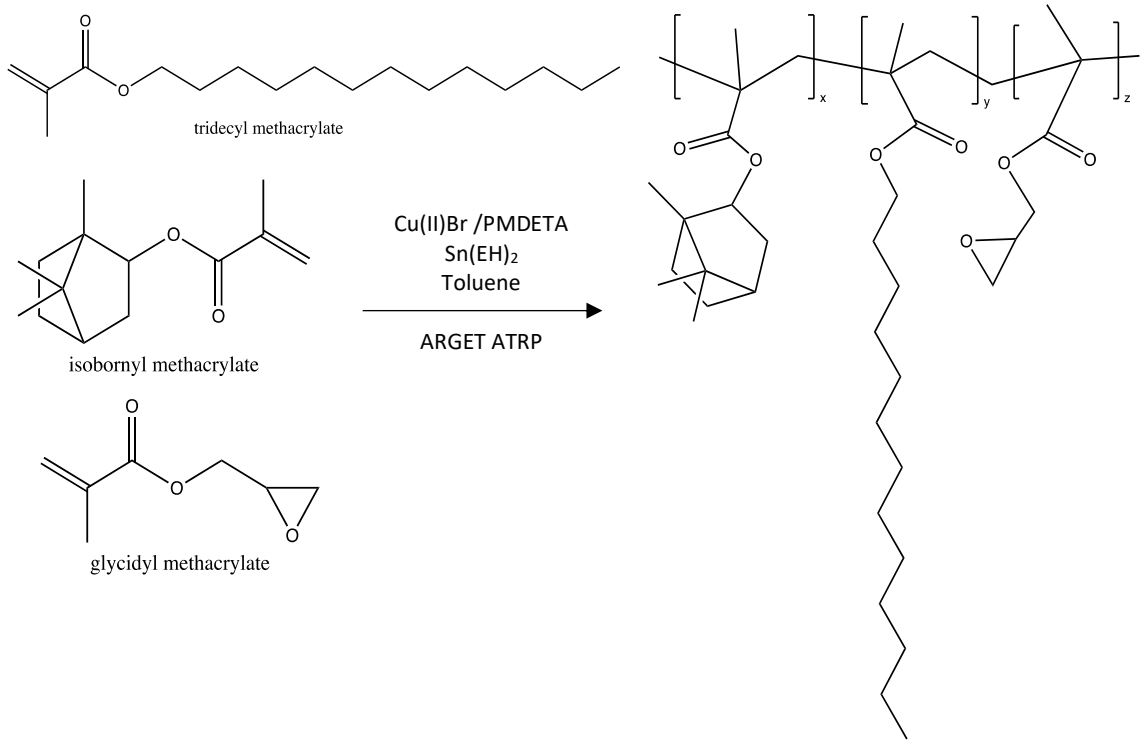

Figure 2.2 The synthesis of terpolymers of IBOMA/C13MA/GMA with Cu(II)Br, PMDETA, and EBiB via ARGET ATRP at 80°C.

2.2.5 Preparation of the Coating Formulation

The acrylic resin used in the coating formulations was based on the bio-based methacrylate monomers IBOMA and C13MA and the epoxy-functional monomer glycidyl methacrylate (GMA). Poly(IBOMA) has a high glass transition temperature and thus imparts hardness and strength to the resin, whereas poly(C13MA) has a low glass transition temperature which enhances the resin's flexibility. GMA is the epoxy functionality added to the resin that will help with adhesion, cross-linking and curing of the coating. ARGET ATRP was used to broaden the IP portfolio of the varnish formulation and use more widely available components. However, benchmarks made from NMP chemistry used by previous students in this project were synthesized first to ensure the composition for ATRP was acceptable. Resins made by ARGET ATRP were then made to match those by NMP as closely as possible, with the intent of matching the properties. Therefore, here the coatings made by NMP were evaluated initially.

In NMP, acrylonitrile (AN) is used as the controlling comonomer. Hence, when preparing the polymer resins, different ratios of the four monomers, C13MA, IBOMA, GMA, and AN were explored in order to determine the optimal composition that meets adhesion and impact strength requirements as set out by the industrial sponsor. The glass transition temperature T_g of the final polymer depends on the ratio of monomers and their respective glass transition temperatures, where the resultant glass transition temperature is bound between the lowest and the height glass transition temperature of the constituent monomers, according to the Fox equation (equation 2.1) [105]:

$$1/T_{g_{polymer}} = \sum w_i/T_{g_i} \qquad \text{eq 2.1}$$

where w_i and T_{gi} and the mass fraction and glass transition temperature respectively of the component i. Sample calculation for the copolymers' theoretical glass transition temperatures is shown in table 2.5.

Table 2.5 Sample calculation for the theoretical glass transition temperature of an IBOMA/C13MA/GMA terpolymer.

	C13MA	*IBOMA*	*AN*	*GMA*	*Tg Polymer*
Initial mole fraction	0.25	0.25	0.10	0.40	
Mass fraction	0.36	0.30	0.03	0.31	
Tg (°C)	-44	110	95	72	27
Tg (K)	229.15	383.15	368.15	345.15	300

Different terpolymers of IBOMA/C13MA/GMA were prepared with various glass transition temperatures varying from 17-40 °C as shown in table 2.6. Polymers were synthesized via NMP with 10% acrylonitrile (AN) as the controlling comonomer at 90°C in 50wt% dioxane solvent and BlocBuilder(BB) as the initiator.

Table 2.6 Terpolymers of IBOMA/C13MA/GMA with varying glass transition temperatures prepared via NMP with 10% acrylonitrile (AN) as the controlling comonomer at 90°C in 50wt% dioxane solvent and BlocBuilder(BB) as the initiator.

Polymer ID	$f_{0.IBOMA}$[a]	$f_{0.C13MA}$[a]	$f_{0.GMA}$[a]	*Tg (°C)*
M1	0.4	0.4	0.1	12
M3	0.35	0.35	0.2	16
M4	0.25	0.25	0.4	26

a. The initial molar fraction of monomers in the initial feed.

The optimal formulation, which gave a nice appearance with a smooth surface and met the criteria for adhesion and hardness, was found to be the one with T_g of around 16°C with 20% GMA and equal molar equivalents of IBOMA and C13MA. This formulation of the terpolymers of IBOMA/C13MA/GMA was then prepared using ARGET ATRP as shown earlier in table 2.4 earlier.

To prepare the coatings, the resin was dissolved in toluene in a 30wt% solution. The dimer diamine crosslinker (Priamine 1075) was then added to the solution and mixed well. The solution was then blade coated on wood samples and left to dry under the fume hood. The samples were assumed to be dry when they were dry to touch. Impact tests were then performed on the dry samples to assess and compare the coating formulations.

2.2.6 Characterization

The overall monomer conversion X was determined gravimetrically according to the formula shown in equation 2.2:

$$Conversion\ X = \frac{m_{polymer\ obtained}}{m_{monomer\ added}} = \frac{m_{dry\ sample} - m_{tare\ vial}}{m_{wet\ sample} - m_{wet\ vial}} \qquad \text{eq. 2.2}$$

The M_n and Đ were evaluated by GPC (Waters Breeze) with HPLC grade THF as a mobile phase and a differential refractive index detector (RI 2414). The GPC was equipped with three Waters Styragel HR columns (HR1 with a molecular weight measurement range of $1\times10^2 - 5\times10^3$ g/mol, HR2 with a molecular weight measurement range of $5\times10^2 - 2\times10^4$ g/mol, and HR4 with a molecular weight measurement range of $5\times10^3 - 6\times10^5$ g/mol), and a guard column was used. A mobile phase flow rate of 0.3 mL/min was applied, and the columns were heated to 40°C during the characterization. The molecular weights were determined by calibration with linear narrow molecular weight distribution PMMA standards at 40°C without applying the Mark–Houwink–Sakurada equation as the MHS constants for P(IBOMA) and P(C13MA) are not available.

2.2.6.1 Impact test

The impact test can be used to determine the stone-chip resistance of the coating; it provides a good estimate of adhesion as it evaluates the coating's resistance to cracking and flexibility [20], [106]. A dynamic deformation is induced by an abrupt dropping of a spherical indenter onto the coated panel in the falling weight impact test. The apparatus, shown in figure 2.3, consists of a vertical guide tube with a fixed scale for the drop height. The weight goes down vertically perpendicular to the surface of the sample placed on the base plate [106].

Figure 2.3 Falling weight impact test apparatus.

The energy of deformation is equal to the height from which it was dropped multiplied by the mass of the falling weight. Using this apparatus, a classification test is performed in which the minimum height to cause deformation (chipping) of the coating is determined. Then, the drop height is increased gradually until a crack or peeling of the coating is observed [6].

Several parameters can affect the adhesion performance, including the type of resin, thickness, and dryness of the coating. The thickness of the coating film has a significant impact on the performance of the coating in terms of adhesion and cracking. In thick films, a larger area is impacted than thin films because stress is distributed across a larger area. In thin films, the detachment is concentrated in the region on which the impact hits the surface [20]. The results of the impact testing are summarized later in the research findings section. Pictures of the coated wood samples after impact testing are shown in figure A.5 in the appendix.

3. Research findings: Results and Discussion

3.1 Traditional ATRP: Kinetics and Characterization of IBOMA/C13MA Copolymers

3.1.1 Study of the Kinetics

Homopolymers and copolymers of IBOMA and C13MA were prepared using traditional ATRP with the morpholine-based initiator 4-(2-isobutyrate ethyl morpholine bromide) (ME-Br). In all reactions, the diphenyl ether solvent was in 50 wt% concentration with monomer and the polymerization temperature was 80°C. The experimental results for poly(IBOMA), poly(C13MA), and poly(IBOMA-*stat*-C13MA) production by normal ATRP are summarized in table 3.1. Throughout the reaction, samples were taken periodically for the kinetic study and the conversion at different reaction times was measured gravimetrically. The start of the reaction (time zero) was considered when the reaction mixture reached the set temperature. Starting at time zero, samples were taken every 20 minutes until the solution became very viscous and the reaction is stopped; for reactions with a shorter time frame, a sample after the first 10 minutes was also taken. Reaction time was steady at 80 minutes across the polymerization reactions of the different copolymers of IBOMA and C13MA, except for the homopolymer of IBOMA which was only 50 minutes due to the fast polymerization rate of IBOMA. Kinetic plots of monomer conversion (X) in the form of $\ln[1/(1 - X)]$ versus time show good linear fits over the time periods studied for the different IBOMA/C13MA compositions; figure 3.1 shows the kinetic plots for the traditional ATRP experiments. The slopes of the semi-logarithmic plot of conversion with time provide an estimate of the apparent rate constant in $k_p[P\bullet]$, where k_p is the propagating rate constant and $[P\bullet]$ is the concentration of propagating macroradicals. The slopes were measured using the four points obtained in the kinetic study which showed linear correlation. The IBOMA-rich compositions show higher slopes than the C13MA-rich compositions, indicating a faster polymerization rate for

IBOMA than C13MA. For example, the value of $k_p[P\bullet]$ for the IBOMA homopolymer IB_C13MA_1 ($4.05x10^{-4}$ s^{-1}) is higher than that of the C13MA homopolymer IB_C13MA_7 ($1.73x10^{-4}$ s^{-1}). This result is in agreement with previously reported data for the polymerization of IBOMA and C13MA by nitroxide mediated polymerization (NMP) done in our research group where it was also found that IBOMA had a faster polymerization rate than C13MA [52].

Samples obtained throughout the homopolymerization and copolymerization reactions of IBOMA and C13MA; were analyzed by GPC (relative to PMMA standards at 40°C in THF) to determine the number average molecular weight (M_n) and dispersity (Đ) of the polymer chains. The conversion was calculated gravimetrically; the samples were precipitated in an anti-solvent, methanol, in order to obtain a dry polymer sample to be weighed for conversion. The solvent used in the polymerization was DPE, which is solid at room temperature, is hard to remove and may be still present in the samples after precipitation. Therefore, the conversion samples were dissolved and reprecipitated twice to ensure all solvent and unreacted monomers are removed. The M_n vs. conversion graphs for all the different copolymers were constructed, and the kinetic plots are displayed in figure 3.2. The kinetic plots show a steady increase in the molecular weight as the reactions progressed indicating well-controlled ATRP reactions; a well-controlled ATRP process exhibits a linear increase of molecular weight with the monomer conversion and narrow molecular weight distribution (Đ). The data obtained from the copolymerization of IBOMA and C13MA is linear with high conversions of up to 99% and low molecular weight distribution (Đ = 1.16-1.52). Although the samples were dissolved and reprecipitated to ensure complete removal of the solvent, some solvent may have remained in the dry polymer samples and affected the conversion results. It was observed that the copolymerization reactions of IBOMA with C13MA at nearly equal ratios (IB_C13MA_– IB_C13MA_5) displayed higher conversions compared to the those obtained from

the homopolymerization of the individual monomers and the IBOMA and C13MA rich copolymers (IB_C13MA_2, and IB_C13MA_6). Moreover, it was observed that in the case of those copolymers, the target molecular weight was exceeded notably (IB_C13MA_5 and IB_C13MA_6). An analysis of the M_n vs. conversion graphs showed that points obtained were close to the theoretical value shown in the predicted line (the predicted line assumes the polymer reaches the target molecular weight Mn = 22.3kg/mol at 100% conversion). However, two data sets of C13MA rich copolymers (IB_C13MA_5 and IB_C13MA_6) deviated notably from the predicted line. The higher values of molecular weight could be due to inefficient initiation of the system [107]. Moreover, the GPC results for the C13MA rich compositions may be inaccurate as the molecular weights are measured relative to PMMA standards, and the hydrodynamic volume of poly(C13MA) may be quite different in solution.

The dispersity (Đ = Mw/Mn) represents the breadth of the molecular weight distribution; in a well-controlled polymerization reactions the Đ is low indicating a narrow molecular weight distribution. In typical ATRP reactions, Đ is expected to decrease with monomer conversion [76]; on the contrary, experimental results show a slight increase in the Đ at very high conversions. In the case of the homopolymers and copolymers of IBOMA and C13MA, the Đ values obtained were relatively low, indicating well-controlled reactions. Đ varied between 1.2-1.3 with conversion as shown in figure 3.3, with slightly increasing Đ typically at the last 1-2 data points at the highest conversions. However, in the case of the first copolymerization reaction (IB_C13MA_2), the Đ was low at low conversion (Đ~1.2) and then a high jump as observed as conversion increased yielding a high final Đ value (Đ=1.53). The value of Đ depends on the concentration of the activator and deactivator species, and the fraction of terminated chains [76]. The increase in the Đ

at high conversion is due to the unavoidable termination reactions that are more significant at higher conversion, as is the case with any monomer [76].

Table 3.1 Experimental results for the homopolymerization and copolymerization for different ratios of IBOMA and C13MA.

Experiment ID	*T °C*	*t (min)*	$f_{IBOMA,0}$[a]	F_{IBOMA}[b]	*Conversion X (%)*	*Mn (kg/mol)*[c]	*Đ*[c]
IB_C13MA_1	80	50	1.00	1.00	73	17.7	1.28
IB_C13MA_2	80	80	0.90	0.91	80	17.0	1.53
IB_C13MA_3	80	80	0.70	0.68	98	21.6	1.25
IB_C13MA_4	80	80	0.50	0.47	99	24.5	1.21
IB_C13MA_5	80	80	0.30	0.30	95	28.8	1.31
IB_C13MA_6	80	80	0.10	0.09	84	31.6	1.24
IB_C13MA_7	80	80	0.00	0.00	58	19.1	1.35

a. The initial molar fraction of IBOMA in the initial feed.
b. The final molar fraction of IBOMA in the terpolymer (F_{IBOMA}) as determined by 1H NMR in CDCl3.
c. The final product's number average molecular weight (Mn) and dispersity (Đ) as determined by GPC with PMMA standards at 40°C in THF.

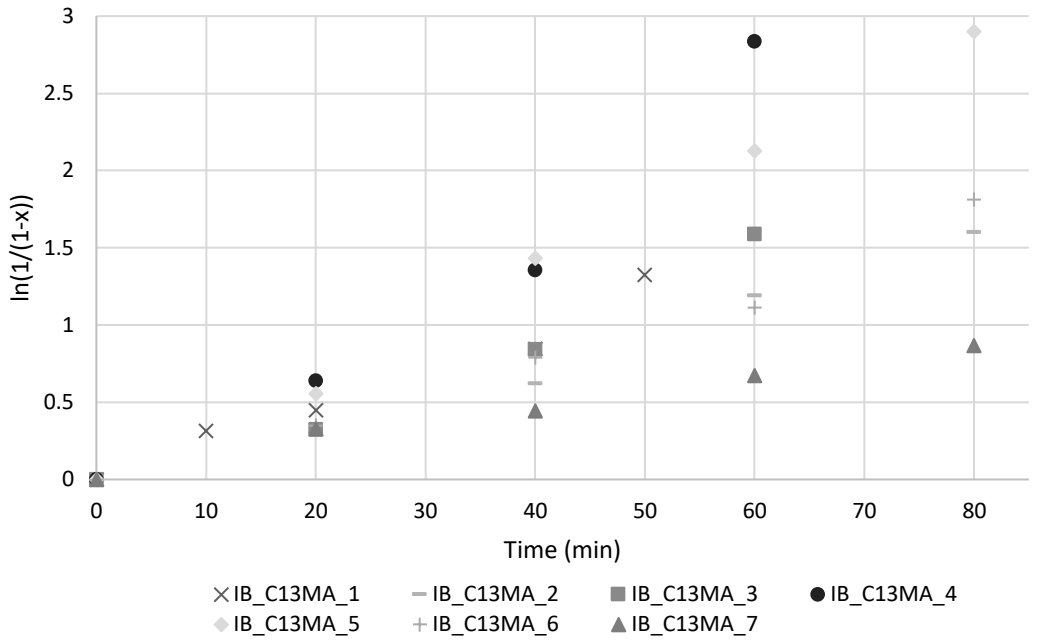

Figure 3.1 Kinetic plot for homopolymers, and copolymers with different ratios of IBOMA and C13MA by standard ATRP at 80°C with ME-Br initiator in diphenyl ether solvent.

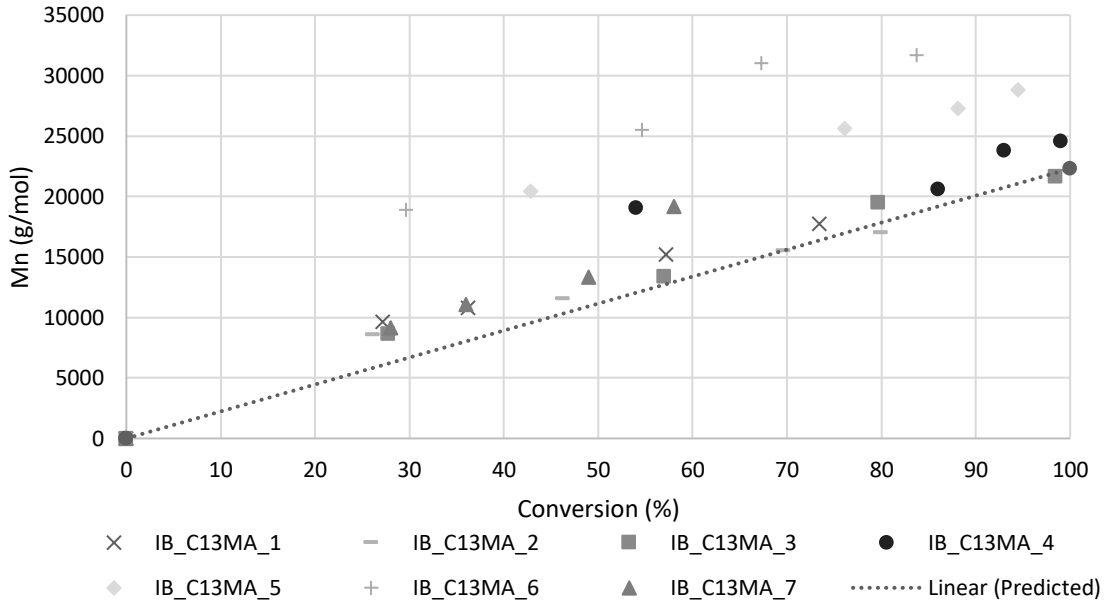

Figure 3.2 Plot of number average molecular weight and conversion for homopolymers and copolymers with different ratios of IBOMA and C13MA by standard ATRP at 80°C with ME-Br initiator in diphenyl ether solvent.

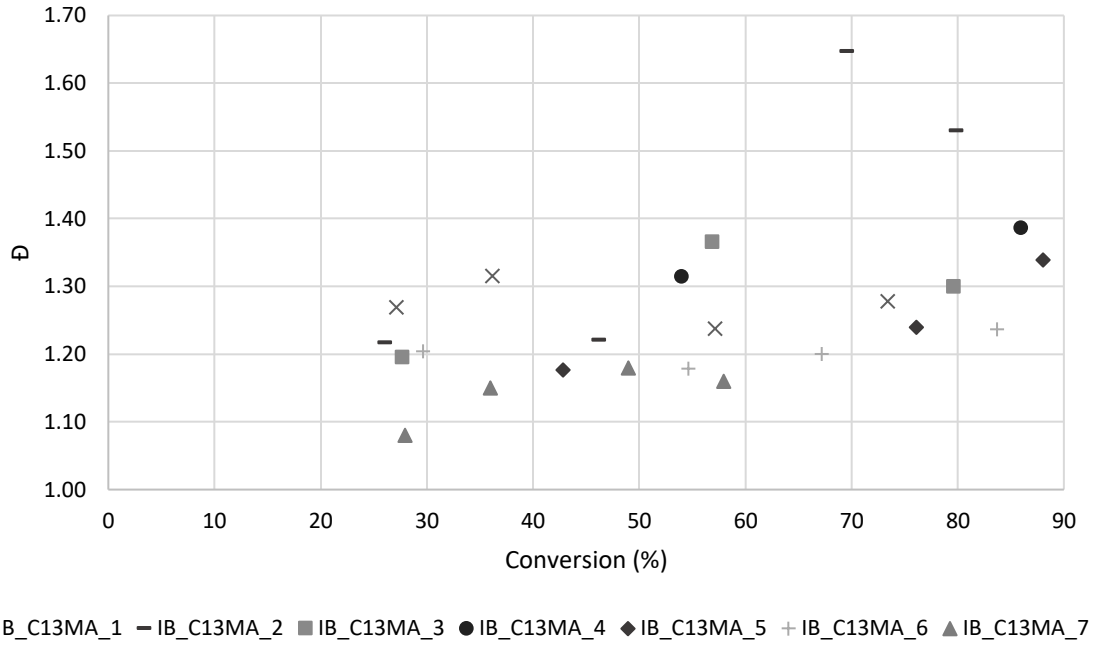

Figure 3.3 Đ and conversion for homopolymers and copolymers with different ratios of IBOMA and C13MA by standard ATRP at 80°C with ME-Br initiator in diphenyl ether solvent.

3.1.2 Determination of Reactivity Ratios

The homopolymers and five different ratios of copolymer of IBOMA and C13MA were prepared by normal ATRP. The final polymer samples were analyzed by ^{1}H NMR to check the final polymer composition (F_{IBOMA} and F_{C13MA}); the results are reported in table 3.1. For example, the copolymer (IB_C13MA-3) had an initial monomer feed ratio of $f_{IBOMA,0} = 0.7$ and $f_{C13MA,0} = 0.3$. A low dispersity blue-tinged polymer was obtained (M_n = 21.6 kg/mol, Đ =1.25); this sample was analyzed using ^{1}H NMR to obtain the final composition of the copolymer. The ^{1}H NMR spectra for (IB_C13MA_3) after 80 minutes of starting the reaction was indexed as follows: ^{1}H NMR (CDCl3, ppm),δ: 6.10-6.14 (m,1 H^{C13MA}), 6.07-6.10 (m,1 H^{IBOMA}), 5.55-5.57 (m,1 H^{C13MA}), 5.51-5.55 (m,1 H^{IBOMA}), 4.29-4.46 (d,1 $H^{P(IBOMA)}$), 3.83-4.06 (s,2 $H^{P(C13MA)}$), 3.75-3.80 (m, 2 $H^{P(C13MA)}$ + 1 $H^{P(IBOMA)}$), 1.93-1.98 (m, 3 H^{IBOMA} + 3 H^{C13MA}), 1.68-1.79 (m, 2 $H^{P(IBOMA)}$+ 2 $H^{P(C13MA)}$), 1.51-

1.68 (m, 7 $H^{P(IBOMA)}$+ 2 $H^{P(C13MA)}$), 1.21-1.41 (m, 3 $H^{P(IBOMA)}$+ 23 $H^{P(C13MA)}$ + 22 H^{C13MA}), 1.07-1.17 (m, 9 $H^{P(IBOMA)}$),1.01-1.06 (s, 9 H^{IBOMA}), 0.71-1.07 (m, 3 H^{C13MA} + 3 $H^{P(C13MA)}$).

The reactivity ratios were determined using the Mayo-Lewis equation via nonlinear least-square fitting of the data for the initial monom34 and final copolymer composition ratios. Equation 3.1 shows the Mayo-Lewis approach for the calculation of the reactivity ratios for IBOMA/C13MA.

$$F_{IBOMA} = \frac{r_{IBOMA} f_{IBOMA,0}{}^2 + f_{IBOMA,0} f_{C13MA,0}}{r_{IBOMA} f_{IBOMA,0}{}^2 + 2 f_{IBOMA,0} f_{C13MA,0} + r_{C13MA,0} f_{C13MA,0}{}^2} \qquad \text{eq. 3.1}$$

The nonlinear least-square fitting of the data performed by Excel Solver and gave the values of r_{IBOMA}=0.93±0.01 and r_{C13MA}=1.08±0.01. This provides an estimate of the reactivity ratios but is not necessarily accurate as the data was taken at high conversion values, and the reactivity ratios may vary due to compositional drift that occurs during the polymerization. In order to get a more accurate estimate of the values of the reactivity ratios, data must be obtained at low conversion.

In order to account for the compositional drift, the reactivity ratios were also determined by fitting the data to the Kelen-Tudos plot [108], [109] Equation 3.2 shows the Fineman-Ross linearization method; however, this results in heavily biased data towards one end of the plot. Thus, Kelen-Tudos scaling was used; equation 3.3 represents the Kelen-Tudos plot [108], [109]. This method assumes the samples were obtained at low conversion; hence, since the results were obtained at high conversion values, this will result in an error in the final reactivity ratio values calculated.

$$\frac{f_1}{1-f_1}\left(\frac{1-2F_1}{F_1}\right) = r_1\left(\frac{f_1}{1-f_1}\right)^2\left(\frac{F_1}{1-F_1}\right) + r_2 \qquad \text{eq. 3.2}$$

$$\eta = \left(r_1 + \frac{r_2}{\alpha}\right)\varepsilon - \frac{r_2}{\alpha}\,,\eta = \frac{G}{\alpha+H}\,,\varepsilon = \frac{H}{\alpha+H}\,,\alpha = \sqrt{H_{min}H_{max}} \qquad \text{eq. 3.3}$$

A plot of η vs. ε (figure 3.4) gives a straight line in which the slope equals $r_1 + r_2/\alpha$ and the y-intercept equals $-r_2/\alpha$ [110]. The values for reactivity ratios obtained were r_{IBOMA}=1.17±0.01 and r_{C13MA}=1.34±0.01. The numerical data for this calculation is provided in the appendix, table A.1.

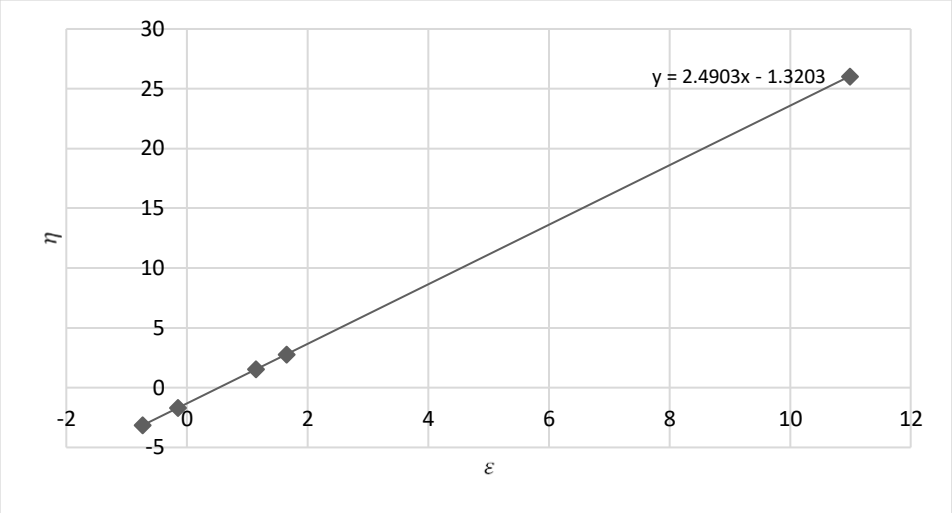

Figure 3.4 The Kelen-Tudos plot for the determination of the reactivity ratios of IBOMA and C13MA.

The extended Kelen-Tudos equation which is modified for higher conversion data and accounts for the compositional drift was then used and G and H are redefined according to equation 3.4, where w is the weight percent conversion of total monomers.

$$G = \frac{f-1}{z} and\ H = \frac{F}{z^2}\ where\ z = \frac{\log(1-\tau_1)}{\log(1-\tau_2)};\ \tau_2 = \left(\frac{w}{100}\right)\left(\frac{\mu+f}{\mu+F}\right), \tau_1 = \tau_2\left(\frac{F}{f}\right) \quad \text{eq. 3.4}$$

$$\mu = (mol.wtmonomer2/mol.wt\ monomer\ 1)$$

A plot of η vs. ε (figure 3.5) gives a straight line in which the slope equals $r_1 + r_2/\alpha$ and the y-intercept equals $-r_2/\alpha$ [110]. The reactivity ratios obtained were r_{IBOMA}=0.89±0.01 and r_{C13MA}=0.84±0.01. The numerical data for this calculation is provided in the appendix, table A.2. However, both the classic and the extended Kelen-Tudos equations assume a linear fitting of the data; as the data is nonlinear, the least-square fitting to the Mayo-Lewis equation provides more accurate results.

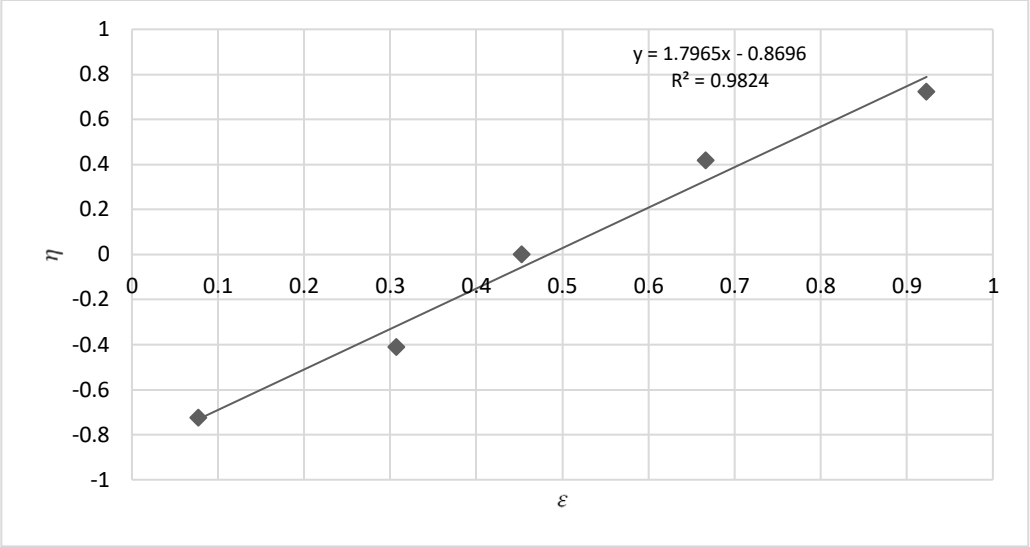

Figure 3.5 The extended Kelen-Tudos plot for the determination of the reactivity ratios of IBOMA and C13MA.

These results show that the reactivity ratios of IBOMA and C13MA are very similar; the product is almost equal to one, which means the copolymerization produces essentially random statistical copolymers. This indicates that both monomers were equally consumed in the reaction since it is equally likely for either monomer to add to the other on the active monomer site. The Mayo–Lewis plot, shown in figure 3.6, shows that the ATRP synthesized poly(IBOMA-stat-C13MA) was a random statistical copolymer ($r_{IBOMA}.r_{C13MA} \approx 1$) with azeotropic composition observed at $f_{IBOMA,0}$ =0.3. The copolymerization of IBOMA and tridecyl methacrylate (TDMA) via nitroxide mediated polymerization previously reported by our group obtained reactivity ratio values of r_{IBOMA} = 0.83 and r_{TDMA} = 1.12 [52], which is in agreement with the results obtained in this work.

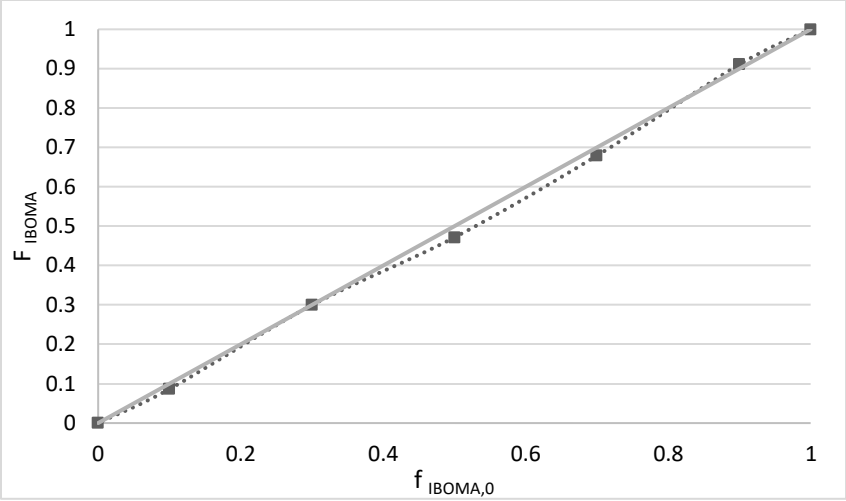

Figure 3.6 Mayo_lewis plot for IBOMA/C13MA copolymers in terms of the initial and final composition of IBOMA in the polymer, $f_{IBOMA,0}$ and F_{IBOMA}, respectively. The solid line indicates the azeotropic composition ($f_{IBOMA,0} = F_{IBOMA}$) and the fitted statistical data is indicated by the open squares and the dashed line.

3.1.3 Thermal Properties

The thermal properties of the IBOMA and C13MA homopolymers and IBOMA and C13MA-rich copolymers were characterized using differential scanning calorimetry (DSC) and thermal gravimetric analysis (TGA). DSC was performed to provide data on the glass transition temperatures (T_g) of the polymers. The glass transition temperature was measured using DSC under a nitrogen atmosphere at a heating/cooling rate of 10 °C/min using three scans per cycle (heat/cool/heat). The values of T_g were obtained by the inflection point method [111] on DSC traces obtained from the first heat run. The T_g values observed for four different compositions are reported in table 3.2. The IBOMA homopolymer had a T_g of 118°C, whereas the C13MA homopolymer had a T_g of -44°C, which agrees with previously reported data [52]. The values of T_g are then tuned within the range -44 -118°C for different copolymer ratios of IBOMA and C13MA.

Table 3.2 DSC analysis results for the glass transitions temperatures of IBOMA and C13MA rich compositions.

Experiment ID	*F_{IBOMA}*[a]	*Predicted Tg (°C)* [b]	*Experimental Tg (°C)*[c]
IB_C13MA_1	1.00	120	118
IB_C13MA_2	0.91	88	77
IB_C13MA_6	0.09	-36	-42
IB_C13MA_7	0.00	-44	-45

a. The final molar fraction of IBOMA in the terpolymer (F_{IBOMA}) as determined by 1H NMR in CDCl3.
b. The predicted Tg as reported in literature for the homopolymers [52] and calculated by the fox equation for the copolymers.
c. Experimental Tg measured by DSC under a nitrogen atmosphere at a rate of 10 °C min−1 using three scans per cycle (heat/cool/heat).

TGA analysis was also done on the homopolymers of IBOMA and C13MA to test their thermal stability. TGA was performed at a temperature ramp rate of 15°C/min from 25°C to 550°C under nitrogen. The TGA results for different copolymer compositions are shown in table 3.3. For example, the IBOMA homopolymer (IB_C13MA_1) TGA results, shown in figure 3.7, indicates that the temperature at which the sample started to decompose (onset temperature, Tdec,1) was at 312°C and it decomposed completely at 465°C (Tdec,2) with only 1.5% ash content remaining. The derivative of weight percent (wt%/°C) shows the temperature $T_{dec,max}$, which corresponds to the highest peak at which there is the most apparent weight loss (in this case 316°C). An apparent decrease in the decomposition temperatures of the copolymers is observed as the mole fraction of C13MA increases in the polymer composition. Therefore, IBOMA rich compositions are more thermally stable than C13MA rich compositions with higher decomposition temperatures ($T_{dec1,IBOMA}$=308°C, $T_{dec1,\ C13MA}$=115°C).

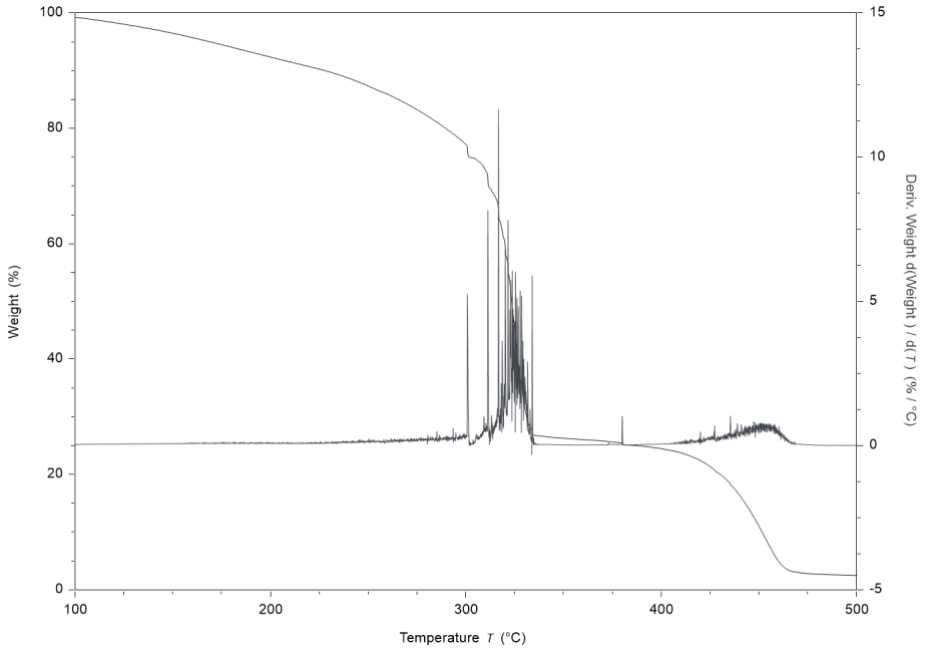

Figure 3.7 TGA analysis for the IBOMA homopolymer (IB_C13MA_1). The plot of Weight % with temperature and the first derivative in (wt%/°C).

Table 3.3 TGA analysis results for the decomposition temperatures.

Experiment ID	F_{IBOMA}[a]	*Tdec 1(°C)*[b]	*Tdec 2(°C)*[b]	*Tdec 3(°C)*[b]
IB_C13MA_1	1.00	308	316	465
IB_C13MA_2	0.91	301	320	460
IB_C13MA_4	0.47	282	315	335
IB_C13MA_5	0.30	276	321	348
IB_C13MA_6	0.09	114	260	277
IB_C13MA_7	0.00	115	152	243

a. The final molar fraction of IBOMA in the terpolymer (F_{IBOMA}) as determined by 1H NMR in CDCl3.
b. Tdec,1 (onset of decomposition), Tdec,2 (the temperature at which weight loss is most apparent), and Tdec,3 (end of decomposition) measured by TGA under nitrogen flow at a ramp rate of 15°C/min.

3.2 ARGET ATRP: Kinetics and Characterization of IBOMA/C13MA Homopolymers, Copolymers, and Terpolymers

3.2.1 Homopolymers of Isobornyl Methacrylate by ARGET ATRP

Activator regenerated by electron transfer (ARGET ATRP) allows ATRP to be conducted with significantly lower amounts of copper in the system in the presence of a reducing agent. Copper in its higher oxidation state is used in a low concentration; this concentration is maintained through the regeneration of the activator complex by the reducing agent. The experimental results for poly(IBOMA) production by ARGET ATRP are summarized in table 3.4. Various reaction parameters were varied in order to obtain a controlled ARGET ATRP reaction with a linear increase in the molecular weight with conversion and low Đ. The type of solvent and initiator were varied across the experiments. Different temperatures were studied along with different ligand to copper ratios and reducing agent to copper ratios. The amount of copper used was 250 ppm (the amount of copper was calculated on a molar basis as the ratio of the concentration of catalyst to monomer, [Cu(II)Br]:[IBOMA]=250 ppm) except in (AR_IB_1 and AR_IB_2) and (AR_IB_11) where the concentration of copper was increased to 500 ppm to study the effect of the copper concentration on the Đ value and the general control over the polymerization.

The first experiment (AR_IB_1) was performed using the ME-Br initiator with a reactants feed ratio of $[IBOMA]_0/[ME\_Br]_0/[SnEH_2]_0/[CuBr_2]_0/[PMDETA]_0$ = 100/1/0.37/0.025/0.25 in a 30wt% diphenyl ether (DPE) solution. The reaction was un-controlled, and the solution became very viscous in only 10 minutes when the reaction was stopped. The concentration of DPE solvent was then increased to a 50 wt% solution and the amount of copper was doubled to 500 ppm (AR_IB_2); the polymerization was not controlled, and the reaction was stopped in 30 mins yielding a very high molecular weight (higher than expected) with a broad molecular weight distribution (Đ = 2.18, M_n= 62.3 kg/mol). The DPE solvent initially used was then switched to

toluene which was fixed throughout the experiments (AR_IB_4-11). In the experiment (AR_IB_4), the concentration of copper was increased to 500 ppm to have better control over the polymerization; the reaction was performed using ME-Br initiator with the reactant feed ratio of $[IBOMA]_0/[ME\_Br]_0/[SnEH_2]_0/[CuBr_2]_0/[PMDETA]_0$ = 100/1/0.37/0.05/0.75 in 50wt% toluene solution. The resultant polymer had a high molecular weight and lower Đ (M_n=27.2 kg/mol, Đ =1.41). Having achieved low Đ, the reactants feed ratio was fixed (same as AR_IB_4), but the concentration of copper was halved to 250 ppm (AR_IB_5). The feed ratio was ($[IBOMA]_0/[ME\_Br]_0/[SnEH_2]_0/[CuBr_2]_0/[PMDETA]_0$ = 100/1/0.37/0.025/0.375 in 50 wt% toluene solution). Expectedly, the lower amount of copper resulted in lower control over the reaction resulting in a higher than predicted molecular weight polymer with a high Đ (M_n=32.7 kg/mol, Đ =1.73). The feed ratio used was fixed for the set of reactions (AR_IB_5-8) and only the temperature was varied to study thermal effects. There was no significant change in the properties of the polymer produced as they had very similar molecular weights and Đ (M_n= 27.3-32.7 kg/mol and Đ =1.71-1.80). The molecular weight exceeded the target molecular weight in all reactions, suggesting poor control over the polymerization. Therefore, the initiator was switched to ethyl α-bromoisobutyrate (EBiB, AR_IB_9), using the same feed ratio as the previous reactions(AR_IB_5-8). This resulted in better control over the polymerization reaction, yielding a polymer within the target molecular weight and with low Đ in only 60 minutes (M_n=14 kg/mol, Đ =1.50). The molecular weight versus conversion plot deviated from the predicted line, indicating the possibility of having dead chains. In order to improve the "livingness" of the polymerization, the concentration of the reducing agent used was decreased to only ten times the copper concentration and the feed ratio used was as follows: ($[IBOMA]_0/[EBiB]_0/[SnEH_2]_0/[CuBr_2]_0/[PMDETA]_0$ = 100/1/0.25/0.025/0.375 in 50 wt% toluene solution, AR_IB_10). High conversion

was achieved, and the resultant polymer had relatively high molecular weight and a reasonable Đ (M_n=20.6 kg/mol, Đ =1.65). The reaction was repeated with 500 ppm of copper to study the effect of increasing the copper concentration on the Đ index (AR_IB_11). Better control over the polymerization was achieved and the polymer produced had a lower Đ (M_n=15.7 kg/mol, Đ =1.46).

Table 3.4 Experimental results for the homopolymerization of IBOMA by ARGET ATRP with variable solvents, reaction temperatures, and reactants feed ratio.

Experiment ID	Temp (°C)	Time (min)	Mn, GPC (kg/mol)[a]	*Đ* [a]	Conversion %
AR_IB_1	90	10	51.4	2.18	-
AR_IB_2	80	30	62.3	2.51	-
AR_IB_4	80	65	27.2	1.41	81
AR_IB_5	80	60	32.7	1.73	74
AR_IB_6	90	30	28.6	1.71	85
AR_IB_7	85	60	28.0	1.75	78
AR_IB_8	75	70	27.3	1.80	79
AR_IB_9	80	60	14.0	1.50	94
AR_IB_10	80	60	20.6	1.65	97
AR_IB_11	80	60	15.7	1.46	77

a. The final product's number average molecular weight (Mn) and dispersity (Đ) as determined by GPC with PMMA standards at 40°C in THF.

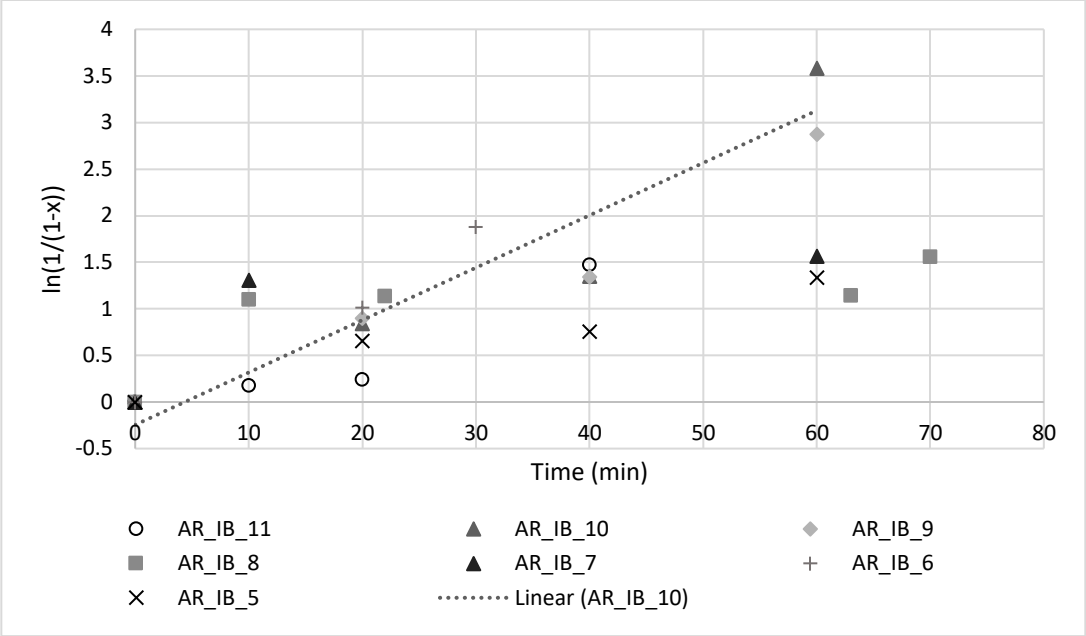

Figure 3.8 Kinetic plot of IBOMA homopolymers by ARGET ATRP with variable solvents, reaction temperatures, and reactants feed ratio.

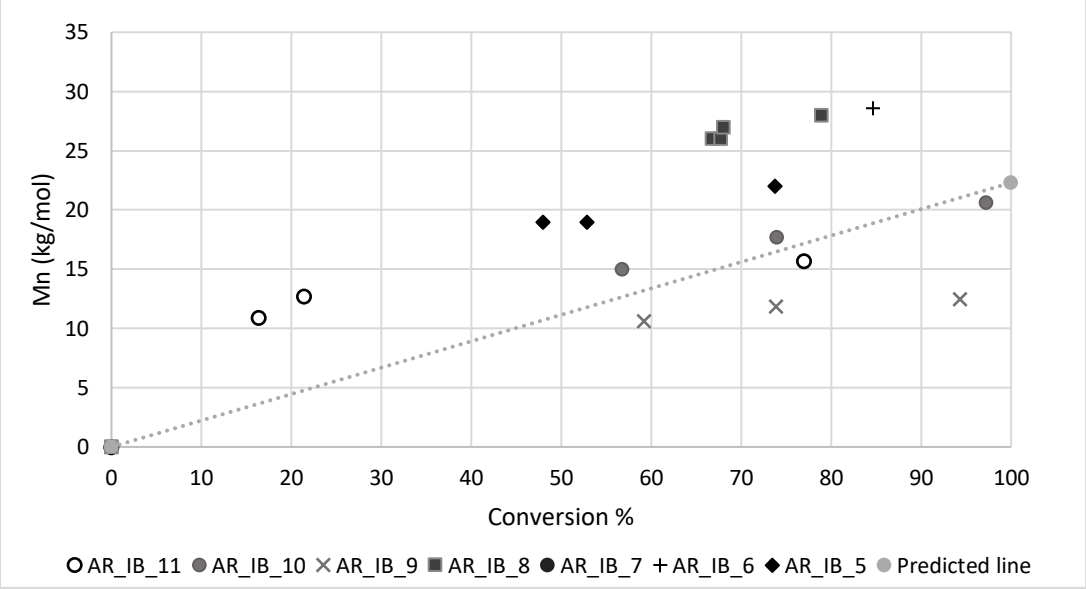

Figure 3.9 Plot of number average molecular weight and conversion for homopolymers of IBOMA by ARGET ATRP with variable solvents, reaction temperatures, and reactants feed ratios.

3.2.1.1 Effect of Solvent

Diphenyl ether is a polar solvent that is typically used in ATRP reactions as it minimizes chain transfer and allows the polymer to reach high molecular weights [79]. Reactions in diphenyl ether using ARGET ATRP were uncontrolled (AR_IB_1-2); the target molecular weight was exceeded in only 10-30 mins; the reaction mixture became very viscous and solidified. Therefore, the solvent was switched to toluene which is a non-polar solvent instead of the polar solvent diphenyl ether [112]. The data for molecular weight relative to conversion obtained was much closer to the predicted values than those obtained with diphenyl ether as a solvent. Matyjaszewski reported that toluene and xylene are more suitable solvent when the target molecular weight is relatively low (~20 kg/mol)[79], and a comparative study on the effect of solvent or the ARGET ATRP system reported that toluene and DMF are the two best solvents and toluene was chosen because it has a lower boiling point which makes the polymer recovery easier [99]. Reactions in toluene exhibited better control where a lower Đ and a more reasonable time frame (60-80 mins) were obtained; thus, toluene was fixed as the reaction solvent.

3.2.1.2 Effect of Ligand

The ligand plays a very important role in controlling ATRP polymerization. The control over the reaction relies on the stability of the metal catalyst complex formed by the metal ion and the ligand [93]. Since only a minimal amount of copper is used in ARGET ATRP, high activity ligands are typically used to form stable complexes. However, due to the high cost of these ligands, this study uses an inexpensive ligand (PMDETA) for its industrial applicability and commercial availability [95]. In order to make up for the lower activity that PMDETA has, it should be used in high excess; the excess ligand increases the rate of polymerization and the concentration of the activator species in the ATRP reaction [99]. A study done using PMDETA as a ligand in ARGET ATRP concluded

that the concentration of the ligand PMDETA should be atleast 10 times the concentration of Cu(II)Br in order to minimize side reactions of Cu(II)Br that may take place if insufficient amounts of the ligand are available ([PMDETA]:[Cu(II)Br] ≥10) [96]. Hence, the concentration of PMDETA initially used was ten times the concentration of copper (AR_IB_1). High Đ was obtained (Đ =2.2) suggesting poor control over the polymerization that may be due to side reactions of Cu(II)Br and inefficient catalyst activity due to the low activity of the PMDETA ligand . The concentration of PMDETA was then increased to 15 times the copper concentration (AR_IB_4, [PMDETA]:[Cu(II)Br] ≥10), and a significant decrease in the Đ was observed (Đ =1.41) indicating better control which is reflected in the narrow molecular weight distribution observed. Therefore, the ratio of the concentration of ligand to copper was fixed to 15 for the ARGET ATRP reactions ([PMDETA]:[Cu(II)Br]=15).

3.2.1.3 Copper(II) Bromide Concentration

The copper(II) bromide complexes with the ligand to form the catalyst complex that controls the ATRP equilibrium. ARGET ATRP allows the use of only trace amounts of copper catalyst to mediate the ATRP equilibrium as the Cu(I) activator complex is continuously regenerated from the Cu(II) by the excess reducing agent present in the reaction mixture. This not only allows a more environmentally benign reaction, but also minimizes the side reactions the copper catalyst may have with the active chain ends allowing the polymerization to reach high molecular weights while maintaining a narrow molecular weight distribution [92], [95]. However, a sufficient concentration of the catalyst complex must be present throughout the reaction to mediate the equilibrium and maintain control over the polymerization reaction. Thus, copper should be minimized to avoid any problems with discoloration while maintaining a sufficient concentration to ensure control over the reaction. Using 500 ppm of copper catalyst ([Cu(II)Br]:[IBOMA]=500

ppm), high conversion was achieved and a low Đ polymer was obtained (AR_IB_4, X=81%, Đ =1.4). The concentration of copper was then halved to minimize the discoloration and study the effects of the lower amount of copper on the system's control. With only 250 ppm of Cu(II)Br (AR_IB_5), the Đ increased (Đ =1.7), indicating lower levels of control over the polymerization. In another experiment (AR_IB_11), the concentration of the copper complex was doubled from 250 ppm (AR_IB_10) to 500 ppm to study the effect on the control; the Đ decreased from Đ =1.65 with 250 ppm of Cu(II)Br to Đ =1.46 with 500 ppm of Cu(II)Br. Further lowering of the copper concentration to below 50 ppm is possible but would result in very high Đ values if the low activity ligand PMDETA is used; it can be accomplished with a highly active ligand such as Me_6TREN or TREN [95], [97] , which was not pursued in this study due to their high cost which makes them inapplicable on the industrial scale.

3.2.1.4 Effect of Temperature

The temperature was varied to study its effect on the polymerization with a fixed feed ratio of [PMDETA]:[Cu(II)Br]=15 and 250 ppm of Cu(II)Br in 50wt% toluene. The temperature was varied in 5 degree intervals from 75°C to 90°C. No significant difference in Đ was observed, but slightly lower Đ was observed at higher temperatures. At higher temperatures, both the rate constant for radical propagation and the atom transfer equilibrium constant increase resulting in higher polymerization rate [79]. Expectedly, higher reaction rates were obtained at higher temperatures as the reaction time was only 30 mins long at 90°C (AR_IB_6) to get to a conversion of 87.5%, whereas it was 70 mins at 75°C (AR_IB_8) to get a conversion of 79%. Therefore, the optimal reaction temperature was 80°C as it provides a reasonable reaction rate and sufficiently low Đ.

3.2.1.5 Effect of Initiator

The initiator plays an important role in ATRP as the initiator's concentration determines the number of growing polymer chains; fast and efficient initiation is key to the success of ATRP [78]. However, the molecular weights obtained were higher than the target molecular weight in all reactions and the graphs of the molecular weights vs. conversion (figure 3.9) were not linear and deviated from the predicted line indicating low initiator efficiency. The low initiator efficiency could be caused by inefficient deactivation of the active radicals resulting in termination [113]. Therefore, in order to ensure efficient initiation, the initiator should be chosen to match the structure of the particular monomer used [76]. In that sense, ethyl α-bromoisobutyrate (EBiB) was chosen as an alternative initiator as it resembles the structure of methyl methacrylate and hance would be a good choice for the methacrylic monomers IBOMA and C13MA. Therefore, the morpholine-based initiator was switched EBiB to study the effect of a different initiator. Using EBiB, more efficient initiation was observed as lower Đ polymer was achieved (AR_IB_9, Đ =1.5) compared to (AR_IB_5, Đ =1.8) with ME-Br as an initiator at 80°C. After achieving low Đ and reasonable conversion, the ratios [PMDETA]:[Cu(II)Br]=15 with 250 ppm of Cu(II)Br in 50wt% toluene at 80°C with the ratio of reducing agent [$Sn(EH)_2$]:Cu(II)Br=15 were used to synthesize a set of IBOMA/C13MA copolymers.

3.2.1.6 Effect of Reducing Agent

Despite lower Đ values obtained in (AR_IB_9), the molecular weight versus conversion plot still does not confirm the active nature of the polymerization. The points obtained deviate from the predicted line in the molecular weight-conversion plot, which indicates the possibility of side reactions such as chain transfer or irreversible termination. Moreover, the curvature in the kinetic plots shown in figure 3.8 indicates irreversible termination and the formation of dead chains [97],

[113]. The dead chains may have formed due to side reactions with the oxidized reducing agent. The excess reducing agent is necessary for the continuation of the ARGET polymerization as it facilitates the regeneration of the copper complex to ensure the continuation of the ARGET ATRP reaction. However, a high excess may lead to side reactions of the oxidized reducing agent with the catalyst complex [93]. Therefore, the concentration of reducing agent was kept in excess but was reduced from 15 times the concentration of Cu(II)Br to 10 times to study the effect of the concentration of the reducing agent (AR_IB_10, $[Sn(EH)_2]$:Cu(II)Br=10). A slightly higher Đ was observed (Đ =1.65), but the molecular weight conversion graph was very similar to the predicted line indicating efficient initiation, high control over the polymerization reaction, and high chain-end fidelity. The kinetic graph of ln(1/1-X) show a good linear fit with time for (AR_IB_10) as indicated by the dashed line in figure 3.8. The GPC chromatogram for the homopolymerization of IBOMA (AR_IB_10) with a feed ratio of $[IBOMA]_0/[EBiB]_0/[SnEH_2]_0/ [CuBr_2]_0 /[PMDETA]_0$ =100/1/0.25/0.025/0.25, shown in figure 3.10, shows a clear shift towards higher molecular weight at different values of conversion indicating activity of the chains and nearly simultaneous growth of all chains. The reaction was repeated with 500 ppm of copper catalyst (AR_IB_11) with a feed ratio of ($[IBOMA]_0/[EBiB]_0/[SnEH_2]_0/[CuBr_2]_0 /[PMDETA]_0$ = 100/1/0.5/0.05/0.5 in 50 wt% toluene solution). Lower Đ was observed, and the linear kinetic plots displayed good control over the polymerization (M_n=15.7 kg/mol, Đ =1.46). To confirm the polymer's chain-end fidelity (ability to form block copolymers), chain extension was performed on the IBOMA homopolymer synthesized via ARGET ATRP (AR_IB_11).

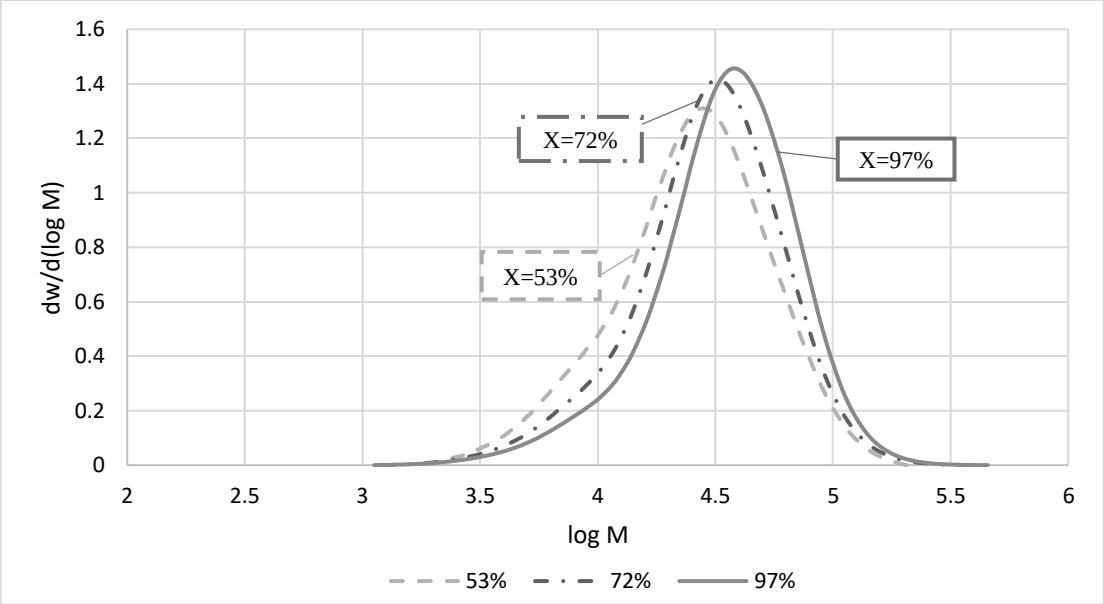

Figure 3.10 GPC peak signal for the homopolymerization of IBOMA by ARGET ATRP (AR_IB_10) with a feed ratio $[IBOMA]_0/[EBiB]_0/[SnEH2]_0/[CuBr2]_0/[PMDETA]_0$= 100/1/0.25/0.025/0.25 at 80°C with EBiB initiator in 50wt% toluene solution. The three curves correspond to three samples taken throughout the reaction with different conversion values (53%, 72% and 97%).

3.2.2 IBOMA and C13MA Copolymers via ARGET ATRP

Copolymerization of IBOMA withC13MA was first done with EBiB initiator and a feed ratio of $[EBiB]_0/[SnEH2]_0/[CuBr_2]_0/[PMDETA]_0$=1/0.37/0.025/0.25 in a 50 wt% toluene solution. The monomer concentrations were calculated based on the target DP, moles of initiator, and the initial mole fractions of the respective monomer; target DP was around 100 corresponding to a target molecular weight ($M_{n,\ target}$=22.3 kg/mol). The results for the homopolymers and copolymers of IBOMA and C13MA prepared are summarized in table A.3 in the appendix. The kinetic plots (fig A.1 and A.2, appendix) show some curvature in the C13MA rich compositions suggesting that side reactions were taking place, which leads to the formation of dead chains [97], [113]. Therefore, the experiments were repeated with a lower concentration of reducing agent ($[Sn(EH)_2]$:Cu(II)Br=10). Different copolymers of IBOMA and C13MA were synthesized using the feed ratio $[EBiB]_0/[SnEH_2]_0/[CuBr_2]_0$ /$[PMDETA]_0$ = 1/0.25/0.025/0.25 in 50wt% toluene at

80°C. The results for the homopolymers and copolymers of IBOMA and C13MA prepared are summarized in table 3.5. The kinetic plots, shown in figure 3.11, show a linear increase with time; the molecular weight versus conversion graphs show a linear increase aligned with the predicted line as shown in figure 3.12. This indicates a well-controlled polymerization reaction and confirms that decreasing the reducing agent concentration, while keeping it in slight excess, increases the control over the polymerization by decreasing the possibility of having side reactions that lead to the formation of dead chains.

Table 3.5 Experimental results for the copolymerization of IBOMA and C13MA by ARGET ATRP at 80°C in 50wt% toluene solution with a feed ratio of $[EBiB]_0/[SnEH_2]_0/[CuBr_2]_0/[PMDETA]_0$ = 100/1/0.25/0.025/0.25.

Experiment ID	Temp (°C)	Time (min)	Mn (kg/mol)[a]	$Đ^a$	Conversion (%)
AR_10_IB	80	60	20.6	1.65	97
ARG_10_IB_C13MA_70_30	80	80	15.2	1.51	98
ARG_10_IB_C13MA_30_70	80	80	18.0	1.53	68
ARG_10_C13MA_100	80	80	18.3	1.56	87

a. The final product's number average molecular weight (Mn) and dispersity (Đ) as determined by GPC with PMMA standards at 40°C in THF.

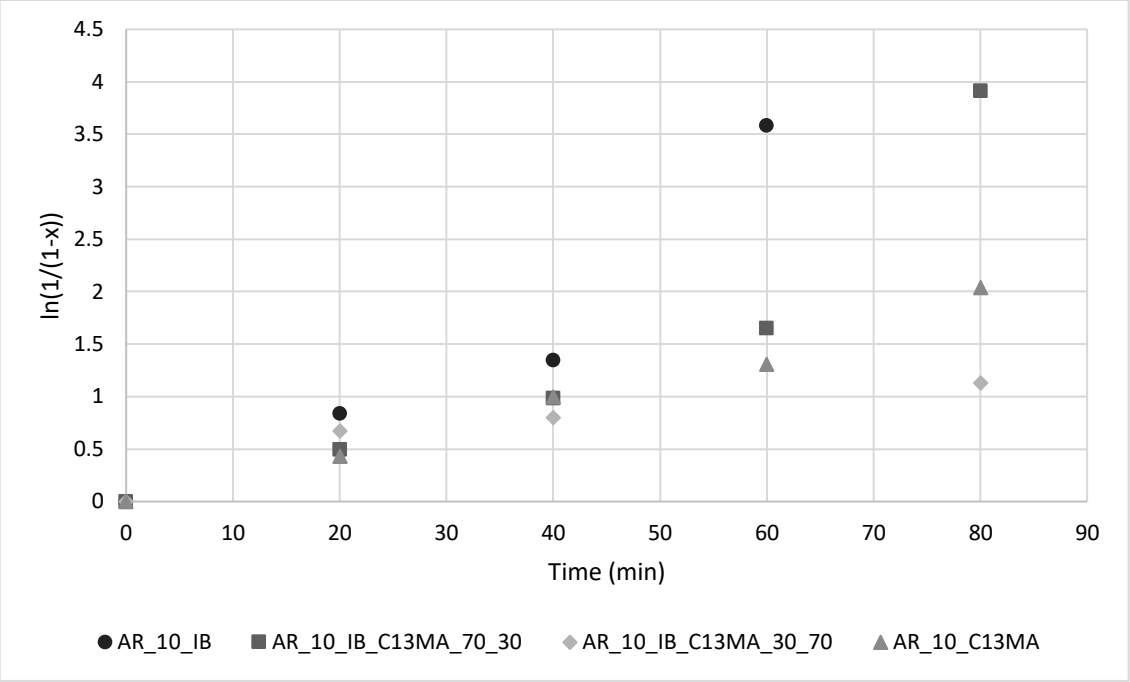

Figure 3.11 Kinetic plot for the copolymerization of different ratios of IBOMA and C13MA by ARGET ATRP at 80°C in 50wt% toluene solution with a feed ratio of $[EBiB]_0/[SnEH2]_0/[CuBr2]_0$ /$[PMDETA]_0$ = 1/0.25/0.025/0.25.

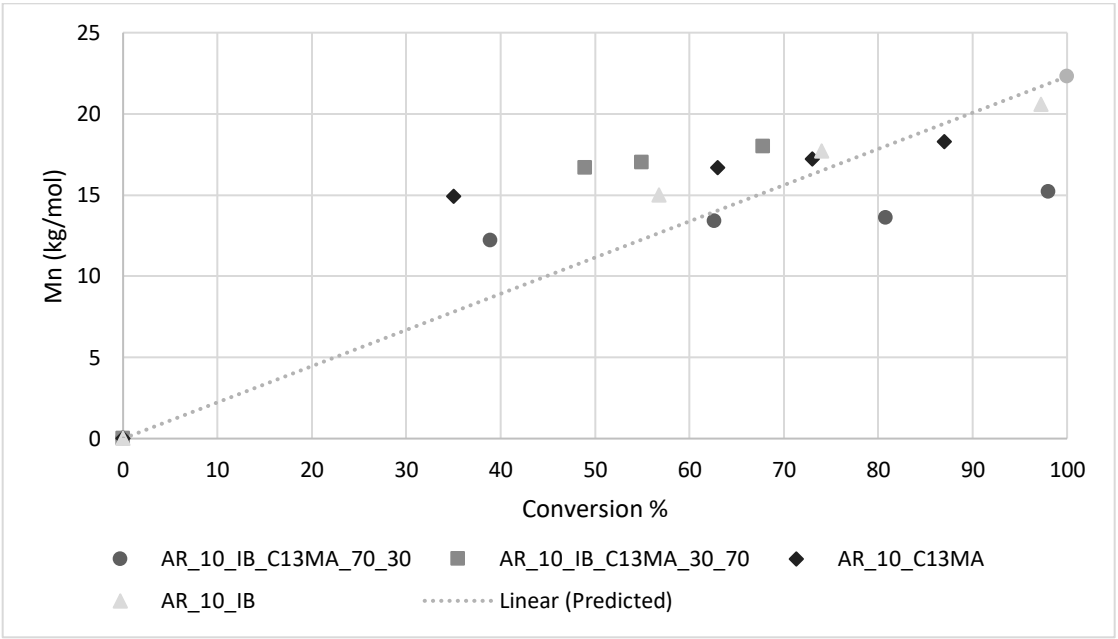

Figure 3.12 Plot of number average molecular weight and conversion for the copolymerization of different ratios of IBOMA and C13MA by ARGET ATRP at 80°C in 50wt% toluene solution with a feed ratio of $[EBiB]_0/[SnEH2]_0/[CuBr2]_0$ /$[PMDETA]_0$ = 1/0.25/0.025/0.25.

3.2.3 Chain Extension of Poly(IBOMA) with C13MA via ARGET ATRP

To examine the chain end fidelity of the polymers produced, chain extension of the IBOMA homopolymer poly(IBOMA) (AR_IB_11, M_n=15.7 kg/mol, Đ=1.46) was performed with C13MA to form a block copolymer. The reaction was carried out at 80°C in a 50wt% solution of toluene with a feed composition of $[Monomer]_0/[EBiB]_0/[SnEH_2]_0/[CuBr_2]_0/[PMDETA]_0$= 100/1/0.25/0.025 /0.25 and with poly(IBOMA) as a macroinitiator. The reaction yielded an IBOMA/C13MA block copolymer with 48% C13MA in the final polymer composition, the experimental results are summarized in table 3.6. Therefore, successful chain extension was accomplished, which was confirmed from the GPC data shown in figure 3.13, where a clear monomodal shift towards a higher molecular is observed for poly(IBOMA)-b-poly(C13MA). This indicates high activity of the macroinitiator and nearly simultaneous growth of all chains. The ^{1}H NMR spectra, shown in figure 3.14, clearly shows the poly(IBOMA) and the poly(C13MA) blocks, further confirming the chain extension.

Table 3.6 Experimental results for the poly(IBOMA)-block-poly(C13MA) copolymer formed by chain extension of IBOMA homopolymer with C13MA by ARGET ATRP.

A. Macroinitiator				
AR_IB_11	Time (min)	Conversion %	Mn (kg/mol)[a]	Đ[a]
	60	77	15.7	1.46
B. Chain Extended Copolymer				
poly(IBOMA)-b-poly(C13MA)	Conversion %	F_{IBOMA}[b]	Mn (kg/mol)[a]	Đ[a]
	76	0.52	22.7	1.43

a. The final product's number average molecular weight (Mn) and dispersity (Đ) as determined by GPC with PMMA standards at 40°C in THF.
b. The final molar fraction of IBOMA in the terpolymer (F_{IBOMA}) as determined by 1H NMR in CDCl3.

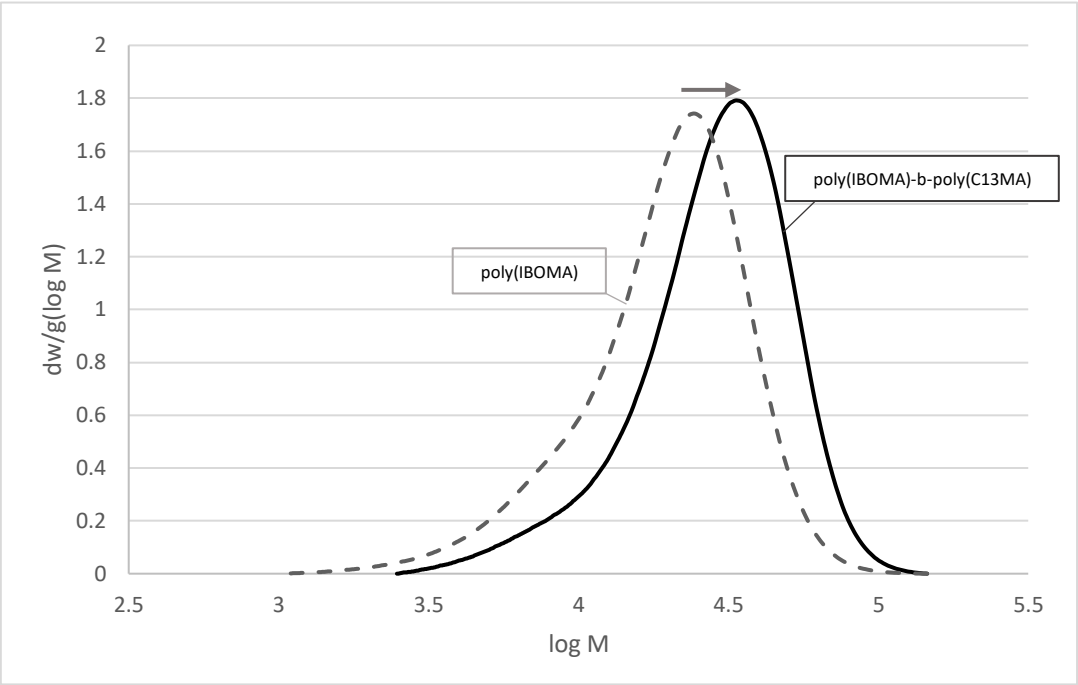

Figure 3.13 GPC traces of IBOMA homopolymer and the chain extended IBOMA/C13MA block copolymer (poly(IBOMA)-b-poly(C13MA). Chain extension was performed by ARGET ATRP with 500ppm Cu(II)Br at 80°C in 50wt% toluene solution with a feed ratio of $[Monomer]_0/[EBiB]_0/[SnEH_2]_0/[CuBr_2]_0$ /$[PMDETA]_0$ = 100/1/0.25/0.025/0.25.

In conclusion, ARGET ATRP was successful in producing well-defined homopolymers and copolymers of IBOMA with C13MA, as well as terpolymers of IBOMA, C13MA, and GMA. Different reaction parameters were optimized to get a well-controlled ARGET ATRP polymerization, including temperature, type of initiator and solvent, and concentration of solvent, catalyst, ligand, and reducing agent. The optimized feed ratio of reactants was determined experimentally ($[IBOMA]_0/[EBiB]_0/[SnEH_2]_0/[CuBr_2]_0/[PMDETA]_0$ = 100/1/0.25/0.025/0.25 in 50 wt% toluene solution) where EBiB is the initiator, $SnEH_2$ is the reducing agent, $CuBr_2$ is the metal catalyst, and PMDETA is the ligand. Using the optimized feed ratio, copolymers of IBOMA and C13MA were successfully produced by ARGET ATRP with only 250ppm of copper producing nearly colorless polymers with relatively low Đ (Đ=1.51-1.61). The chain end fidelity

of the polymer was confirmed by the chain extension of IBOMA with C13MA via ARGET ATRP yielding a low Đ block copolymer of IBOMA and C13MA.

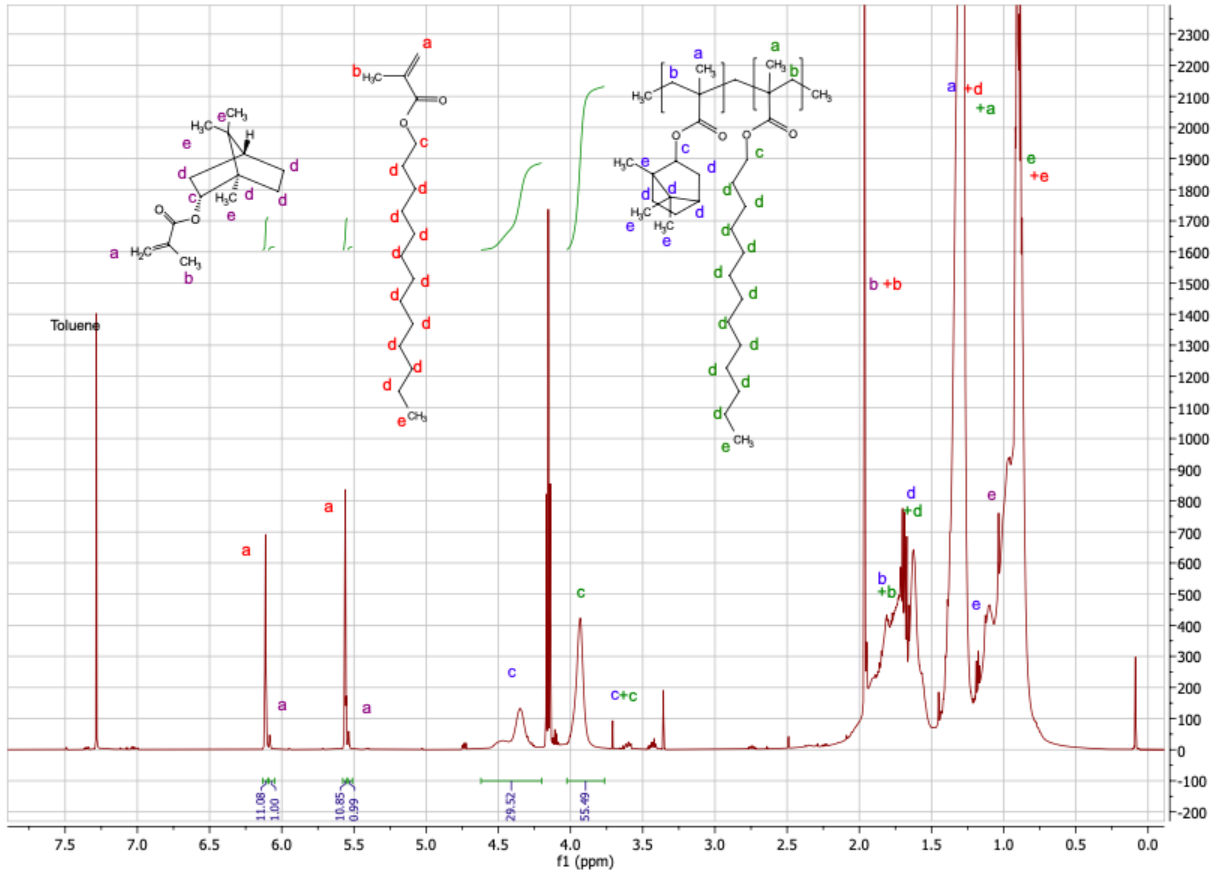

Figure 3.14 ^{1}H NMR spectra for the chain extended IBOMA/C13MA block copolymer (poly(IBOMA)-b-poly(C13MA)) after 60 minutes of starting the reaction. ^{1}H NMR (CDCl3, ppm): 6.17-6.22 (m, 1 H^{C13MA}), 6.14-6.17 (m, 1 H^{IBOMA}), 5.59-5.63 (m, 1 H^{C13MA}), 5.56-5.59 (m, 1 H^{IBOMA}), 4.25-4.65 (d, 1 $H^{P(IBOMA}$), 3.83-4.04 (s, 2 $H^{P(C13MA)}$), 3.66-3.76 (m, 2 $H^{P(C13MA)}$ + 1 $H^{P(IBOMA}$), 1.93-2.02 (m, 3 H^{IBOMA} + 3 H^{C13MA}), 1.77-1.83 (m, 2 $H^{P(IBOMA)}$+ 2 $H^{P(C13MA)}$), 1.64-1.76 (m, 7 $H^{P(IBOMA}$ + 2 $H^{P(C13MA)}$), 1.21-1.44 (m, 3 $H^{P(IBOMA}$ + 23 $H^{P(C13MA)}$ + 22 H^{C13MA}), 1.14-1.19 (m, 9 $H^{P(IBOMA}$), 1.01-1.06 (s, 9 H^{IBOMA}), 0.81-0.96 (m, 3 H^{C13MA} + 3 $H^{P(C13MA)}$).

3.3 Coatings: Varnish Formulation

This project was done to support the development of a super varnish for wood aircraft interiors. The varnish must meet the criteria for performance, including sufficient adhesion/peel strength, anti-flammability, and exhibit no cracking and aging. The varnish formulation was initially prepared using nitroxide mediated polymerization (NMP); however, some weaknesses become apparent as this varnish is being scaled-up for industrial production. The cost and unavailability of the initiators for NMP make it challenging for scale-up, and the long reaction times required for NMP reactions may also be problematic. Therefore, alternative controlled radical polymerization should be explored for the varnish formulation; therefore, ATRP was pursued to protect the formulation broadly. From an industrial perspective, ATRP has many advantages over NMP chemistry; it generally has a shorter reaction time, and all the reactants are commercially available. However, the most significant disadvantage associated with ATRP is the blue color that appears in the final polymer product due to the presence of the copper catalyst. However, with the reduced catalyst ATRP methods (ARGET ATRP), it became possible to produce colorless polymers that do not require any further purification or post-treatment modification. In the initial stage of the varnish coating testing, NMP was used to make the polymer resins used to prepare the varnish formulation and tested. The system was then switched to an ARGET ATRP system to prepare, test, and compare the coatings results to the initial NMP coatings.

3.3.1 IBOMA/C13MA/GMA terpolymers

Terpolymers of IBOMA, C13MA, and GMA were prepared to be used in the varnish formulation. IBOMA imparts hardness and strength to the coating resin, C13MA provides flexibility and lowers the glass transition temperature, and GMA adds the epoxy functionality to facilitate crosslinking and curing of the coating. The polymer resin used in the varnish formulation was initially prepared

with nitroxide mediated polymerization (NMP) and then an ARGET system was adopted; both those systems produce colorless polymers that can be used directly in the varnish formulation without the need for any further purification or treatment. The terpolymers all initially consist of 40% IBOMA, 40% C13MA, and 20% GMA; the experimental results for the terpolymers prepared by ARGET ATRP are presented in table 3.7. The first experiment (AR_IB_C13MA_GMA_1) was accomplished with 250 ppm of copper and a feed ratio of $[EBiB]_0/[SnEH_2]_0/[CuBr_2]_0$ $/[PMDETA]_0$ = 1/0.37/0.025/0.25 in 50 wt% toluene. The monomer concentrations were calculated based on the target DP, moles of initiator, and the initial mole fractions of the respective monomer. The terpolymer obtained had a light white color with a relatively high molecular weight and low Đ (Mn=19 kg/mol , Đ =1.50). The reaction was repeated with a lower copper concentration of only 200 ppm to achieve an utterly colorless polymer (AR_IB_C13MA_GMA_2). The polymer obtained was nearly colorless and had a similar molecular weight to the previous, but a slightly higher Đ was obtained (Mn=18.3 kg/mol, Đ =1.71). In the third experiment (AR_IB_C13MA_GMA_3), the feed ratio was kept constant, but the target molecular weight was lowered to 12 kg/mol to lower the viscosity of the polymer resin to enable decreasing the amount of solvent used. A lower molecular weight polymer was obtained with a low Đ (M_n=9.0 kg/mol, Đ =1.53). The polymers prepared were used as resins in the varnish coating formulation and applied on wood substrates for testing.

Table 3.7 Experimental results of the IBOMA, C13MA, GMA terpolymers prepared by ARGET ATRP at 80°C in 50wt% toluene solution with a feed ratio of *[*$[EBiB]_0/[SnEH2]_0/[CuBr2]_0$ /$[PMDETA]_0$ = 1/0.37/0.025/0.25.

Experiment ID	*Temp (°C)*	*Time (min)*	*Conversion %*	Mn_{targer} *(kg/mol)*	Mn_{exp} [a] *(kg/mol)*	Đ [a]
AR_IB_C13MA_GMA_1	80	80	79	22.3	19.0	1.50
AR_IB_C13MA_GMA_2	80	80	62	22.3	18.3	1.71
AR_IB_C13MA_GMA_3	80	60	84	12.0	9.0	1.53

a. The final product's number average molecular weight (Mn) and dispersity (Đ) as determined by GPC with PMMA standards at 40°C in THF.

3.3.2 Varnish Formulation

The polymers were dissolved in a 70wt% solution of toluene and left overnight to ensure complete dissolution to prepare the coatings. Diamine crosslinker (Priamine 1075) was then added in 10wt% of the polymer to the polymer solution. The wood samples were buffed, cleaned with water, and dried before use. The thickness of the wood substrates was measured at five different points to obtain an average thickness before applying the coating. The solution was mixed well and then blade coated by direct application of the coating using a pipette onto clean wood substrates. The coated wood samples were left under the fume hood to dry. The resulting coated substrates were assessed based on coating thickness, appearance, and impact resistance; the results were compared with the coatings prepared earlier using NMP chemistry.

In the first set of experiments, polymer resins were prepared by NMP with different IBOMA/C13MA/GMA ratios to obtain different glass transition temperatures. All the NMP polymerization reactions were performed with 10% acrylonitrile (AN) as the controlling co-monomer at 90°C in50wt% dioxane solvent with BlocBuilder as the initiator; the experimental results of the NMP synthesized polymers are shown in table 3.8. The NMP reactions exhibited long reaction times that varied between 200-270 mins and gave high Đ polymers (Đ=1.61-2.87).

The polymers were used in coating formulations with different amounts of diamine crosslinker; the diamine was added at levels of 10 wt% of the polymer and 20wt% of the polymer (table 3.9, M1* and M3*) to investigate the optimal amount of diamine crosslinker needed. The samples with 20wt% diamine exhibited shrinkage and cracking, so 10wt% diamine was pursued for the following samples. Assessment of the results of the dry coated wood sample, shown in table 3.9, showed that the resin M3 was the optimum choice (Tg= 16°C; $f_{IBOMA,0}$=0.35, $f_{C13MA,0}$=0.35, $f_{GMA,0}$=0.2, $f_{AN,0}$=0.1). Impact tests performed on the prepared samples gave relatively high heights for fracture indicating good adhesion to the substrate. The thickness of the coatings was not optimized, but it was used as an indicator on the effect of thickness on adhesion and drying time. The thickness did not have a significant effect on the impact test results; however, the thicker coatings had a higher impacted surface area whereas the thin coatings had a more localized and concentrated detachment.

This formulation prepared via NMP resulted in a smooth colorless coating with an aesthetic finish, free of any bubbles or shrinkage, and high impact resistance. However, the long drying time requirement of almost four weeks is a significant setback for this formulation. Pictures of the coated wood samples are shown in figure A.3 in the appendix.

Table 3.8 Experimental results of the terpolymers prepared by NMP with different theoretical glass transition temperatures corresponding to different initial monomer ratios.

Sample Name	$f_{GMA,0}$[a]	$f_{IBOMA,0}$[a]	$f_{C13MA,0}$[a]	T_g (°C)[b]	*Time (min)*	*Mn (kg/mol)*[c]	*Đ*[c]
M1	0.10	0.40	0.40	12	200	26.30	2.21
M3	0.20	0.35	0.35	16	255	13.00	1.61
M4	0.40	0.25	0.25	26	260	15.8	2.87

a. The initial molar fraction of IBOMA in the initial feed.
b. The predicted glass transition temperature as calculated by the Fox equation.
c. The final product's number average molecular weight (Mn) and dispersity (Đ) as determined by GPC with PMMA standards at 40°C in THF.

Table 3.9 Coated sample results for polymer resins prepared by NMP.

Sample Name	T_g (°C)[a]	*Diamine*[b]	*Average thickness (mm)*[c]	*Height for fracture (±1 cm)*	*Notes*
M1	12	10%	0.4-0.5	15	Clear matte finish
*M1**	12	20%	0.39-0.49	N/A	Shrinkage
M3	16	10%	0.2-0.3	15	Clear matte finish
*M3**	16	20%	0.35-0.45	18	Shrinkage
M4	26	10%	0.3-0.4	17	Clear matte finish

a. The predicted glass transition temperature as calculated by the Fox equation.
b. The amount of diamine cross-linker (Priamine-1075) added to the coating formulation expressed as the weight percent of the polymer.
c. The average thickness of the dried coating film was measured as an average of the thickness taken at five different locations on the wood substrate.
d. The height for fracture determined is the drop height that results in a crack or peeling of the coating using the impact test apparatus.

The chosen formulation of the IBOMA/C13MA/GMA terpolymer was then prepared using ARGET ATRP, shown earlier in table 3.7. The main problem associated with the formulation is the long drying time; using the ARGET ATRP prepared polymer resins, different parameters were studied to optimize the coatings' drying time. The parameters varied include the molecular weight of the polymer, the type of solvent, and the amount and ratio of solvents used; the coated wood samples results are shown in table 3.10. In the first set of experiments, the polymer

(AR_IB_C13MA_GMA_1) was dissolved in 70wt% toluene solution and mixed with diamine (10wt% of the polymer). The solution was mixed well and then applied as a thin layer on 3 different clean buffed wood substrates. The resultant coating dried after 4 weeks in the fume hood, and it had a good appearance with a matte finish. The average thickness varied (0.24-0.57 mm), and the height for fracture was the same for all three samples (~4 cm). To improve the appearance of the coating, the polymer prepared with only 200 ppm of copper (AR_IB_C13MA_GMA_2) was used for the second set of experiments. This polymer was nearly colorless since it had a lower amount of copper in the polymerization reaction. It was dissolved in a mixture of toluene and 2-methyl tetrahydrofuran (2-MeTHF) as co-solvents. 2-MeTHF is a volatile solvent with a boiling point of 80°C; it was added to lower the solvent's boiling point to allow faster evaporation and have a shorter drying time. Different ratios of solvents were explored to optimize the drying time. For the first set of coatings (AR_IB_C13MA_GMA_2*), the polymers were dissolved in the solvent and applied on the same day. This resulted in shrinkage and a lousy appearance as the polymers did not dissolve well before application. The same resin was used to prepare another set of samples that were left to dissolve overnight in the solvent mixture before being mixed with the diamine crosslinker and applied. These coatings gave a nice clean finish with some small discolored patches caused by the fast evaporation of the solvent that is rich in 2 Me-THF. However, the volatile solvent (2-Me-THF) did not significantly affect the drying time and was ineffective in speeding up the evaporation process. A lower molecular weight polymer (AR_IB_C13MA_GMA_3) was then used to prepare the next set of samples. The lower molecular weight polymer will have lower viscosity to allow decreasing the amount of solvent used. Two samples were prepared, one with 70 wt% solvent and the other contained only 50wt% solvent. The samples had a nice, aesthetic appearance without any bubbles or discoloration. The sample with less solvent had a faster drying

time of around 3 weeks compared to 4 weeks with more solvent. The overall appearance of the polymer was significantly better when a low molecular weight polymer was used. Pictures of the coated wood samples are shown in figure A.3 in the appendix.

Table 3.10 Experimental results for the coated wood samples. All samples contain 10wt% diamine crosslinker(Priamine1075), and the polymer resins are synthesized via ARGET ATRP.

Sample Name	Sample	Solvent: Polymer	Solvent		Thickness [a] Average (mm)	Height [b] for fracture (±1 cm)	Notes
			Toluene	2-MeTHF			
AR_IB_ C13MA_GMA_1	1	0.7 : 0.3	100%	0%	0.24	4	Clear matte finish
	2	0.7 : 0.3	100%	0%	0.27	4	
	3	0.7 : 0.3	100%	0%	0.58	4	
AR_IB_ C13MA_GMA_2[c]	1	0.7: 0.3	50%	50%	0.73	9	Shrinkage and cracking
	2	0.7: 0.3	70%	30%	0.36	7	
	3	0.7: 0.3	90%	10%	0.41	9	
AR_IB_ C13MA_GMA_2	1	0.7: 0.3	50%	50%	0.47	10	Clear matte finish with some discolored patches
	2	0.7: 0.3	90%	10%	0.37	7	
AR_IB_ C13MA_GMA_3	1	0.7 : 0.3	100%	0%	0.52	2	Clear matte finish
	2	0.7 : 0.3	100%	0%	0.41	2	
	3	0.5 : 0.5	100%	0%	0.47	2	Shrinkage and cracking
	4	0.5 : 0.5	100%	0%	0.48	2	

a. The average thickness of the dried coating film measured as an average of the thickness taken at five different locations on the wood substrate.
b. The height for fracture determined is the drop height that results in a crack or peeling of the coating using the impact test apparatus.
c. Samples were dissolved and applied as coatings in the same day.

The developed coating formulation meets the appearance criteria as it forms a nice clear matte coating, and it also meets the adhesion and hardness criteria. The main disadvantage associated

with the developed coating formulation is the toluene solvent which is not only a concern from an environmental perspective, but also prolongs the drying time significantly. To address this issue, two approaches were taken. First, a co-solvents mixture was employed to lower the boiling point and decrease the amount of toluene used by mixing it with a bio-sourced solvent. 2-MeTHF is a bio-based solvent with a boiling point around 80°C that was used to lower the boiling point of toluene (110°C) in order to speed up drying by increasing the volatility of the solvent. Moreover, unlike toluene, 2-MeTHF is a REACH approved solvent that is safe to use for coatings. However, after investigation of different co-solvent ratios, it was found that the use of 2-MeTHF did not help speed up the drying process and decrease the drying time. Thus, another approach to reduce the drying time was employed which was to decrease the amount of solvent used in the coating formulation. Initially, the coating has 70wt% solvent and only 30wt% solid content (resin). In order to lower the solvent content without significantly increasing the viscosity of the polymer, a low molecular weight resin with low viscosity should be used. Hence, a lower molecular weight polymer was prepared, and two sets of coatings were made, one with 50wt% solvent and the other with 70wt% solvent for comparison. There was no significant change in the drying time between the high-solid content coating and the previous; the high-solid content coating had a bad appearance where some solvent seemed to be trapped below the surface of the coating causing discoloration of the wood substrate and a tacky finish. Since, both approaches were not successful in decreasing the drying time of the coating, other more advanced alternatives should be pursued. Solventless liquid coating formulations is a promising alternative to be pursued. Using reactive binders that can be cured by UV light radiation, or using a reactive diluents to replace solvents, could eliminate the need for using a solvent [13], [20]. Another possible alternative would be a

hot-melt adhesive type coatings which employs a solventless solid coating formulation that is the melted on the surface to form a thin coating film [13], [20].

4. Conclusion

4.1 Experimental Conclusions

In this study, traditional ATRP was successful in producing well-defined homopolymers and statistical copolymers of IBOMA and C13MA with high conversion (up to 99%) and low Đ (Đ=1.16-1.52). The kinetic study of the copolymerization reaction showed higher reaction rates for IBOMA rich compositions in comparison to C13MA rich compositions. H^1NMR analysis of the copolymers produced allowed the deduction of the final polymer compositions, which was used to determine the reactivity ratios of the monomers (r_{IBOMA}=0.93±0.01, r_{C13MA}=1.08±0.01). The reactivity ratios of IBOMA and C13MA are very similar suggesting that both monomers were equally consumed throughout the reaction to form random copolymers. The thermal properties of the polymers were assessed by TGA and DSC. The DSC results gave the glass transitions temperatures for IBOMA and C13MA to be $T_{g,IBOMA}$ =118°C and $T_{g,C13MA}$=-44°C. TGA analysis was also performed on the samples to understand the degradation process and the thermal stability of the copolymers. IBOMA rich compositions were more thermally stable with higher decomposition temperatures than C13MA rich compositions ($T_{dec1,IBOMA}$=308°C, $T_{dec1,C13MA}$=115°C).

In the second part of the study, ARGET ATRP was successful in producing well-defined homopolymers and copolymers of IBOMA with C13MA, as well as terpolymers of IBOMA, C13MA, and GMA. ARGET ATRP efficiently produced tailor-made polymer structures with only ppm amounts of copper, thereby eliminating post-polymerization purification requirements. ARGET ATRP was first applied for the synthesis of IBOMA homopolymers. Different reaction

parameters, including temperature, type of initiator and solvent, and concentration of solvent, catalyst, ligand, and reducing agent were all investigated and optimized to obtain a well-controlled polymerization. The optimized feed ratio of reactants was determined experimentally ($[IBOMA]_0/[EBiB]_0/[SnEH_2]_0/[CuBr_2]_0/[PMDETA]_0$ = 100/1/0.25/0.025/0.375 in 50 wt% toluene solution) where EBiB is the initiator, SnEH2 is the reducing agent, $CuBr_2$ is the metal catalyst, and PMDETA is the ligand. Using the optimized feed ratio, copolymers of IBOMA and C13MA were successfully produced by ARGET ATRP with only 250ppm of copper producing nearly colorless polymers with relatively low Đ (Đ=1.51-1.61). Chain extension of IBOMA with C13MA via ARGET ATRP was successfully performed yielding a block copolymer of IBOMA and C13MA, which confirms the chain end fidelity and activity/livingness of the polymer chains. ARGET ATRP was also successful in producing nearly colorless terpolymers of IBOMA, C13MA, and GMA to be used as the polymer resin for the varnish coating formulation. Both high and low molecular weight terpolymers (Mn_{target}=22.3kg/mol and Mn_{target}=12.0 kg/mol) were prepared and applied in the varnish formulation. The coatings had a clear matte finish and good impact resistance; ARGET ATRP resins matched the NMP resins and resulted in coatings with very similar appearance and properties as those made by NMP.

4.2 General Conclusion

ATRP proved to be an efficient method for the production of controlled polymer structures with pre-determined molecular weights and low molecular weight distribution. The wide applicability of ATRP across various monomers and the commercial availability of all reactants makes it an industrial viable choice. New advances in low catalyst ATRP methods allows the synthesis of colorless controlled polymer structures that do not require any purification or post-polymerization treatment. ARGET ATRP was successfully used to synthesize polymer resins that constitute of

terpolymers of bio-based methacrylic monomers and functional epoxy groups that were incorporated in varnish formulations. The varnish formulation produced require no further purification or processing and meets the criteria for hardness, adhesion, and appearance; however, the main set back of this formulation is the long drying time. New methods that diminish and even eliminate the use of solvent will be pursued in future work in order to speed up the drying process.

4.3 Future Work

Recent developments in ATRP allowed the synthesis of tailor-made polymers with various shapes, architectures, and functionalities; high molecular weights while maintaining low Đ and using only trace amounts of the metal catalyst. The commercial availability, versatility, and ease of application of advanced ATRP methods provides access and opportunity for the synthesis of advanced materials and polymer structures. The success of ARGET ATRP in producing low Đ polymer resins in this work paves the way for the investigation of other more advanced reduced catalyst ATRP methods that can further lower the metal catalyst requirement or even eliminate it entirely.

Photo-induced polymerization is a very promising polymerization method that will be the focus of the future work for polymer synthesis. Utilizing visible light for the initiation of ATRP is a very interesting concept recently highlighted [90], [114]. Photo-induced ATRP follows the same mechanism as conventional ATRP; the main difference is that it uses a photo-induced radical initiator instead of the traditional thermal initiator[115]. This process allows control over polymerization through the manipulation of the light source[114]. Photo-induction was carried out on several variations of ATRP methods, including using very low amounts of metal catalysts such as copper [90] or iron [116], and using organic catalysts (organo-catalyzed ATRP) which is also known as metal-free ATRP [117].

Ultimately, photo-induced metal-free ATRP is nearly ideal as it completely eliminates metal catalyst and allows retraction of the the post-polymerization purification steps [118]. Using organo-catalyzed polymerization successfully produced well-defined polymers; however, the molecular weight distributions were slightly broader than other ATRP variants [119]. Although this method still requires improvement to obtain narrow molecular weight distribution, it poses as a promising environmentally friendly controlled polymerization method as it can be relevant industrially in the electronics and biomaterials sectors [120]. This advancement is revolutionary both environmentally and industrially as the use of organic catalyst retracts the need the purification and post-polymerization steps allowing industrial scale production without worrying about metal contamination or the costs and removal of the metal catalyst.

In terms of coatings, future work will employ solventless coating formulations to eliminate the use of chemical solvents and speed up the drying process. Functional monomers will be incorporated into the polymer resin to allow different reactive chemistries, such as thiol-ene click chemistry, to aid with the curing of the coatings. UV light curable coatings that employ reactive binders or use reactive diluents to replace solvents will be investigated, along with hot-melt adhesive type coatings which employs a solventless solid coating formulation that is the melted on the surface to form a thin coating film [13], [20].

References

[1] J. Chi, G. Zhang, Q. Xie, C. Ma, and G. Zhang, "High performance epoxy coating with cross-linkable solvent via Diels-Alder reaction for anti-corrosion of concrete," *Prog. Org. Coatings*, vol. 139, no. September 2019, p. 105473, 2020, doi: 10.1016/j.porgcoat.2019.105473.

[2] P. Król and P. Chmielarz, "Recent advances in ATRP methods in relation to the synthesis of copolymer coating materials," *Prog. Org. Coatings*, vol. 77, no. 5, pp. 913–948, 2014, doi: 10.1016/j.porgcoat.2014.01.027.

[3] M. Montazeri and M. J. Eckelman, "Life cycle assessment of UV-Curable bio-based wood flooring coatings," *J. Clean. Prod.*, vol. 192, pp. 932–939, 2018, doi: 10.1016/j.jclepro.2018.04.209.

[4] G. de With, *Polymer Coatings: A Guide to Chemistry, Characterization, and Selected Applications*. 2018.

[5] E. Scrinzi, S. Rossi, F. Deflorian, and C. Zanella, "Evaluation of aesthetic durability of waterborne polyurethane coatings applied on wood for interior applications," *Prog. Org. Coatings*, vol. 72, no. 1–2, pp. 81–87, 2011, doi: 10.1016/j.porgcoat.2011.03.013.

[6] I. De Windt, J. Van Den Bulcke, I. Wuijtens, H. Coppens, and J. Van Acker, "Outdoor weathering performance parameters of exterior wood coating systems on tropical hardwood substrates," *Eur. J. Wood Wood Prod.*, vol. 72, no. 2, pp. 261–272, 2014, doi: 10.1007/s00107-014-0779-7.

[7] J. E. P. Custódio and M. I. Eusébio, "Waterborne acrylic varnishes durability on wood surfaces for exterior exposure," *Prog. Org. Coatings*, vol. 56, no. 1, pp. 59–67, 2006, doi: 10.1016/j.porgcoat.2006.02.008.

[8] F. Bulian and J. A. Graystone, "Markets for Wood and Wood Coatings," *Wood Coatings*, pp. 1–14, 2009, doi: 10.1016/b978-0-444-52840-7.00001-1.

[9] A. S. Kimerling and S. R. Bhatia, "Block copolymers as low-VOC coatings for wood: Characterization and tannin bleed resistance," *Prog. Org. Coatings*, vol. 51, no. 1, pp. 15–26, 2004, doi: 10.1016/j.porgcoat.2004.03.006.

[10] M. de Meijer and J. Nienhuis, "Influence of internal stress and extensibility on the exterior durability of wood coatings," *Prog. Org. Coatings*, vol. 65, no. 4, pp. 498–503, 2009, doi: 10.1016/j.porgcoat.2009.04.011.

[11] C. M. Popescu and A. Pfriem, "Treatments and modification to improve the reaction to fire of wood and wood based products—An overview," *Fire Mater.*, vol. 44, no. 1, pp. 100–111, 2020, doi: 10.1002/fam.2779.

[12] G. de With., "Polymer Coatings," in *Polymer Coatings: A Guide to Chemistry, Characterization, and Selected Applications*, 2018, pp. 1–17.

[13] G. de With., "Basic Coating Formulations," in *Polymer Coatings: A Guide to Chemistry, Characterization, and Selected Applications*, 2018, pp. 71–108.

[14] K. Dušek and M. Dušková-Smrčková, "Network structure formation during crosslinking of organic coating systems," *Prog. Polym. Sci.*, vol. 25, no. 9, pp. 1215–1260, 2000, doi: 10.1016/S0079-6700(00)00028-9.

[15] F. Bulian and J. A. Graystone, "Classification and Formulation of Wood Coatings," *Wood Coatings*, pp. 137–154, 2009, doi: 10.1016/b978-0-444-52840-7.00005-9.

[16] G. de With., "Additives and Particulates," in *Polymer Coatings: A Guide to Chemistry, Characterization, and Selected Applications*, 2018, pp. 109–134.

[17] B. De Clercq, J. Laperre, and L. Ruys, “The controlled radical polymerisation process as an instrument for tailor-made coating applications,” *Prog. Org. Coatings*, vol. 53, no. 3, pp. 195–206, 2005, doi: 10.1016/j.porgcoat.2005.03.001.
[18] G. de With, “Petro-based Thermoset Resins,” in *Polymer Coatings: A Guide to Chemistry, Characterization, and Selected Applications*, 2018, pp. 47–69.
[19] J. D. Gasper and R. A. Lombardi, “Acrylic Polymers,” in *Coatings Materials and Surface Coatings*, 2006, pp. 1–10.
[20] Arthur A. Tracton, *Coatings Technology Handbook*, 3rd editio. Taylor & Francis, 2005.
[21] G. (Bert) de With, *Polymer coatings: a guide to chemistry, characterization, and selected applications*. Wiley-VCH Verlag, 2018.
[22] U. Kästner, “The impact of rheological modifiers on water-borne coatings,” *Colloids Surfaces A Physicochem. Eng. Asp.*, vol. 183–185, pp. 805–821, 2001, doi: 10.1016/S0927-7757(01)00507-6.
[23] R. F. G. Brown, “Additives in coatings - a necessary evil?,” 2007.
[24] C. W. Macosko, “Viscous Liquids,” *Rheol. Princ. Meas. Appl.*, pp. 65–108, 1994.
[25] K. Matyjaszewski, “Controlling polymer structures by Atom Transfer Radical Polymerization and other controlled/living radical polymerizations,” in *Macromolecular Symposia*, 2003, vol. 195, pp. 25–32, doi: 10.1002/masy.200390131.
[26] K. Matyjaszewski, “Advanced Materials by Atom Transfer Radical Polymerization,” *Adv. Mater.*, vol. 30, no. 23, pp. 1–22, 2018, doi: 10.1002/adma.201706441.
[27] F. Paquin, J. Rivnay, A. Salleo, N. Stingelin, and C. Silva, “Multi-phase semicrystalline microstructures drive exciton dissociation in neat plastic semiconductors,” *J. Mater. Chem. C*, vol. 3, pp. 10715–10722, 2015, doi: 10.1039/b000000x.
[28] A. Van Herk, “General Aspects of Copolymerization,” in *Synthesis and Applications of Copolymers*, vol. 9781118057, 2014, pp. 54–66.
[29] M. Nejad and P. Cooper, “Exterior wood coatings. Part-2: Modeling correlation between coating properties and their weathering performance,” *J. Coatings Technol. Res.*, vol. 8, no. 4, pp. 459–467, 2011, doi: 10.1007/s11998-011-9331-4.
[30] I. González, D. Mestach, J. R. Leiza, and J. M. Asua, “Adhesion enhancement in waterborne acrylic latex binders synthesized with phosphate methacrylate monomers,” *Prog. Org. Coatings*, vol. 61, no. 1, pp. 38–44, 2008, doi: 10.1016/j.porgcoat.2007.09.012.
[31] F. Tronc *et al.*, “Epoxy-functionalized, low-glass-transition-temperature latex. II. Interdiffusion versus crosslinking in the presence of a diamine,” *J. Polym. Sci. Part A Polym. Chem.*, vol. 40, no. 22, pp. 4098–4116, 2002, doi: 10.1002/pola.10462.
[32] J. M. Geurts, P. E. Jacobs, J. C. Muijs, J. J. G. Steven Van Es, and A. L. German, “Molecular mass control in methacrylic copolymer latexes containing glycidyl methacrylate,” *J. Appl. Polym. Sci.*, vol. 61, no. 1, pp. 9–19, 1996, doi: 10.1002/(sici)1097-4628(19960705)61:1<9::aid-app2>3.0.co;2-p.
[33] M. A. Shenoy and D. J. D’Melo, “Effect of cross-linking density on coating properties of a polyurea coating system,” *Surf. Coatings Int. Part B Coatings Trans.*, vol. 89, no. 3, pp. 221–230, 2006, doi: 10.1007/BF02699664.
[34] M. Ogata, N. Kinjo, and T. Kawata, “Effects of crosslinking on physical properties of phenol–formaldehyde novolac cured epoxy resins,” *J. Appl. Polym. Sci.*, vol. 48, no. 4, pp. 583–601, 1993, doi: 10.1002/app.1993.070480403.
[35] H. Bakhshi, M. J. Zohuriaan-Mehr, H. Bouhendi, and K. Kabiri, “Effect of functional

monomer GMA on the physical-mechanical properties of coatings from poly(BA-MMA) latexes," *J. Mater. Sci.*, vol. 46, no. 8, pp. 2771–2777, 2011, doi: 10.1007/s10853-010-5151-7.
[36] M. Alam, D. Akram, E. Sharmin, F. Zafar, and S. Ahmad, "Vegetable oil based eco-friendly coating materials: A review article," *Arab. J. Chem.*, vol. 7, no. 4, pp. 469–479, 2014, doi: 10.1016/j.arabjc.2013.12.023.
[37] M. Irimia-Vladu *et al.*, "Natural resin shellac as a substrate and a dielectric layer for organic field-effect transistors," *Green Chem.*, vol. 15, no. 6, pp. 1473–1476, 2013, doi: 10.1039/c3gc40388b.
[38] Y. Farag and C. S. Leopold, "Investigation of drug release from pellets coated with different shellac types," *Drug Dev. Ind. Pharm.*, vol. 37, no. 2, pp. 193–200, 2011, doi: 10.3109/03639045.2010.504210.
[39] R. B. Seymour and G. B. Kauffman, "The rise and fall of celluloid," *J. Chem. Educ.*, vol. 69, no. 4, pp. 311–314, 1992, doi: 10.1021/ed069p311.
[40] L. B. Mehta, K. K. Wadgaonkar, and R. N. Jagtap, "Synthesis and characterization of high bio-based content unsaturated polyester resin for wood coating from itaconic acid: Effect of various reactive diluents as an alternative to styrene," *J. Dispers. Sci. Technol.*, vol. 40, no. 5, pp. 756–765, 2019, doi: 10.1080/01932691.2018.1480964.
[41] M. A. R. Meier, J. O. Metzger, and U. S. Schubert, "Plant oil renewable resources as green alternatives in polymer science," *Chem. Soc. Rev.*, vol. 36, no. 11, pp. 1788–1802, 2007, doi: 10.1039/b703294c.
[42] M. Azam Ali, T. L. Ooi, A. Salmiah, U. S. Ishiaku, and Z. A. M. Ishak, "New polyester acrylate resins from palm oil for wood coating application," *J. Appl. Polym. Sci.*, vol. 79, no. 12, pp. 2156–2163, 2001, doi: 10.1002/1097-4628(20010321)79:12<2156::AID-APP1023>3.0.CO;2-K.
[43] S. Cousinet, A. Ghadban, E. Fleury, F. Lortie, J. P. Pascault, and D. Portinha, "Toward replacement of styrene by bio-based methacrylates in unsaturated polyester resins," *Eur. Polym. J.*, vol. 67, pp. 539–550, 2015, doi: 10.1016/j.eurpolymj.2015.02.016.
[44] E. de Jong, A. Higson, P. Walsh, and M. Wellisch, "Task 42 Biobased Chemicals - Value Added Products from Biorefineries," *A Rep. Prep. IEA Bioenergy-Task*, p. 36, 2011.
[45] IEA Bioenergy Task42, "Bio-Based Chemicals: a 2020 Update," 2020.
[46] R. Tajau, M. I. Ibrahim, N. M. Yunus, M. H. Mahmood, M. Z. Salleh, and N. G. N. Salleh, "Development of palm oil-based UV-curable epoxy acrylate and urethane acrylate resins for wood coating application," *AIP Conf. Proc.*, vol. 1584, no. February 2015, pp. 164–169, 2014, doi: 10.1063/1.4866125.
[47] Y. Lu and R. C. Larock, "Novel polymeric materials from vegetable oils and vinyl monomers: Preparation, properties, and applications," *ChemSusChem*, vol. 2, no. 2, pp. 136–147, 2009, doi: 10.1002/cssc.200800241.
[48] M. R. Van De Mark and K. Sandefur, "Vegetable oils in paint and coatings," *Inf. - Int. News Fats, Oils Relat. Mater.*, vol. 16, no. 8, p. 478, 2005, doi: 10.1201/9781439822388.ch8.
[49] A. Parthiban, "Monomers and Polymers Derived from Renewable or Partially Renewable Resources," in *Synthesis and Applications of Copolymers*, vol. 9781118057, 2014, pp. 101–124.
[50] C. Fang, X. Zhu, Y. Cao, X. Xu, S. Wang, and X. Dong, "Toward replacement of methyl methacrylate by sustainable bio-based isobornyl methacrylate in latex pressure sensitive

adhesive," *Int. J. Adhes. Adhes.*, vol. 100, no. April, 2020, doi: 10.1016/j.ijadhadh.2020.102623.
[51] L. Chen, Z. Bao, Z. Fu, and W. Li, "Preparation and characterisation of novel cross-linked poly (IBOMA-BA-DFMA) latex," *Pigment Resin Technol.*, vol. 44, no. 6, pp. 333–338, 2015, doi: 10.1108/PRT-01-2015-0007.
[52] F. Hajiali, A. Métafiot, L. Benitez-Ek, L. Alloune, and M. Marić, "Nitroxide mediated polymerization of sustainably sourced isobornyl methacrylate and tridecyl methacrylate with acrylonitrile co-monomer," *J. Polym. Sci. Part A Polym. Chem.*, vol. 56, no. 21, pp. 2422–2436, 2018, doi: 10.1002/pola.29216.
[53] D. Saal, J. Knebel, and A. Haehnlein, "Process of Synthesis of Isobornyl (Meth)Acrylate," US 6,329,543 B1, 2001.
[54] P. Anastas and N. Eghbali, "Green Chemistry: Principles and Practice," *Chem. Soc. Rev.*, vol. 39, no. 1, pp. 301–312, 2010, doi: 10.1039/b918763b.
[55] P. G. Jessop, "Searching for green solvents," *Green Chem.*, vol. 13, no. 6, pp. 1391–1398, 2011, doi: 10.1039/c0gc00797h.
[56] V. Pace, P. Hoyos, L. Castoldi, P. Domínguez De María, and A. R. Alcántara, "2-Methyltetrahydrofuran (2-MeTHF): A biomass-derived solvent with broad application in organic chemistry," *ChemSusChem*, vol. 5, no. 8, pp. 1369–1379, 2012, doi: 10.1002/cssc.201100780.
[57] D. F. Aycock, "Solvent applications of 2-methyltetrahydrofuran in organometallic and biphasic reactions," *Org. Process Res. Dev.*, vol. 11, no. 1, pp. 156–159, 2007, doi: 10.1021/op060155c.
[58] J. E. Camp, "Bio-available Solvent Cyrene: Synthesis, Derivatization, and Applications," *ChemSusChem*, vol. 11, no. 18, pp. 3048–3055, 2018, doi: 10.1002/cssc.201801420.
[59] B. Yamada and P. B. Zetterlund, *General Chemistry of Radical Polymerization*. 2003.
[60] M. K. Nicolay V. Tsarevsky, "Environmentally Benign Atom Transfer Radical Polymerization: Towards \Green" Processes and Materials," *J. Polym. Sci. Part A Polym. Chem.*, vol. 44, no. October 2005, pp. 5098–5112, 2006, doi: 10.1002/POLA.
[61] A. V. Ambade, "Controlled radical polymerization," *Met. Polym. Fundam. to Appl.*, vol. 1, no. 12, pp. 161–178, 2017, doi: 10.1201/b19905.
[62] G. Wenz, *Advances in Polymer Science: Preface*, vol. 222, no. 1. 2009.
[63] C. Le Mercier *et al.*, "Use of phosphonylated nitroxides and alkoxyamines in controlled/"living" radical polymerization," *ACS Symp. Ser.*, vol. 768, pp. 108–122, 2000, doi: 10.1021/bk-2000-0768.ch008.
[64] K. Matyjaszewski and J. Spanswick, "Controlled/living radical polymerization," *Mater. Today*, vol. 8, no. 3, pp. 26–33, 2005, doi: 10.1016/S1369-7021(05)00745-5.
[65] E. Rizzardo, J. Chiefari, R. T. A. Mayadunne, G. Moad, and S. H. Thang, "Synthesis of Defined Polymers by Reversible Addition-Fragmentation Chain Transfer: The RAFT Process," in *Controlled/Living Radical Polymerization*, vol. 276, 2000, pp. 278–296.
[66] M. Destarac, "Controlled radical polymerization: Industrial stakes, obstacles and achievements," *Macromol. React. Eng.*, vol. 4, no. 3–4, pp. 165–179, 2010, doi: 10.1002/mren.200900087.
[67] J. S. Wang and K. Matyjaszewski, "Controlled/'Living' Radical Polymerization. Atom Transfer Radical Polymerization in the Presence of Transition-Metal Complexes," *J. Am. Chem. Soc.*, vol. 117, no. 20, pp. 5614–5615, 1995, doi: 10.1021/ja00125a035.
[68] M. Kato, M. Kamigaito, M. Sawamoto, and T. Higashimura, "Polymerization of Methyl

Methacrylate with the Carbon Tetrachloride/Dichlorotris-(triphenylphosphine)ruthenium(II)/ Methylaluminum Bis(2,6-di-tert-butylphenoxide) Initiating System: Possibility of Living Radical Polymerization," *Macromolecules*, vol. 28, no. 5, pp. 1721–1723, 1995, doi: 10.1021/ma00109a056.

[69] M. Nikolic, J. M. Lawther, and A. R. Sanadi, "Use of nanofillers in wood coatings: a scientific review," *J. Coatings Technol. Res.*, vol. 12, no. 3, pp. 445–461, 2015, doi: 10.1007/s11998-015-9659-2.

[70] W. A. Braunecker and K. Matyjaszewski, "Controlled/living radical polymerization: Features, developments, and perspectives," *Prog. Polym. Sci.*, vol. 32, no. 1, pp. 93–146, 2007, doi: 10.1016/j.progpolymsci.2006.11.002.

[71] K. Min and K. Matyjaszewski, "Atom transfer radical polymerization in aqueous dispersed media," *Cent. Eur. J. Chem.*, vol. 7, no. 4, pp. 657–674, 2009, doi: 10.2478/s11532-009-0092-1.

[72] K. Min, H. Gao, and K. Matyjaszewski, "Development of an ab initio emulsion atom transfer radical polymerization: From microemulsion to emulsion," *J. Am. Chem. Soc.*, vol. 128, no. 32, pp. 10521–10526, 2006, doi: 10.1021/ja0629054.

[73] M. Li and K. Matyjaszewski, "Reverse atom transfer radical polymerization in miniemulsion," *Macromolecules*, vol. 36, no. 16, pp. 6028–6035, 2003, doi: 10.1021/ma034109d.

[74] K. Min, H. Gao, and K. Matyjaszewski, "Preparation of homopolymers and block copolymers in miniemulsion by ATRP using activators generated by electron transfer (AGET)," *J. Am. Chem. Soc.*, vol. 127, no. 11, pp. 3825–3830, 2005, doi: 10.1021/ja0429364.

[75] T. Cuneo, R. W. Graff, X. Wang, and H. Gao, "Synthesis of Highly Branched Copolymers in Microemulsion," *Macromol. Chem. Phys.*, vol. 220, no. 6, pp. 1–8, 2019, doi: 10.1002/macp.201800546.

[76] P. Krys and K. Matyjaszewski, "Kinetics of Atom Transfer Radical Polymerization," *Eur. Polym. J.*, vol. 89, pp. 482–523, 2017, doi: 10.1016/j.eurpolymj.2017.02.034.

[77] V. M. C. Coessens and K. Matyjaszewski, *Fundamentals of atom transfer radical polymerization*, vol. 87, no. 9. 2010.

[78] Q. Lou and D. A. Shipp, "Recent developments in atom transfer radical polymerization (ATRP): Methods to reduce metal catalyst concentrations," *ChemPhysChem*, vol. 13, no. 14, pp. 3257–3261, 2012, doi: 10.1002/cphc.201200166.

[79] K. Matyjaszewski, "Mechanistic Aspects of Atom Transfer Radical Polymerization," in *Controlled Radical Polymerization*, vol. 685, 1998, pp. 258–283.

[80] P. T. Anastas and M. M. Kirchhoff, "Origins, current status, and future challenges of green chemistry," *Acc. Chem. Res.*, vol. 35, no. 9, pp. 686–694, 2002, doi: 10.1021/ar010065m.

[81] J. Kreutzer and Y. Yagci, "Metal free reversible-deactivation radical polymerizations: Advances, challenges, and opportunities," *Polymers (Basel).*, vol. 10, no. 1, 2017, doi: 10.3390/polym10010035.

[82] Y. Shen, H. Tang, and S. Ding, "Catalyst_separation_in_atom_transfer_rad.pdf," *Prog. Polym. Sci.*, vol. 29, no. 10, pp. 1053–1078, 2004.

[83] N. Chan, M. F. Cunningham, and R. A. Hutchinson, "Copper-mediated controlled radical polymerization in continuous flow processes: Synergy between polymer reaction engineering and innovative chemistry," *J. Polym. Sci. Part A Polym. Chem.*, vol. 51, no.

15, pp. 3081–3096, 2013, doi: 10.1002/pola.26711.
[84] K. Matyjaszewski *et al.*, "Diminishing catalyst concentration in atom transfer radical polymerization with reducing agents," *Proc. Natl. Acad. Sci. U. S. A.*, vol. 103, no. 42, pp. 15309–15314, 2006, doi: 10.1073/pnas.0602675103.
[85] K. Matyjaszewski, T. E. Patten, and J. Xia, "Controlled/'living' radical polymerization. Kinetics of the homogeneous atom transfer radical polymerization of styrene," *J. Am. Chem. Soc.*, vol. 119, no. 4, pp. 674–680, 1997, doi: 10.1021/ja963361g.
[86] W. Tang and K. Matyjaszewski, "Kinetic modeling of normal ATRP, normal ATRP with [CuII] 0, reverse ATRP and SR & NI ATRP," *Macromol. Theory Simulations*, vol. 17, no. 7–8, pp. 359–375, 2008, doi: 10.1002/mats.200800050.
[87] J. Gromada and K. Matyjaszewski, "Simultaneous reverse and normal initiation in atom transfer radical polymerization," *Macromolecules*, vol. 34, no. 22, pp. 7664–7671, 2001, doi: 10.1021/ma010864k.
[88] W. Jakubowski and K. Matyjaszewski, "Activator generated by electron transfer for atom transfer radical polymerization," *Macromolecules*, vol. 38, no. 10, pp. 4139–4146, 2005, doi: 10.1021/ma047389l.
[89] D. R. D'Hooge, D. Konkolewicz, M. F. Reyniers, G. B. Marin, and K. Matyjaszewski, "Kinetic modeling of ICAR ATRP," *Macromol. Theory Simulations*, vol. 21, no. 1, pp. 52–69, 2012, doi: 10.1002/mats.201100076.
[90] X. Pan, N. Malhotra, A. Simakova, Z. Wang, D. Konkolewicz, and K. Matyjaszewski, "Photoinduced Atom Transfer Radical Polymerization with ppm-Level Cu Catalyst by Visible Light in Aqueous Media," *J. Am. Chem. Soc.*, vol. 137, no. 49, pp. 15430–15433, 2015, doi: 10.1021/jacs.5b11599.
[91] B. L. Ramsey, R. M. Pearson, L. R. Beck, and G. M. Miyake, "Photoinduced Organocatalyzed Atom Transfer Radical Polymerization Using Continuous Flow," *Macromolecules*, vol. 50, no. 7, pp. 2668–2674, 2017, doi: 10.1021/acs.macromol.6b02791.
[92] Y. Kwak and K. Matyjaszewski, "ARGET ATRP of methyl methacrylate in the presence of nitrogen-based ligands as reducing agents," *Polym. Int.*, vol. 58, no. 3, pp. 242–247, 2009, doi: 10.1002/pi.2530.
[93] N. Chan, M. F. Cunningham, and R. A. Hutchinson, "ARGET ATRP of methacrylates and acrylates with stoichiometric ratios of ligand to copper," *Macromol. Chem. Phys.*, vol. 209, no. 17, pp. 1797–1805, 2008, doi: 10.1002/macp.200800328.
[94] A. Simakova, S. E. Averick, D. Konkolewicz, and K. Matyjaszewski, "Aqueous ARGET ATRP," *Macromolecules*, vol. 45, no. 16, pp. 6371–6379, 2012, doi: 10.1021/ma301303b.
[95] Y. Kwak, A. J. D. Magenau, and K. Matyjaszewski, "ARGET ATRP of methyl acrylate with inexpensive ligands and ppm concentrations of catalyst," *Macromolecules*, vol. 44, no. 4, pp. 811–819, 2011, doi: 10.1021/ma102665c.
[96] J. Li *et al.*, "Synthesis of amphiphilic block copolymers via ARGET ATRP using an inexpensive ligand of PMDETA," *React. Funct. Polym.*, vol. 73, no. 11, pp. 1517–1522, 2013, doi: 10.1016/j.reactfunctpolym.2013.07.012.
[97] K. Tanaka and K. Matyjaszewski, "Copolymerization of (meth)acrylates with olefins using activators regenerated by electron transfer for atom transfer radical polymerization (ARGET ATRP)," *Macromol. Symp.*, vol. 261, no. 1, pp. 1–9, 2008, doi: 10.1002/masy.200850101.
[98] P. Król and P. Chmielarz, "Synthesis of PMMA-b-PU-b-PMMA tri-block copolymers

through ARGET ATRP in the presence of air," *Express Polym. Lett.*, vol. 7, no. 3, pp. 249–260, 2012, doi: 10.3144/expresspolymlett.2013.23.
[99] A. Dhar, B. P. Koiry, and D. J. Haloi, "Synthesis of poly(methyl methacrylate) via ARGET ATRP and study of the effect of solvents and temperatures on its polymerization kinetics," *Int. J. Chem. Kinet.*, vol. 50, no. 10, pp. 757–763, 2018, doi: 10.1002/kin.21210.
[100] W. Jakubowski and K. Matyjaszewski, "Activators regenerated by electron transfer for atom-transfer radical polymerization of (meth)acrylates and related block copolymers," *Angew. Chemie - Int. Ed.*, vol. 45, no. 27, pp. 4482–4486, 2006, doi: 10.1002/anie.200600272.
[101] N. Chan, J. Meuldijk, M. F. Cunningham, and R. A. Hutchinson, "Continuous ARGET ATRP of methyl methacrylate and butyl acrylate in a stirred tank reactor," *Ind. Eng. Chem. Res.*, vol. 52, no. 34, pp. 11931–11942, 2013, doi: 10.1021/ie4011996.
[102] H. Dong, W. Tang, and K. Matyjaszewski, "Well-defined high-molecular-weight polyacrylonitrile via activators regenerated by electron transfer ATRP," *Macromolecules*, vol. 40, no. 9, pp. 2974–2977, 2007, doi: 10.1021/ma070424e.
[103] K. L. Robinson, J. V. M. Weaver, S. P. Armes, E. D. Marti, and F. C. Meldrum, "Synthesis of controlled-structure sulfate-based copolymers via atom transfer radical polymerisation and their use as crystal habit modifiers for BaSO4," *J. Mater. Chem.*, vol. 12, no. 4, pp. 890–896, 2002, doi: 10.1039/b200348c.
[104] J. V. M. Weaver *et al.*, "Stimulus-Responsive Water-Soluble Polymers Based on 2-Hydroxyethyl Methacrylate," *Macromolecules*, vol. 37, no. 7, pp. 2395–2403, 2004, doi: 10.1021/ma0356358.
[105] L. A. Wood, "Glass Transition Temperatures of Copolymers," *J. Polym. Sci.*, vol. 28, pp. 319–330, 1958, doi: 10.1016/0032-3861(73)90127-4.
[106] H.-J. Streitberger and K.-F. Dossel, *Automotive Paints and Coatings*. Wiley-VCH Verlag, 2008.
[107] J. L. De La Fuente, M. Fernández-Sanz, M. Fernández-García, and E. L. Madruga, "Solvent effects on the synthesis of poly(methyl methacrylate) by atom-transfer radical polymerization (ATRP)," *Macromol. Chem. Phys.*, vol. 202, no. 12, pp. 2565–2571, 2001, doi: 10.1002/1521-3935(20010801)202:12<2565::AID-MACP2565>3.0.CO;2-4.
[108] K. B. WOOD and V. T. STANNETT, "Analysis of Copolymerization Systems Involving Multiple Reaction Pathways," vol. 30, pp. 13–19, 1992.
[109] T. Kelen, F. Tüdös, and B. Turcsányi, "Confidence intervals for copolymerization reactivity ratios determined by the Kelen-Tüdös method," *Polym. Bull.*, vol. 2, no. 1, pp. 71–76, 1980, doi: 10.1007/BF00275556.
[110] A. D. Azzahari, R. Yahya, A. Hassan, and M. R. K. Sheikh, "Synthesis and characterization of new copolymers from glycidyl methacrylate and tetrahydrofurfuryl acrylate: Determination of reactivity ratios," *Fibers Polym.*, vol. 13, no. 5, pp. 555–563, 2012, doi: 10.1007/s12221-012-0555-4.
[111] M. J. Richardson and N. G. Savill, "Derivation of Accurate Glass Transition Temperatures By Differential Scanning Calorimetry.," *Rubber Chem. Technol.*, vol. 49, no. 2, pp. 224–232, 1976, doi: 10.5254/1.3534959.
[112] P. F. Cañamero, J. L. De La Fuente, E. L. Madruga, and M. Fernández-García, "Atom transfer radical polymerization of glycidyl methacrylate: A functional monomer," *Macromol. Chem. Phys.*, vol. 205, no. 16, pp. 2221–2228, 2004, doi: 10.1002/macp.200400186.

[113] J. Xia and K. Matyjaszewski, “Controlled/"living" radical polymerization. Homogeneous reverse atom transfer radical polymerization using AIBN as the initiator,” *Macromolecules*, vol. 30, no. 25, pp. 7692–7696, 1997, doi: 10.1021/ma9710085.
[114] D. Konkolewicz, K. Schröder, J. Buback, S. Bernhard, and K. Matyjaszewski, “Visible light and sunlight photoinduced ATRP with ppm of Cu catalyst,” *ACS Macro Lett.*, vol. 1, no. 10, pp. 1219–1223, 2012, doi: 10.1021/mz300457e.
[115] X. Jiang, J. Wu, L. Zhang, Z. Cheng, and X. Zhu, “Highly active ppm level organic copper catalyzed photo-induced ICAR ATRP of methyl methacrylate,” *Macromol. Rapid Commun.*, vol. 35, no. 21, pp. 1879–1885, 2014, doi: 10.1002/marc.201400393.
[116] G. X. Wang *et al.*, “Photo-induced atom transfer radical polymerization in ionic liquid,” *J. Polym. Res.*, vol. 22, no. 4, pp. 20–25, 2015, doi: 10.1007/s10965-015-0707-5.
[117] X. Liu, L. Zhang, Z. Cheng, and X. Zhu, “Metal-free photoinduced electron transfer-atom transfer radical polymerization (PET-ATRP) via a visible light organic photocatalyst,” *Polym. Chem.*, vol. 7, no. 3, pp. 689–700, 2016, doi: 10.1039/c5py01765c.
[118] J. Yan, X. Pan, M. Schmitt, Z. Wang, M. R. Bockstaller, and K. Matyjaszewski, “Enhancing Initiation Efficiency in Metal-Free Surface-Initiated Atom Transfer Radical Polymerization (SI-ATRP),” *ACS Macro Lett.*, vol. 5, no. 6, pp. 661–665, 2016, doi: 10.1021/acsmacrolett.6b00295.
[119] X. Pan *et al.*, “Mechanism of Photoinduced Metal-Free Atom Transfer Radical Polymerization: Experimental and Computational Studies,” *J. Am. Chem. Soc.*, vol. 138, no. 7, pp. 2411–2425, 2016, doi: 10.1021/jacs.5b13455.
[120] G. S. Park, J. Back, E. M. Choi, E. Lee, and K. sun Son, “Visible light-mediated metal-free atom transfer radical polymerization with N-trifluoromethylphenyl phenoxazines,” *Eur. Polym. J.*, vol. 117, pp. 347–352, 2019, doi: 10.1016/j.eurpolymj.2019.05.023.

Appendix

Table A. 1 Calculations of the reactivity ratios by Kelen-Tudos.

f[a] (IBOMA)	F[b] (IBOMA)	G	H	ε	η
0.9	0.91	-8.117	-7.943	1.147	1.172
0.7	0.68	-1.231	-2.572	1.656	0.793
0.5	0.47	0.121	-1.121	10.991	-1.185
0.3	0.30	0.574	-0.430	-0.729	0.974
0.1	0.09	1.065	-0.131	-0.147	1.199

a. The initial molar fraction of IBOMA in the initial feed.
b. The final molar fraction of IBOMA in the terpolymer (F_{IBOMA}) as determined by 1H NMR in CDCl3.

Table A. 2 Calculations of the reactivity ratios by Kelen-Tudos extended.

f[a] (IBOMA)	F[b] (IBOMA)	G	H	ε	η
0.9	0.91	9.065	11.556	0.923	0.724
0.7	0.68	1.210	1.921	0.666	0.419
0.5	0.47	0.000	0.796	0.452	0.000
0.3	0.30	-0.570	0.427	0.307	-0.410
0.1	0.09	-0.756	0.080	0.077	-0.724

a. The initial molar fraction of IBOMA in the initial feed.
b. The final molar fraction of IBOMA in the terpolymer (F_{IBOMA}) as determined by 1H NMR in CDCl3.

Table A. 3 Copolymers of IBOMA and C13MA by ARGET ATRP with a feed ratio of $[Monomer]_0/[EBIB]_0/[SnEH2]_0/[CuBr2]_0/[PMDETA]_0 = 100/1/0.37/0.025/0.25$

Experiment ID	Temp (°C)	Time (min)	Conversion %	Mn[a], GPC (kg/mol)	$Đ^a$
AR_IB_9	80	60	0.94	12.497	1.57
ARG_IB_C13MA_70_30	80	40	0.82	14.5	1.53
ARG_IB_C13MA_30_70	80	60	0.88	19.5	1.55
ARG_C13MA_100	80	80	0.71	22.3	1.68

a. The final product's number average molecular weight (Mn) and dispersity (Đ) as determined by GPC with PMMA standards at 40°C in THF.

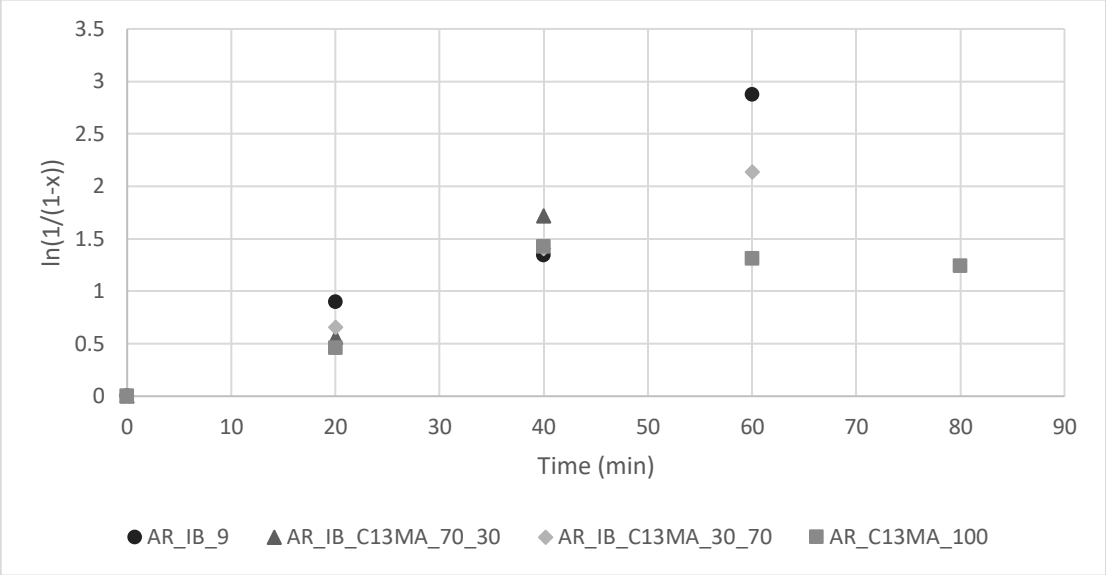

Figure A.1 Kinetic plot of ln(1/(1-X) with time, where X is conversion, for IBOMA and C13MA by ARGET ATRP with a feed ratio of $[Monomer]_0/[EBIB]_0/[SnEH2]_0/[CuBr2]_0/[PMDETA]_0 = 100/1/0.37/0.025/0.25$

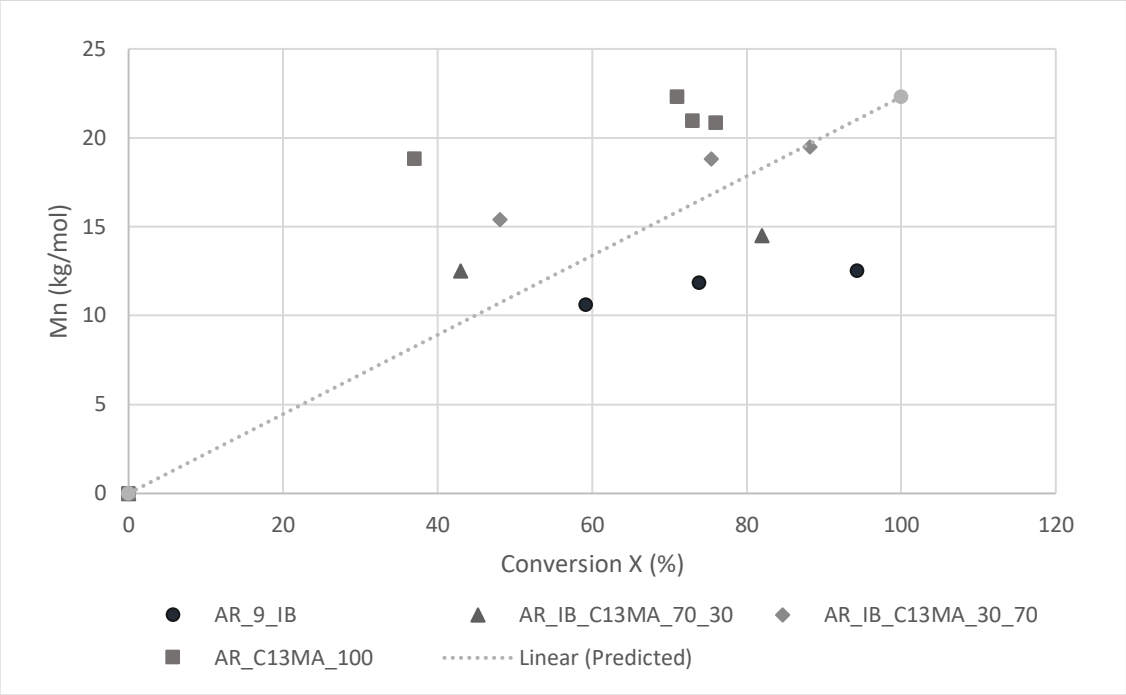

Figure A.2 Kinetic plot of molecular weight and conversion for IBOMA and C13MA by ARGET ATRP with a feed ratio of $[Monomer]_0/[EBIB]_0/[SnEH2]_0/[CuBr2]_0/[PMDETA]_0$ = 100/1/0.37/0.025/0.25.

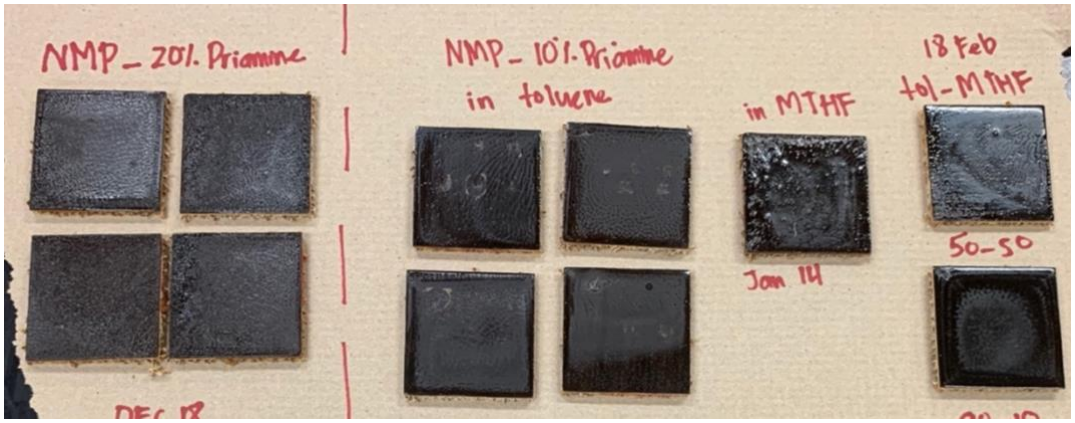

Figure A.3 Coated wood samples_ NMP polymer resins.

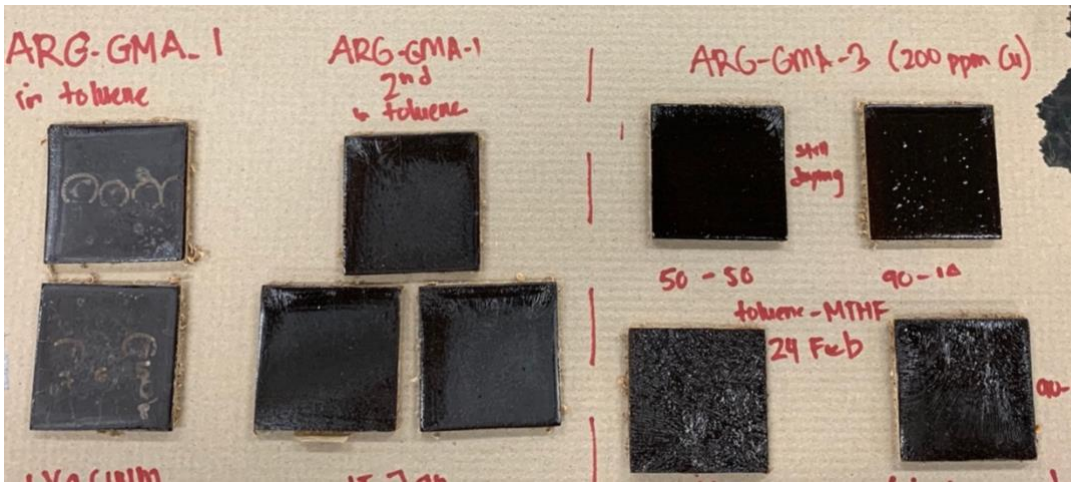

Figure A.4 Coated wood samples_ ARGET polymer resins.

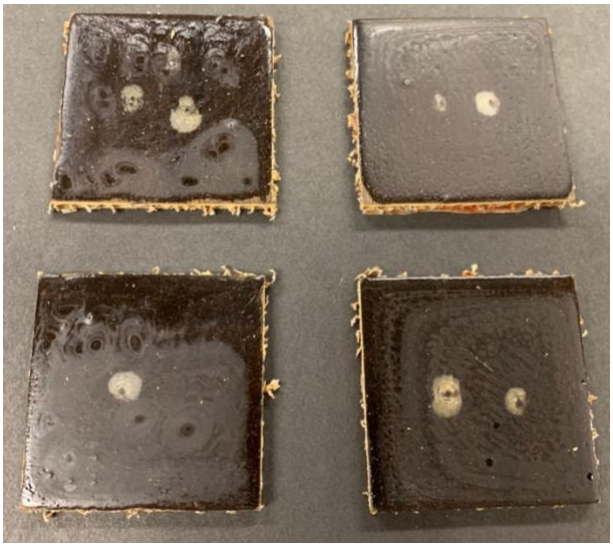

Figure A.5 Wood samples after impact testing.